REPORT NO. CASD-NAS74-008
CONTRACT NAS8-29060

EVALUATION OF SOFT RUBBER GOODS

FINAL REPORT

GENERAL DYNAMICS
Convair Division

EVALUATION OF SOFT RUBBER GOODS

Final Report

Report No. CASD-NAS-74-008
July 1972 to February 1974

P. L. Merz

Contract No. NAS8-29060
Control No. 1-2-50-23699 (1F)

February 1974

National Aeronautics and Space Administration
George C. Marshall Space Flight Center
Astronautics Laboratory
Materials Division, Nonmetallics Branch
Huntsville, Alabama

GENERAL DYNAMICS
Convair Aerospace Division
San Diego, California

TABLE OF CONTENTS

LIST OF FIGURES

LIST OF FIGURES-Continued

LIST OF FIGURES-Continued

LIST OF TABLES

LIST OF TABLES-Continued

LIST OF TABLES-Continued

LIST OF TABLES-Continued

SUMMARY

Twelve potential seal candidates were evaluated for the following Space Shuttle systems:

Hydraulic System - MIL-H-83282 Fluid, 233K (-40F) to 422K (300F)

Main Propellent System - LH_2 and LO_2, 80K (-320F) to 344K (160F)

Orbital Maneuvering System - N_2O_4 and Monomethyl Hydrazine, 222K (-60F) to 378K (220F)

Tensile coupons were employed for all of the various compatibility tests (thermal cycling, long term aging, etc.) with the exception of the liquid oxygen impact testing. O-ring configurations were employed for cyclic load deflection, stress relaxation, cyclic compression and static sealibility tests. Basic rheological properties such as cyclic hysteresis and apparent modulus of the O-rings themselves were calculated from these tests.

Low temperature Viton rubbers offer a good combination of cyclic load bearing and rheological properties, as well as sealability and compatibility against MIL-H-83282 fluid even at high temperatures. Although the subject Vitons display excellent high temperature elastic properties, they have relatively poor low temperature properties, and are suitable only for service from 422K (300F) to~243K (-22F).

Crosslinked Halar, which is liquid oxygen compatible, exhibited outstanding performance in the cyclic compression sealability test at 83K (-310F). Stress relaxation, cyclic compression set, and load deflection measurements, however, suggest that higher degrees of radiation crosslinking are desirable in order to develop the full potential of Halar seals.

Linear Tefzel displayed the greatest chemical resistance, being virtually unaffected by ten months' immersion in either nitrogen tetroxide or monomethyl-hydrazine. Unfortunately, linear Tefzel has extremely poor high temperature sealing properties, and failed completely in the cyclic sealability test at 377K (220F).

Due to their capacity to be radiation crosslinked, both Halar and Tefzel offer promise of developing into superior seals with improved thermal capabilities. However, considerable work remains to be done before crosslinked Halar (for example) can be seriously considered as a replacement for the current cryogenic seal materials, thermoplastic Teflon and Kel-F.

SECTION 1

INTRODUCTION

This report describes the work accomplished by General Dynamics/Convair Aerospace for the George C. Marshall Space Flight Center under Contract NAS8-29060 during the period 29 June 1972 through 30 December 1973. The primary objectives of this program were to study the performance of rubber goods suitable for use as O-rings, seals, gaskets, bladders and diaphragms under conditions simulating those of the Space Shuttle. High reliability throughout the 100 flight missions planned for the Space Shuttle was considered of overriding importance. Accordingly, in addition to a rank ordering of the selected candidate materials based on prolonged fluid compatibility and sealability behavior, basic rheological parameters (such as cyclic hysteresis, stress relaxation, indicated modulus, etc.) were determined in an attempt to develop methods capable of predicting the cumulative effect of these multiple reuse cycles.

Although this contract was limited to state-of-the-art materials, the extreme cyclic variations in the Space Shuttle flight environments, coupled with reusability and quick turn-around requirements (all superimposed on the usual high reliability spacecraft requirements) precluded using conventional seal materials. For example, raising the upper operating temperature of the space shuttle hydraulic system to 422K (300F) through use of the new MIL-H-83282 hydraulic fluid effectively excluded the proven MIL-P-25732 type seal rubbers. Similarly, the thermoplastic nature of the current preferred seal materials for liquid oxygen use (filled fluorocarbons such as Teflon and Kel-F) suggested a low survival probability for the space shuttle time-temperature requirements without softening and deforming. It was, therefore, necessary to select new, unproven seal materials which, on the basis of their chemical structure and physical properties, appeared to offer the greatest chance of success for withstanding the severe conditions of the space shuttle missions.

In this report, the SI system of units is shown as the primary system with English units following in parentheses, although the English system of units (ft, lb, sec) has been used for all measurements and calculations.

SECTION 2

MATERIAL SELECTION AND PROCUREMENT

2.1 Seal Candidate Selection

Selection was based on prior knowledge of aerospace sealing requirements plus the general relationships which exist between molecular structure and the chemical compatibility, thermal stability, and rheological behavior of polymers. Materials were selected in an effort to match the various specific requirements which are peculiar to the three (3) different seal areas of Space Shuttle (i. e., the hydraulic system, the main propulsion system, and the orbital maneuvering system). Hydraulic system seals were selected primarily for their oil resistance, creep resistance at 422K (300F), resiliance, and compliance at 233K (-40F). Similarly, the main propulsion seals were selected mainly for their LO_2 compatibility, their rheological behavior at cryogenic temperatures, and minimum creep at 344K (160F).

By contrast, chemical resistance is the overriding concern in the case of the orbital maneuvering system. It would be desirable to minimize the variety of space shuttle seal materials. This program, therefore, attempted to develop a single seal material for each of the three mentioned systems. Unfortunately, the main propulsion system and the orbital maneuvering system each encompasses its own oxidizer/fuel combination. Any oxidizer/fuel combination inherently poses conflicting compatibility requirements. This is particularly true of the high energy oxidizer/fuel combination [nitrogen tetroxide (N_2O_4) and hydrazine (N_2H_4)] employed in the orbital maneuvering system. For the orbital maneuvering system, different seal materials would probably be required for the N_2O_4 and for the N_2H_4 portions of the system.

Twelve different polymeric compounds were selected for this program. Their chemical structure (if known), principal characteristics, and suppliers are listed below according to their specific end use. New, contemporary organic polymers predominate, because the older, tried and proven seal materials would not satisfy the severe, long term requirements demanded by the space shuttle. Utilization of these new untried materials, of course, poses greater risk of failure. Accordingly, a number of alternate (i. e., "back up") materials were included for each of the three systems in case some, or all, of the preferred materials failed to meet the Space Shuttle requirements. Since most of the polymeric compounds are extremely new, and many were available only in small (laboratory or semicommercial) quantities, the individual vendors were contacted to obtain data on optimum compounding, processing, and curing conditions. In addition, special molds were purchased which are capable of meeting the critical high temperature molding requirements demanded by some of these new seal materials.

2.1.1 Hydraulic System

Principal Candidates:

Viton ECD-3234/carbon black filled

This is a special perfluoropropylene/vinylidine fluoride copolymer,

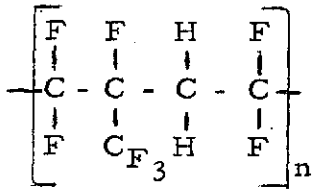

called LD-487 with an E-60C type cure. It has superior low temperature properties.

Vendor: DuPont

Fluorosilicone LS-2380

A special silicone,

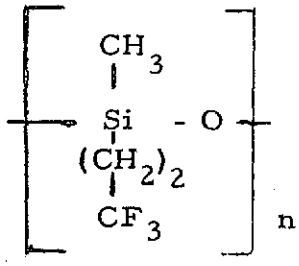

having an unusually high tensile strength; T_S = 9.1 MN/m^2 (1320 psi) and low compression set, 70 hr/423K (302F) = 15%.

Vendor: Dow Corning

Phosphazine Fluoroelastomer

A novel, new elastomer derived from phosphonitrilic chloride with the copolymer structure,

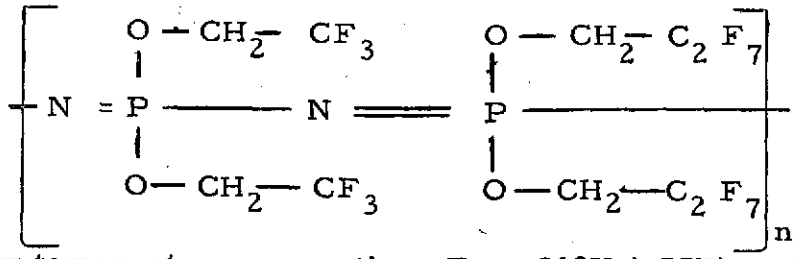

It has excellent low temperature properties, T_G = 212K (-77F) and oil resistance.

Vendor: Horizons, Inc. (via NASA)

Alternate Candidates:

Viton ECD-3233/carbon black filled

Similar to ECD-3234 (above) but better low temperature properties, T_G = 243K (-22F). Less likely to be commercialized than -3234.

Vendor: DuPont

Viton E-60C/carbon black filled

Similar to -3243 but cheaper and with poorer low temperature properties.

Vendor: DuPont

Fluorosilicone LS-2249

Similar to LS-2380 (above) but having lower modulus and much higher tear strength.

Vendor: Dow Corning

2.1.2 Main Propellent System

Principal Candidates:

AF-E-124D or Viton ECD-006

An unusual copolymer of tetrafluoroethylene/perfluoromethyl vinyl ether,

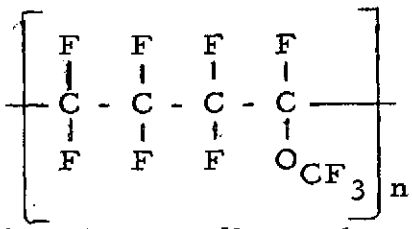

It is LO_2 compatible, has excellent solvent resistance, and temperature capabilities from 233K to 561K (-40F to 550F). Available in limited quantities, but is expensive.

Vendor: DuPont

Viton ECD-3234/Cab-O-Lite filled

Similar to ECD-3234 (black) but a non-black stock. May be LO_2 compatible.

Vendor: DuPont

Phosphazine Fluoroelastomer

See 2.1.1. Presumed to be LO_2 compatible.

Vendor: Horizons, Inc.

Crosslinked Halar

An ethylene/chlorotrifluoroethylene copolymer with good physical properties.

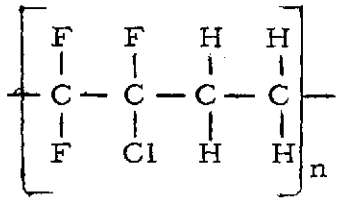

Similar to Kel-F but much better solvent resistance. Inexpensive and easily fabricated. LO_2 compatible. Crosslinked with 5 MRads of radiation.

Vendor: Allied Chemical

Crosslinked Tefzel

An ethylene/tetrafluoroethylene copolymer.

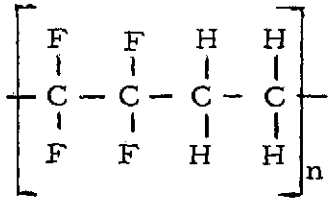

Similar to TFE but much more easily fabricated. Presumed to be LO_2 compatible. Radiation crosslinked.

Vendor: DuPont

Alternate Candidate:

Viton E-60C/ white stock

See 2.1.1. Presumed to be LO_2 compatible.

2.1.3 Orbital Maneuvering System

N_2O_4 Oxidizer

Principal Candidates:

Viton ECD-006 (AF-E-124D)

See 2.1.2. N_2O_4 compatible.

Linear Halar

See 2.1.2. N_2O_4 compatible.

Linear Tefzel

See 2.1.2. Presumed to be N_2O_4 compatible.

Alternate Candidates:

Crosslinked Halar

See 2.1.2.

Crosslinked Tefzel

See 2.1.2.

N_2H_4 Fuel

Principal Candidates:

Phosphazine Fluoroelastomer

See 2.1.1. Presumed to be N_2H_4 compatible.

Linear Halar

See 2.1.2. Presumed to be N_2H_4 compatible.

Linear Tefzel

See 2.1.2. Presumed to be N_2H_4 compatible.

Alternate Candidates:

Crosslinked Halar

See 2.1.2.

Crosslinked Tefzel

See 2.1.2.

Viton ECD-006 (AF-E-124D)

See 2.1.2. N_2H_4 compatible.

2.2 Specimen Fabrication

This program employed four (4) types of specimens:

1. Tensile dumbbells for plastic - ASTM D638-68
2. Tensile dumbbells for rubbers - ASTM D412-61
3. LO_2 impact test specimens - discs 19 mm. OD x 1.27 mm (0.75 by .050 inches)
4. (-224) size O-rings

The tensile dumbbells and impact specimens were machined or die cut from 1.9 mm (0.075 inches) thick sheet stock. The 1.9 mm sheet stock was either obtained directly from the appropriate vendor or was molded by Convair Aerospace using a standard single cavity ASTM test slab mold, 15.25 cm by 15.25 cm by 1.9 mm (6 by 6 by 0.075 inches), which had been electroless-nickel-plated. The -224 size O-rings ID = 44.4 mm (1-3/4 inch); OD = 50.9 mm (2 inches), 3.18 mm (1/8 inch) cross section were also molded at Convair Aerospace in an electroless-nickel-plated, 4-cavity, O-ring mold. A heavy, non-porous, nickel plating is essential for molding the fluorocarbon polymers (such as Halar and Tefzel), which are extremely corrosive at the high temperatures required for molding. O-ring preforms for the rubbers used on this program were prepared by cutting rings from slabbed sheets by means of a concentric "cookie cutter" type die.

By contrast, O-ring preforms for the fluoroplastics were rough machined from 5.08 cm (2 inch) bar stock. After molding, the still uncured O-rings and machined tensile bars of the Halar and Tefzel were radiation cured with 5 megarads by Radiation International at Parsippany, New Jersey, employing a 150,000 curie cobalt-60 source.

In the case of rubbers (such as the Vitons), the raw stock was received as rough slabbed sheets containing some or all of the required compounding ingredients. After mastication, the remaining ingredients were milled in, and the resulting rubber was compression molded and vulcanized in the nickel-plated molds described above. The molded parts were then postcured at elevated temperatures for extended periods of time to improve the physical properties and to minimize any tendency of the vulcanizate to undergo any spontaneous change in physical properties during subsequent long-term service. Postcuring times range from a few hours up to 4 or 5 days at temperatures as high as 558K(545F), depending on the chemical reactivity of the rubber and the crosslinking mechanism involved. The exact formulations and cure schedules of all the seal rubber candidates employed are documented in Appendix A.

No particular difficulty was encountered in fabricating specimens from any of the stocks except for phosphazine fluoroelastomer and the perfluoroelastomer for AF-E-124D. In the first case, the difficulty involved unavailability of the raw uncured phosphazine rubber. The only phosphazine rubber available was four small, cured, tensile slabs marked #1884-34, which was furnished by NASA-Huntsville in October 1973. All phosphazine rubber specimens utilized in this contract were cut from these four tensile slabs. Unfortunately, these #1884-34 slabs represent a very early development by the manufacturer, Horizons, Inc., of Cleveland, Ohio, and are not representative of the present superior generation of phosphazine fluoroelastomer vulcanizates.

By contrast, a 454g (1 lb.) sample of the raw perfluoroelastomer (called Viton ECD-006 by DuPont, and AF-E-124D by the Air Force) was obtained early in the program through the courtesy of Mr. J. K. Sieron of the AFML, Wright-Patterson Air Force Base. The difficulty in this case, is that the raw AF-E-124D stock is extremely viscous even at high temperatures. Due to its poor flow, viscous character, and low cohesion, it was difficult to mold parts (such as O-rings) without massive surface defects such as "backrind," even when molded at the AFML-recommended temperature of 450K (350F). Specification grade O-rings were obtained only when the molding temperature had been reduced by 75K (per suggestion of J. Martin of TRW).

In the case of the plastic candidates (such as Tefzel or Halar), the raw stock was usually received in the form of molded sheet or rod, although in one case, a pound of molding powder was also obtained. Due to the extremely high modulus and poor moldability of these fluorocarbons, considerable expertise is required to mold these basic sheets and rods. For example, DuPont was unable to mold the required 0.19 cm (.075 in.) thick Tefzel tensile slabs directly, and resorted to machining a thicker slab to the required size. Fluorocarbon did indeed succeed in molding two 0.19 cm thick slabs, but it required about three times as long as they initially estimated.

By contrast, Allied Chemical (the manufacturer of Halar) readily molded the required tensile slabs, but experienced difficulty with the 5.08 cm (2 in.) diameter Halar rod. Tensile dumbells were readily machined from the Halar and Tefzel sheets. O-ring preforms were also readily machined from the linear Halar and Tefzel rods, however, in order to obtain satisfactory O-rings from the corresponding machined preforms both the molding conditions and the preform dimensions are critical.

Preliminary experiments proved that the temperatures specified for injection molding these fluoroplastics results in compression molded parts having excessive voids and strains. Compression molding temperatures 55.5K (100F) to 83.4K (150F) degrees lower than those employed for injection molding appear necessary. The use of machined Halar and Tefzel rings, 5.09 cm OD x 4.37 cm ID x 0.363 cm cross section, worked fairly well as preforms for the (-224) O-ring mold. It was found, however, that by changing from a simple square cross section to the half-round cross section shown at the right, parts with less strain and fewer internal voids could be obtained. Preforms of this cross section can be machined from the fluoroplastic rod with only a minimum increase in cost over that of the square sectional preforms.

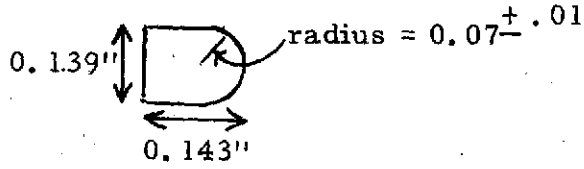

The secret of obtaining good moldings is to subject the preform to compressive loadings throughout the molding operation. For example, by simply increasing the preform OD from 5.08 cm (2.00 $^{+.00}_{-.02}$ in.) to 5.10 cm (2.010 $\pm$ .005 in.), i.e., by only 0.02 cm or 0.01 in. the O-ring rejection rate dropped from 25% to 0%. The exact O-ring molding procedures for these two fluoroplastics are summarized in Appendix B. The integrity of the newly molded O-rings was checked by a simple thermal shock test consisting of immersion in liquid nitrogen (LN_2) followed by warming to room temperature with a heat gun. In contrast to defective O-rings produced by earlier less successful molding procedures, O-rings produced by the methods described in Appendix B showed no evidence of cracking.

2.3 Test Fluid Procurement and Analysis

2.3.1 Hydraulic Fluid MIL-H-83282

Originally, it had been assumed that the Space Shuttle's hydraulic system would be required to operate over the temperature range of 222K (-60F) to 422K (300F). Upon examination of the viscosity/temperature relationship of the new, fire-resistant, synthetic hydrocarbon base MIL-H-83282 hydraulic fluid proposed for Space Shuttle use, it was discovered that MIL-H-83282 fluid has a viscosity of 3,000 centistokes at 233K (-40F) and 22,000 centistokes at 219K (-65F). Since at 219K (-65F) the viscosity of this MIL-H-83282 fluid is ten times that of the present

MIL-H-5606B fluid, it was apparent that the usual low temperature military requirement of 219K (-65F) would have to be waived. It was, therefore, recommended that the low temperature limit of this program be changed from 222K (-60F) to 233K (-40F). This change also significantly expanded the types of oil resistant rubbers which could be used in the subject hydraulic system. At the start of the program, there were only three commercial sources of MIL-H-83282 fluid. Unfortunately, at that time none of the three qualified vendors (Bray, Mobile and Standard Oil Co.) had any fluid which satisfied all the MIL-H-83282 specifications. For example, Mobil Oil Corp.'s sample MIL-H-83282 fluid swelled rubber by only 14.9% compared with the specified 18 to 30% swell. Standard Oil's sample failed to pass the gunfire test. As a result, Convair's initial work employed MIL-H-83282 fluid furnished by Messrs. Schwenker and Snyder of the Lubricants and Tribology Group, AFML, Wright-Patterson Air Force Base. The infrared absorption spectra of this fluid is shown in Figure 1.

As expected, the spectra indicates a largely hydrocarbon structure with, however, a small carbonyl component as indicated by the absorption band at 5.7 μ. At a later date, Mobile Oil and Royal Lubricants both succeeded in producing specification grade MIL-H-83282 fluid. Infrared absorption spectra of these two fluids are reproduced in Figures 2 and 3. It is apparent that although the Royal Lubricants' fluid closely resembles the original WADC fluid, the Mobile Oil fluid has a much higher ester content (note the larger intensity of the carbonyl absorption band at 5.7 μ of Figure 2 compared with those of 1 and 3).

2.3.2 Main Propellants

With the exception of the LO_2-impact tests, LN_2 was used to approximate the LO_2 temperature for all other portions of this program. All LN_2 and liquid hydrogen (LH_2) was government furnished. The LO_2 was obtained from Liquid Carbonics.

2.3.3 Orbital Maneuvering Propellants

Monomethyl Hydrazine
Nitrogen Tetroxide } specified by customer

The following propellants were purchased and used without further purification:

Monomethyl hydrazine, bp87°-89°C, MCB #8427 - Matheson Scientific Co.
Nitrogen tetroxide, 34 lb. lecture bottle, The Matheson Co., Newark, Ca.

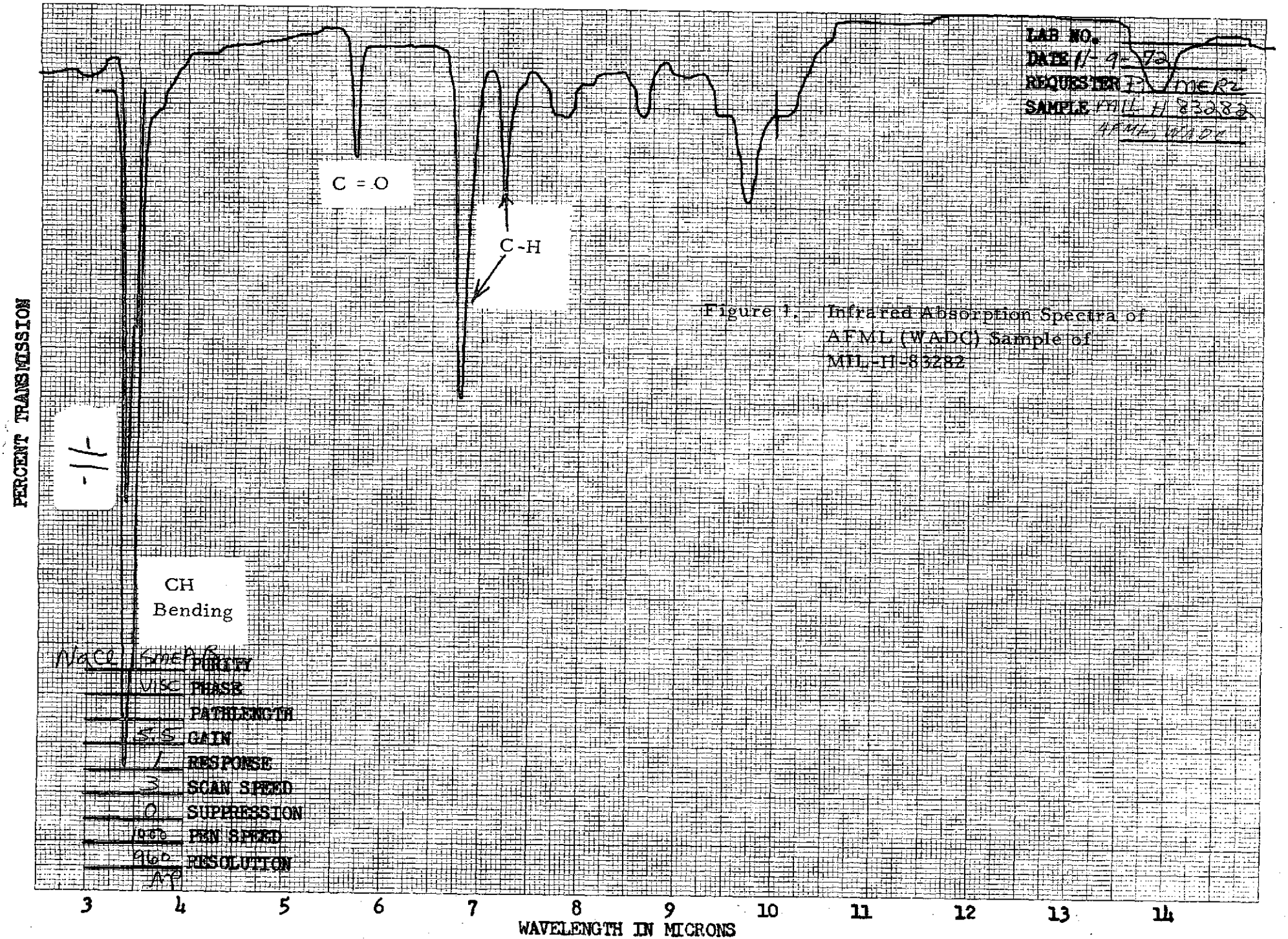

Figure 1. Infrared Absorption Spectra of AFML (WADC) Sample of MIL-H-83282

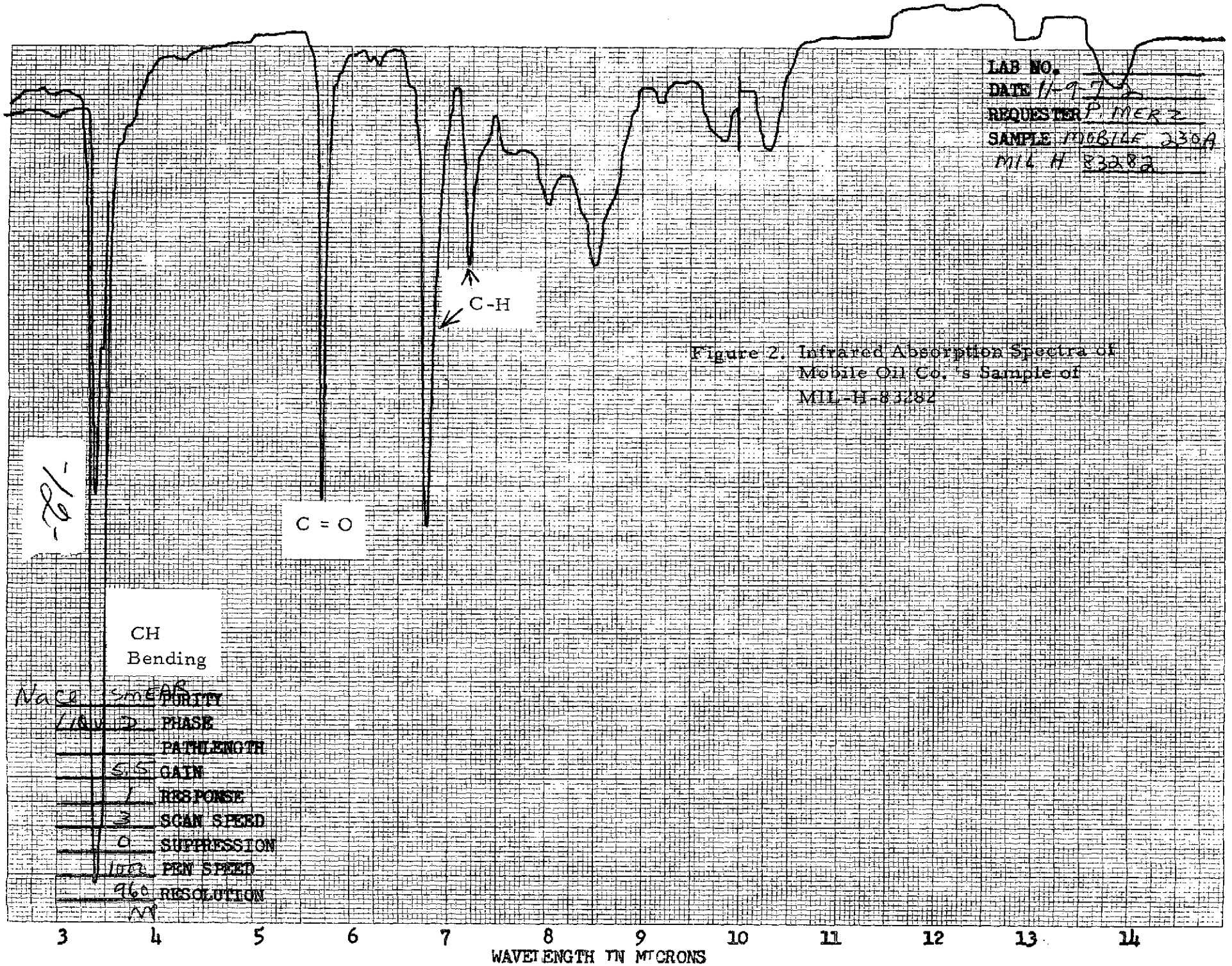

Figure 2. Infrared Absorption Spectra of Mobile Oil Co.'s Sample of MIL-H-83282

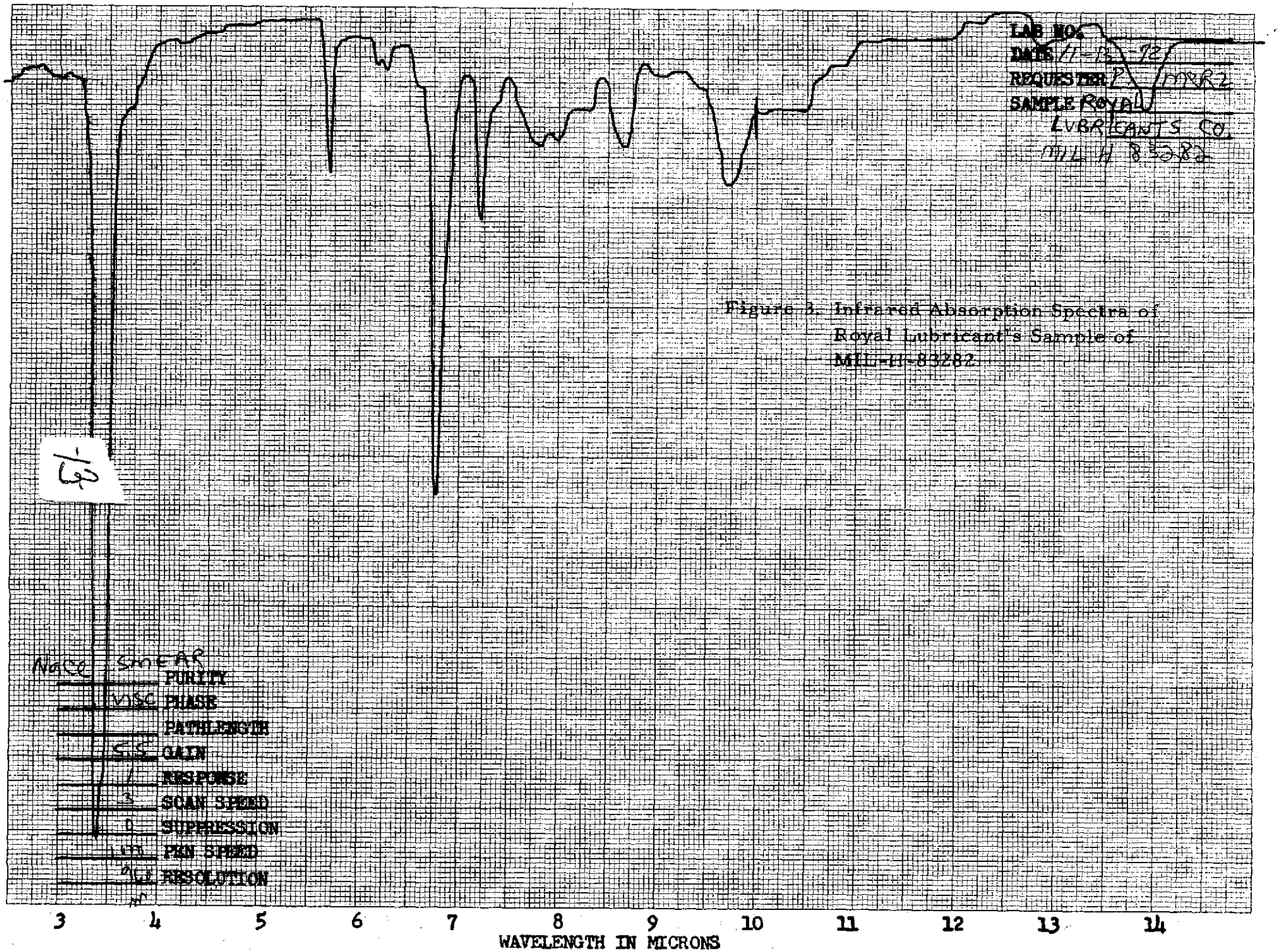

Figure 3. Infrared Absorption Spectra of Royal Lubricant's Sample of MIL-H-83282

SECTION 3

EXPERIMENTAL

3.0 General Plan

In the interest of efficiency and economy, tests were planned to screen out the least desirable seal candidates as quickly as possible. The most destructive tests were therefore performed early in the testing program. Subsequent tests were arranged in increasing order of complexity and cost. This elimination scheme worked reasonably well.

For example, the obviously unsuitable fluorosilicone and phosphazine fluoroelastomer #1884-34(A) were screened out by the first hydraulic system test (the high temperature hydraulic fluid compatability test). Similarly, all but two of the main propellent seal candidates were eliminated by the LO_2-impact test. Unfortunately, in some cases, seal candidates ostensibly satisfied all compatability and rheological requirements up to the end of the program, when they suddenly exhibited an unexpected mode of failure. Thus, the perfluoroelastomer (AF-E-124D) unexpectedly failed the dynamic sealability test at cryogenic temperatures and linear Tefzel O-ring similarly failed at 380K (220F) (Section 3.3.4).

3.1 Hydraulic Seals

3.1.1 High Temperature Hydraulic Fluid Compatibility

3.1.1.1 Experimental Methods

Three tensile specimens of each seal candidate were immersed in the test fluid contained in 38 by 300mm pyrex test tubes equipped with glass beads per ASTM D471-72. Test conditions were 200 hours at 422K (300F). A Blue M Magni Whirl oil bath was used as the constant temperature heat source.

3.1.1.2 Test Results

Tensile specimens of the three principal seal candidates (Viton ECD-3234 (black), fluorosilicone LS-2380, and phosphazine fluoroelastomer #1884-34) were tested for compatibility with samples of MIL-H-83282 hydraulic fluid furnished by AFML (WADC). The results are summarized in Tables 1 to 3.

As a check on the efficacy of Convair's molding and processing technique with these new rubbers, the engineering properties of cured tensile slabs submitted by the various vendors are included in the tables. In the case of the Viton and fluorosilicone rubbers, cured specimens made by the Convair process were used

Table 1. High Temperature Hydraulic Fluid Compatibility Test of Viton ECD-3234 (Black)

Conditions: 200 hours/422K (300F)/AFML MIL-H-83282 Hydraulic Fluid

Test Specimen Description	Ultimate Tensile Strength, MN/m^2	(psi)	Elongation, %	100% Modulus, (M100) MN/m^2	(psi)	Shore A Hardness		Instron Run No.
Viton ECD-3234 (Black)								
1. Virgin, DuPont Factory Slab	11.25	(1631)	190	5.04	(731)	78		4407
2. Virgin, DuPont Factory Slab	11.47	(1663)	190	5.24	(760)	78		4408
3. Virgin, DuPont Factory Slab	10.04	(1456)	170	5.14	(746)	78		4409
Average	10.91	(1583)	183	5.17	(740)	78		
1. Virgin, Convair Slab A	13.23	(1919)	190	5.94	(862)	78		4404
2. Virgin, Convair Slab A	11.85	(1718)	200	5.38	(780)	78		4405
3. Virgin, Convair Slab A	14.15	(2052)	180	6.28	(911)	78		4406
Average	13.22	(1917)	190	5.87	(851)	78		
						Upper	Lower	
1. 200 hr/422K/MIL-H-83282	6.65	(965)	140	4.21	(610)	74	70	4413
2. 200 hr/422K/MIL-H-83282	7.50	(1088)	160	3.93	(570)	74	71	4414
3. 200 hr/422K/MIL-H-83282	7.18	(1041)	160	3.85	(559)	74	72	4415
Average	7.11	(1031)	153	3.85	(559)			
Avg. gain (+) or loss (-)	-6.11	(-886)	-37	-2.01	(-292)	-4	-7	
Avg. % gain or % loss	-46		-19.5	-32		-5	-9	

Table 2. High Temperature Hydraulic Fluid Compatibility Test of Fluorosilicone LS-2380

Conditions: 200 hrs/422K (300F)/AFML MIL-H-83282 Hydraulic Fluid

Test Specimen Description	Ultimate Tensile Strength MN/m^2	Ultimate Tensile Strength (psi)	Elongation, %	100% Modulus, MN/m^2	100% Modulus, (psi)	Shore A Hardness	Instron Run No.
LS-2380							
1. Virgin, Dow-Corning Factory Slab	9.47	(1374)	200	3.98	(577)	70	4470
2. Virgin, Dow-Corning Factory Slab	9.46	(1372)	200	3.75	(544)	71	4471
3. Virgin, Dow-Corning Factory Slab	10.04	(1456)	210	3.94	(571)	70	4472
Average	9.66	(1401)	203	3.96	(574)	70	
1. Virgin, Convair Slab	7.85	(1138)	220	2.98	(432)	72	4410
2. Virgin, Convair Slab	8.24	(1195)	220	3.41	(494)	74	4411
3. Virgin, Convair Slab	8.86	(1285)	240	2.22	(467)	72	4412
Average	8.32	(1206)	227	3.20	(464)	73	
						Upper	Lower
1. 200 hr/300°F/MIL-H-83282	1.18	(171)	25		-	74	60-65 4416
2. 200 hr/300°F/MIL-H-83282	1.10	(159)	30		-	75	60-65 4417
3. 200 hr/300°F/MIL-H-83282	0.38	(55)	-		-	75	60-65 4418
Average	0.88	(128)	27		-		
Average gain (+) or loss (-)	-7.83	(-1078)	-200		-	+2	-10
Average % gain or % loss	-89.4		-88				

Table 3. High Temperature Hydraulic Fluid Compatibility
Test of Phosphazine Fluoroelastomer No. 1884-34

Conditions: 200 hours/422K (300F)/AFML
MIL-H-83282 Hydraulic Fluid

Test specimen Description	Ultimate Tensile Strength, MN/m^2	(psi)	Elongation, %	100% Modulus MN/m^2	(psi)	Shore A Hardness		Instron Run No.
Phosphazine Fluoroelastomer								
1. Virgin, factory slab, #1884-34	8.82	(1279)	150	3.05	(442)	65		4422
2. Virgin, factory slab, #1884-34	9.98	(1303)	130	3.68	(534)	70		4423
Average	8.90	(1291)	140	3.41	(495)	68		
1. Virgin, factory #1884-34(A)	5.81	(843)	200	2.14	(211)	66		4424
						Upper+	Lower+	
1. 200 hr/422K/MIL-H-83282*	1.51	(219)	270	.22	(33)	42	34	4419
2. 200 hr/422K/MIL-H-83282*	2.10	(305)	220	.26	(37)	46	38	4420
3. 200 hr/422K/MIL-H-83282*	1.43	(207)	240	.25	(36)	44	34	4421
Average	1.54	(224)	243	.24	(35)			
Avg. gain (+) or loss (-)	-7.36	(-1067)	+103	-3.17	(-460)	-25	-30	
Avg. % gain or % loss (-)	-82.6		+73.6	-92.3				

+ surface sticky

* MIL-H-83282 immersion specimens were #1884-34 stock

for the actual hydraulic fluid compatibility tests. In the case of the phosphazine fluoroelastomer, however, no uncured rubber was received, and the compatibility test was run on the cured tensile slabs fabricated by the vendor and furnished by NASA-Huntsville.

As Tables 1 and 2 indicate, Convair curing and post curing procedures yielded a strong high modulus Viton, but slightly weaker fluorosilicone. The most important result, of course, is that of the three rubbers tested; the Viton ECD-3234 (black) stock is the only promising seal rubber for these severe conditions. Even this Viton lost 46% of its tensile strength and nearly 20% of its ultimate elongation. Degradation involved softening (note the decrease in M_{100}) for all three candidates with the fluorosilicone, and the phosphazine rubbers losing virtually all engineering integrity. The catastrophic degradation of the fluorosilicone LS-2380 was particularly surprising, since fluorosilicones are known (Ref. 1) to retain their physical properties fairly well in contact with the older MIL-H-5606 hydraulic fluid even at 450K (350F) for up to 170 hours. Apparently, this new MIL-H-83282 hydraulic fluid is much more detrimental, at least to the fluorosilicone rubbers, than MIL-H-5606 fluid.

A second surprising degradative phenomenon was observed in these high temperature compatibility tests. With all three rubbers tested, the lower portions of the tensile dumbells were more severely degraded than the upper portions. This is borne out by the differences in hardness exhibited by the upper and lower portions of the same tensile dumbells after the 200 hour/422K immersion in the MIL-H-83282 hydraulic fluid. This hardness difference between the upper and lower portions of the tensile dumbells ranged from only ~3 Shore A points for the Viton to about 10 Shore A points for the fluorosilicone and phosphazine rubbers. In the case of these last two light-colored compounds, this vertical variation in the extent of degradation was clearly visible. There is no obvious reason for this vertical change in degradation. Both the temperature and the fluid composition were uniform top to bottom. One possible explanation is that the test procedure ASTM D471-72 specifies the use of glass beads as a bumper and the separation of the specimens. Accordingly, the lower part of the tensile dumbells are both slightly compressive loaded and in a region of restricted fluid circulation.

On the basis of this data, further testing of the fluorosilicone and the phosphazine fluoroelastomer as hydraulic system candidates was suspended. Alternate seal candidates, Viton E-60C (black) and Viton ECD-3234 (white) were substituted in their place. At about the same time, the first commercial samples of MIL-H-83282 hydraulic fluid were received from Mobile Oil Co. and Royal Lubricants, Inc. As already described in Section 2.3.1, infrared spectrometry indicated that the chemical composition of the Mobile Oil MIL-H-83282 fluid is significantly different from that of the original WADC fluid. Since

compatibility is a function of chemical composition, it was necessary to directly compare the effect of the Mobile fluid versus the WADC/Royal Lubricants' type of fluid on the subject seal candidates. For this reason, all three fluids were included in this second series of compatibility tests. In addition, since Convair's supply of WADC fluid was limited, it was desirable to minimize the amount of hydraulic fluid used per test. The majority of these new series of immersion tests were therefore performed using 2.54 by 30 cm test tubes, rather than the larger 3.8 by 30 cm test tubes specified by ASTM D3471. Instead of the glass bead spacers specified by D-3471, thin bent glass spacers similar to those used in the sealed tube compatibility tests of the Orbital Maneuvering seals (see Section 3.3.1 and Figure 45) were utilized.

The results of this second series of tests are tabulated in Tables 4 and 5. Table 4 summarized the compatibility data of the Viton E-60C (black) stock with all three hydraulic fluids. It is apparent that the Convair cured Viton was a slightly stronger, higher modulus stock than the factory (duPont) cured stock. Exposure to either the AFML fluid or to the Mobile Oil fluid results in ~30% loss in tensile strength and about a 10 to 15% loss in both ultimate elongation and 100% modulus.

Thus, as far as tensile peoperties are concerned, the MIL-H-83282 fluid produced by Mobile Oil is roughly comparable to the original fluid produced by AFML. By comparison, exposure to the MIL-H-83282 fluid produced by Royal Lubricants, Inc. resulted in a 50% loss in tensile strength, a 30% loss in ultimate elongation, and an 18% loss in 100% modulus. The Royal Lubricants' fluid, which spectrographically closely resembles the original AFML fluid, is much less compatible with the Viton E-60C than the Mobile fluid, which has a significantly higher ester content. Obviously, rubber compatibility cannot be predicted on the basis of the infrared spectra. One additional fact became apparent in these tests. Although all fluids experienced some discoloration during the 200 hour/422K exposure, the Royal Lubricant fluid exhibited the greatest darkening. This poorer(oxidative?) resistance of the Royal Lubricant fluid is tabulated in the left hand columns of Tables 4 and 5.

Table 5 summarizes the 200 hour/422K immersion data obtained with the ECD-3234 Vitons, both black and white stocks. As might be expected, the tensile properties of the virgin white ECD stock are lower than those of the virgin Black ECD stock, and both are slightly inferior to those of the black E-60C stock. For example, both the tensile strength and 100% modulus of the virgin Vitons decrease in the order: E-60C (black) > ECD-3234 (black) > ECD-3234 (white). Unlike the compatibility data obtained with Viton E-60C (black) (see Table 4), the Mobile Oil fluid is definitely less destructive to the ECD-3234 (black) stock than the AFML fluid. Immersion for 200 hours at 422K in the Mobile Oil fluid decreased the tensile strength of the ECD-3234 (black) stock by only 27%, whereas, the AFML fluid produced ~46% loss of strength. Similarly, the 100% modulus of this particular Viton was virtually unaffected by the Mobile Oil fluid, although suffering ~32% loss in the AFML fluid.

Table 4. High Temperature Hydraulic Fluid Compatibility of Viton E-60C (Black)

Conditions: 200 hours/422K (300F) Various MIL-H-83282 Hydraulic Fluids

Rubber Test Specimen	Type of Test Tube	Source of Hydraulic Fluid	Instron Run No.		Tensile Strength Newtons/m^2 in millions	(psi)	% Elongation at Break	Rubber Modulus (*) at 20% Newtons/m^2 in millions	(psi)	at 100% Newton/m^2 in millions	(psi)	Shore A Hardness	Hydraulic Fluid Appearance At Conclusion of Test
Virgin													
Convair Slab	none	none	4750		14.5	(2102)	200	.97	(141)	6.0	(875)	80	-
			4751		13.8	(2002)	170	1.34	(194)	6.9	(1000)	80	
				average	14.2	(2052)	185	1.15	(167)	6.5	(937)	80	
Factory Slab	none	none	4756		11.6	(1689)	190	1.38	(201)	5.8	(840)	80	-
			4757		11.3	(1650)	180	1.31	(190)	6.0	(864)	78	
			4758		11.4	(1659)	180	1.14	(188)	5.4	(784)	80	
				average	11.4	(1666)	183	1.21	(193)	5.7	(833)	79	
200 hr/422K/MIL-H-83282													
Convair Slab	2.54 cm diam.	AFML, WADC	4814		9.6	(1393.7)	170	1.12	(163)	5.2	(755)	72	clear, light
	bent glass		4815		9.1	(1323.5)	150	1.20	(175)	5.8	(837)	72	reddish-brown
	spacers		4816		10.1	(1476.2)	180	1.17	(170)	5.4	(786)	73	color
				average	9.6	(1397.8)	168	1.16	(169)	5.5	(793)	72	
		gain (+) or loss (-) of		average	-4.6	(-655.2)	-17	+0.01	(+2)	-1	-144	-8	
		% gain (+) or loss (-) of		average	-32	-32	-9	+1	+1	-15	-15	-10	
Convair Slab	2.54 cm diam.	Mobile Oil	4817		10.6	(1539.2)	165	1.30	(189)	5.65	(823)	75	clear medium
	bent glass		4818		10.2	(1492.2)	160	1.33	(193)	5.84	(848)	77	orange color
	spacers		4819		8.5	(1237.9)	140	1.30	(189)	5.67	(825)	75	
				average	9.8	(1423.1)	155	1.31	(190)	5.72	(832)	75	
		gain (+) or loss (-) of		average	-4.2	(-629.9)	-30	+.15	(+23)	-.80	(-105)	-5	
		% gain (+) or loss (-) of		average	-30	-30	-16	+14	+14	-12	-11	-6	
Convair Slab	3.8 cm diam.	Royal Lubricants	4820		6.0	(872.8)	115	1.11	(161)	5.2	(753)	72	dark carmine
	ASTM spec		4821		8.9	(1294.6)	150	1.09	(159)	5.5	(797)	71	color
	glass bead		4822		6.3	(912.0)	120	1.08	(158)	5.2	(750)	72	
	spacers			average	7.1	(1026.2)	128	1.09	(159)	5.3	(765)	72	
		gain (+) or loss (-)		average	-7.1	(-1026.8)	-57	-.06	(-8)	-1.2	(-172)	-8	
		% gain (+) or loss (-)		average	-50	-50	-31	-5.5	-5	-18	-18	-10	

(*) Rubber modulus = stress at indicated strain

Table 5. High Temperature Hydraulic Fluid Compatibility of Viton ECD-3234

Conditions: 200 hrs/422K (300F)/MIL-H-83282 Various Hydraulic Fluids

Rubber Test Specimen	Type of Test Tube	Source of Hydraulic Fluid	Instron Run No.	Tensile Strength Newtons/m^2 in millions	Tensile Strength (psi)	% Elongation at Break	Rubber Modulus (*) at 20% Newtons/m^2 in millions	Rubber Modulus (*) at 20% (psi)	Rubber Modulus (*) at 100% Newtons/m^2 in millions	Rubber Modulus (*) at 100% (psi)	Shore A Hardness	Hydraulic Fluid Appearance at Conclusion of Test
Virgin ECD-3234 (Black)												
Convair Slab	none	none	4404	13.2	(1919)	190	1.06	(155)	5.94	(862)	78	-
			4405	11.8	(1718)	200	1.32	(192)	5.38	(780)	78	-
			4406	14.1	(2052)	180	1.08	(157)	6.28	(911)	78	
			average	13.0	(1892)	190	1.15	(168)	5.86	(851)	78	
200 hr/422K/MIL-H-83282, ECD-3234 (Black)												
Convair Slab	3.8 cm diam.	AFML, WADC	4413	6.65	(965)	140	0.62	(89.8)	4.21	(610)	72	clear, reddish-
	ASTM spec.		4414	7.50	(1088)	160	0.92	(133.6)	3.93	(570)	73	brown color
	glass bead		4415	7.18	(1041)	160	0.93	(135.0)	3.85	(559)	73	
	spacers		average	7.04	(1021)	153	0.82	(119.4)	4.00	(579)	73	
		average gain (+) or loss (-)		-5.96	(-876)	-37	-.33	(-48.6)	-1.86	(-272)	-5	
		average % (+) or loss (-)		-46	-46	-19.5	-28.7	-28.9	-31	-32	-6	
Convair Slab	2.54 cm diam.	Mobile Oil	4826	9.24	(1341.4)	145	1.23	(178)	5.53	(802)	72	darker medium
	bent glass		4827	9.71	(1409)	155	1.19	(173)	6.02	(874)	72	orange color
	spacers		4828	9.96	(1445.2)	160	1.19	(173)	5.91	(858)	72	(similar to Mobile Oil
			average	9.64	(1398.5)	153	1.20	(175)	5.82	(845)	72	test on E-60C in Table 4
		average gain (+) or loss (-)		3.36	(-519)	-37	+.05	(+7.0)	-.04	(-6)	-6	but darker)
		average % (+) or loss (-)		-26	-27	-19.5	+4	+4	-0.7	-0.7	-7	
Virgin ECD-3234 (White)												
Convair Slab	none	none	4398	9.49	(1377)	200	1.20	(175)	5.42	(787)	75	-
			4399	10.0	(1458)	200	1.32	(191)	5.78	(838)	75	
			4400	8.12	(1178)	190	1.22	(177)	4.53	(657)	75	
			average	9.20	(1338)	197	1.25	(181)	5.24	(761)	75	
200 hr/422K/MIL-H-83282, ECD-3234 (White)												
Convair Slab	2.54 cm diam.	Royal Lubricant	4823	7.33	(1063.2)	165	.93	(135)	4.55	(660)	70	dark carmine color
	bent glass		4824	7.73	(1121.5)	170	.99	(143)	4.72	(685)	71	
	spacers		4825	7.97	(1156.2)	170	.99	(144)	4.86	(705)	70	
			average	7.67	(1113.6)	168	.97	(140)	4.71	(683)	70	
		average gain (+) or loss (-)		-1.53	(-224.4)	-29.7	-.28	(-41)	-53	(-78)	-5	
		average % (+) or loss (-)		-17	-17	-14.6	-23	-23	-10	-10	-.7	

(*) Rubber modulus = stress at indicated strain

Unfortunately, in the interest of economy, the Viton ECD-3234 (white) stock was tested only in the Royal Lubricant fluid. The Royal Lubricant fluid was, of course, selected because it was presumed to be equivalent to the AFML fluid on the basis of the infrared spectrographic data. Only a modest loss in tensile strength (-17%), elongation (-16%), and 100% modulus (-10%) occurred. Strangely, the 20% modulus decreased by 23%. This is unique. In all other stocks tested, the 20% modulus always decreased less than the 100% modulus. In fact, in two cases, the E-60C (black) and the ECD-3234 (black), both immersed in Mobile fluid, the 20% modulus actually increased.

3.1.1.3 Discussion

It is apparent that as far as high temperature compatibility with rubber Viton seals is concerned, there is not one MIL-H-83282 hydraulic fluid, but at least three different fluids, depending upon the precise manufacturer. To add to the confusion, not only is there no obvious correlation between the high temperature rubber compatibility of the three tested fluids and their chemical composition (as evidenced by infrared spectrometry), but the data obtained in this program suggest that the compatibility rank (or rating) of the fluids change on going from one Viton black rubber to another. For example, although the MIL-H-83282 fluids manufactured by the Mobile Oil Co. and by WADC both attack Viton E-60C (black) specimens equally; the Viton ECD-3234 (black) specimens were attacked much more severely by the WADC fluid than by the Mobile fluid.

In spite of these confusing aspects of the present data, the best overall retention of properties against high temperature MIL-H-83282 fluid is exhibited by the ECD-3234 (white) stock. The lower physical properties exhibited by the virgin 3234-(W) specimens are less important than the absence of large changes in physical properties upon exposure to the hot MIL-H-83282 fluid.

The catastrophic degradation of the fluorosilicone LS-2380 and the phosphazine fluoroelastomer #1884-34 would appear to remove them from further consideration. Unfortunately (see Section 2.1), the phosphazine #1884-34 stock available to this program was a poor representative of the present phosphazine fluoroelastomer technology. Data obtained from Dr. Reynard of Horizons, Inc. (Reference 2) indicated that the current generation of phosphazine fluoroelastomers possess good high temperature compatibility with MIL-H-83282 fluid. This data is summarized in Appendix C. In view of their excellent low temperature properties [glass transition temperature, Tg = 203K (-94F)], these new phosphazine fluoroelastomer vulcanizates should be included in any further hydraulic seal development program.

3.1.2 Thermal Cycling of Hydraulic Seal Candidates

3.1.2.1 Experimental Methods

Three tensile specimens of each of the subject seal candidates were sealed in pyrex glass capsules containing MIL-H-83282 hydraulic fluid. Each capsule had a 1.8mm (0.043 in.) diameter drilled-hole located on the upper shoulder through which a fine thermocouple was threaded. A photograph of a typical thermocoupled, pyrex vial containing three dumbell specimens is shown in Figure 4. The glass ring at the top enabled the capsule to be securely suspended via a fine steel braided cable from the arm of a programmed, mechanical "dipping" machine with a 68.6 cm (27 in.) vertical stroke. As the arm of the dipping machine alternately lowered and raised, the pyrex vial was alternately immersed into a constant temperature, refrigerated bath and then drawn up into a preset, constant temperature, Marshall tube furnace. The internal temperature of the thermocoupled specimen capsule was monitored continually via a Leeds and Northrup, Type G recorder. Freon-MF (i.e. fluorotrichloromethane, bp 296.8K (74.9F); m.p. 162K (-168F) served as the non-flammable, volatile refrigerated bath medium. This refrigerated bath was controlled at 216K (-70F). Originally, the temperature of the Marshall furnace was manually controlled via a variac. Although a constant temperature could be maintained at 504K (450F) over short periods of time (i.e., 2 to 4 hours), the furnace temperature tended to drift over longer periods of time (i.e., 1 to 2 days). This drifting was eliminated by controlling the heater input via a Foxboro potentiometer controller coupled to the furnace thermocouples.

Use of this 216K heat sink and the 504K heat source resulted in a 46 minute temperature cycle from 233K (-40F) to 422K (300F). Of the 46 minutes, 19 minutes was spent in heating the specimen vial and 27 minutes in cooling. A typical thermal cycle recorder trace is shown in Figure 5.

3.1.2.2 Test Results

Tensile specimens of the three most promising hydraulic seal candidates [Viton ECD-3234 (black), Viton E-60C (black), and Viton ECD-3234 (white)] were thermally cycled 200 times between 233K (-40F) and 422K (300F) by means of the automatic dipping machine. Results of these thermal cycling tests are summarized in Table 6. The first stock [ECD-3234 (black)], was cycled in the original sample of MIL-H-83282 hydraulic fluid obtained from AFML (WADC). Due to the short supply of this WADC fluid, the remaining two Viton stocks, E-60C (black) and ECD-3234 (white), were cycled in the fluid produced by Royal Lubricants, Inc. The Royal Lubricants fluid was chosen as the most likely commercial successor to the AFML fluid on the basis of its infrared spectra, as explained earlier. Subsequently, the high temperature hydraulic fluid compatibility tests of 3.1.1.2

Figure 4.

GENERAL DYNAMICS
Convair Division

PYREX SPECIMEN-CAPSULE FOR THERMAL CYCLING STUDIES

Viton ECD-3234 (White) Tensile Dumbbells in MIL-H-83282 Hydraulic Fluid

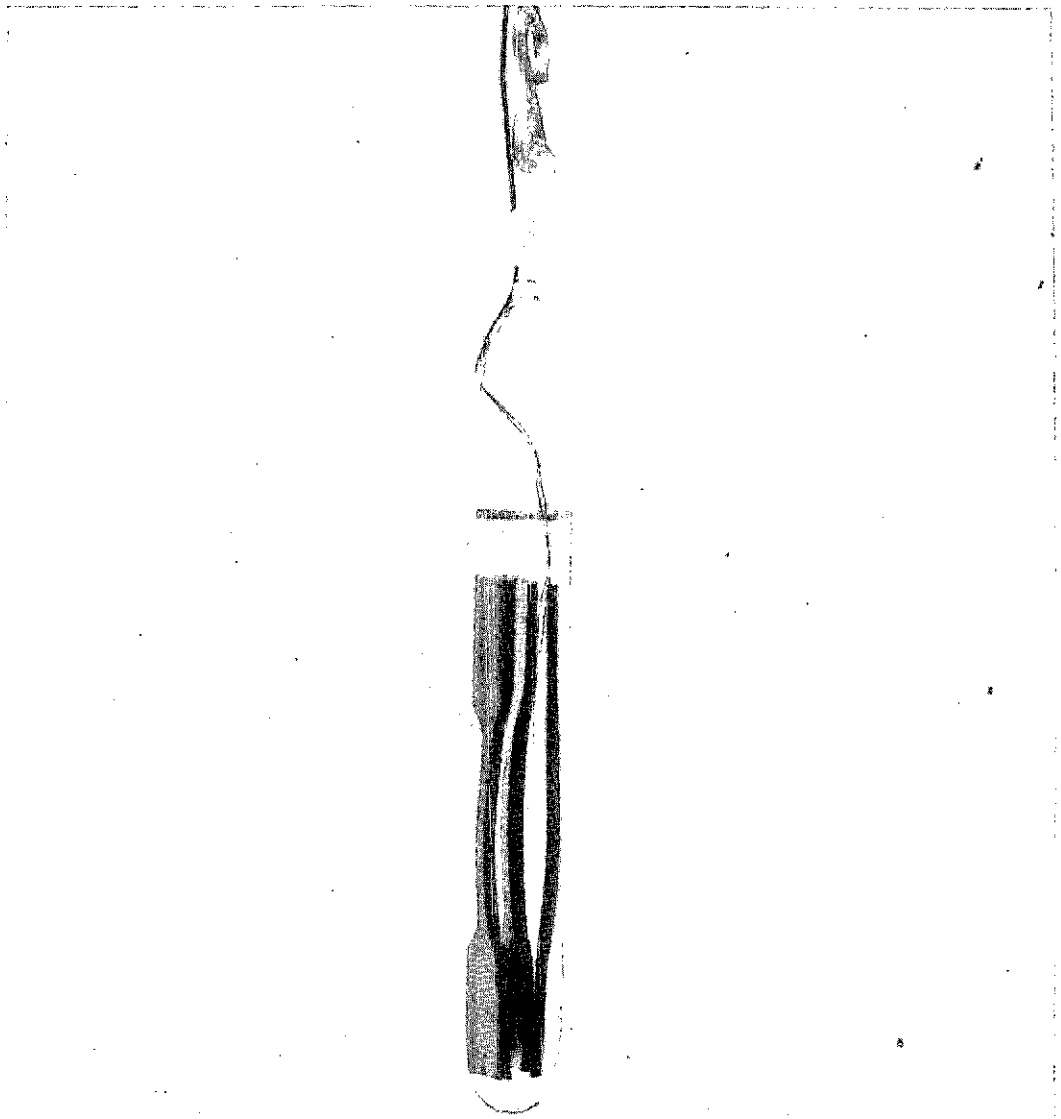

30074CVE5764

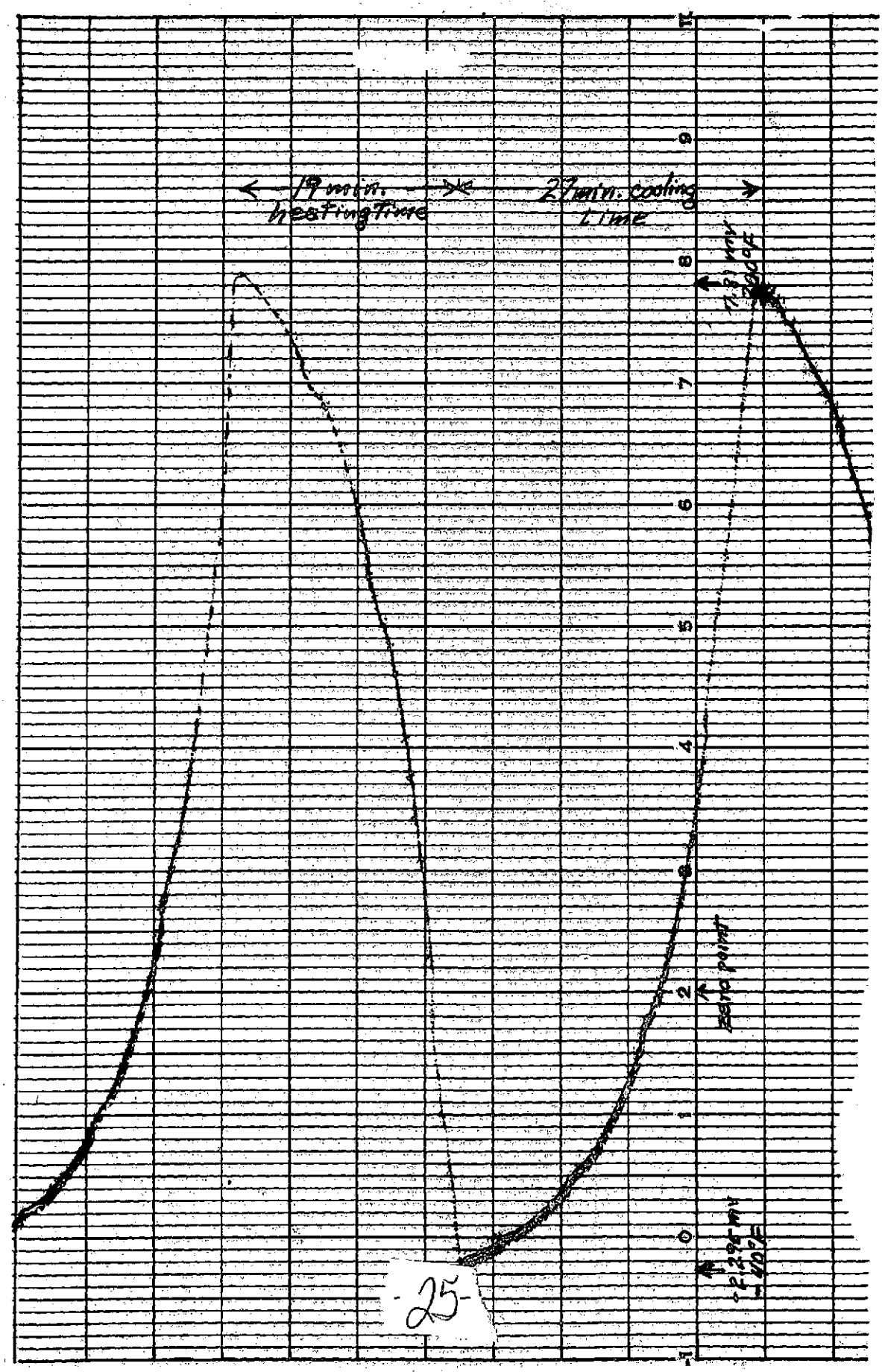

Fig. 5. Recorder Trace of Thermal Cycling of Viton E60-C (Black) Specimen in MIL-H-83282 Fluid

Table 6. Thermal Cycling of Seal Candidates in MIL-H-83282 Hydraulic Fluid

Conditions: 200 cycles/-40° F to 300° F
MIL-H-83282 Hydraulic Fluid

Rubber Compound	Instron Run No.	Tensile Strength Newtons/m^2 in Millions	Tensile Strength (psi)	% Elongation at Break	Rubber Modulus (*) at 20% Newtons/m^2 in Millions	Rubber Modulus (*) at 20% (psi)	Rubber Modulus (*) at 100% Newtons/m^2 in Millions	Rubber Modulus (*) at 100% (psi)	Shore A Hardness
Viton ECD-3234 (Black)									
Virgin (avg)	4404-4406	13.1	(1917)	190%	1.16	(168)	5.86	(851)	78
Cycled in WADC fluid	211	9.4	(1362)	157.5	1.03	(149)	5.34	(775.4)	75
	212	10.9	(1582)	170.	.99	(144)	5.49	(795.8)	77
	213	10.7	(1558)	170	1.00	(145)	5.79	(841.8)	76
	Average	10.3	(1500)	168.8	1.01	146	5.55	(804.3)	77
	Average loss (-)	-2.9	(-417)	-24.2	0.15	-22	-0.31	(-46.7)	-1
	Average % loss	-22%	-22%	-13%	-13%	-13%	-5.3%	-5.5%	-2%
	Range of % loss	-17% to -28%		-11% to -17%	-11% to -14.6%		-1.3% to -9%		
Viton E-60C (Black)									
Virgin (avg)	4750-4751	14.1	(2053)	185	1.15	(167)	6.5	(937)	80
Cycled in Royal Lubricants Inc. Fluid	214	9.3	(1359)	140	1.06	(154.5)	5.96	(865.6)	78
	215	12.3	(1796)	180	1.25	(182.9)	6.34	(920.)	79
	216	5.1	(753)	109	.99	(144.0)	4.95	(719.8)	70
	Average	8.9	(1305)	143	1.10	(160.4)	5.75	(835.1)	77
	Average loss	-5.2	(-148)	-42	-.05	(-6.6)	-0.75	(-101.9)	-3
	Average % loss	-36%	-36%	-23%	-4%	-4%	-11.5%	-11%	-4%
	Range of % gain (+) or % loss (-)	-64% to -13%	-63% to 13%		+8.7% to -14%		-2.5% to -24%		
Viton ECD-3234 (White)									
Virgin (avg)	4398-4400	9.2	(1338)	197	1.24	(181)	5.25	(761)	75
Cycled in Royal Lubricants Inc. Fluid	217	8.79	(1275)	165	.95	(138)	5.67	(823.2)	75
	218	8.39	(1218)	164	.95	(138)	5.66	(821)	74
	219	9.59	(1391)	170	.99	(145.4)	6.35	(924.2)	76
	Average	8.92	(1295)	166.3	.96	(140.4)	5.89	(856.1)	75
	Average gain or loss	-0.28	-43	-30.7%	0.28	-40.9	+0.64	+95	0
	Average % gain or loss	-3%	-3%	-16%	-23%	-23%	+12%	+12%	0%
	Range of % gain (+) or % loss (-)	+4% to -9%	-	-14% to -17%	-19% to -23 1/2%		+8% to +21%		

*Rubber modulus = stress at indicated strain

cast doubt on the practical significance of this infrared spectra similarity. Fortunately, this latter high temperature (200 hour/422K) compatibility data summarized in Tables 4 and 5 offers a direct comparison with the thermal cycling data of Table 6.

Attempts to compare and evaluate the data of Table 6 with Tables 4 and 5 are complicated by the poor checking results obtained from within any single group of black Viton tensile specimens. For example, although the Viton E-60C (black) stock suffered an average loss of 36% tensile strength in the thermal cycling tests, the actual measured losses ranged from 64% to 13% (see Table 6). This wide variation of test results is excessive even for accelerated aging experiments. In general, the thermal cycling data displays wider variations than does the constant 422K compatibility data.

Fortunately, the data obtained with the ECD-3234 (white) stock was more consistant and quite satisfactory for analytical purposes. In spite of the above complications, a simple comparison of Table 6 with Tables 4 and 5 discloses that the three Viton seal candidates degraded in the same order in both the thermal cycling tests and the 200 hour continuous 422K (300F) test, with the E-60C (black) stock suffering the greatest degradation, and the ECD-3234 (white) stock degrading the least. In addition, the extent of this degradation was much greater in the constant 422K (300F) compatibility tests than in the thermal cycling tests. The loss in tensile strength in the latter test ranging from 1/5 for the ECD-3234 (white) stock to 3/4 for the E-60C (black) stock of the tensile loss suffered in the constant 422K (300F) test. Thus, the tensile strength of the E-60C (black) compound decreased by 36% after 200 cycles between 233K and 422K compared with a 50% decrease after 200 hours' continuous immersion at 422K. The ECD-3234 (black) stock showed even greater differences in degradation produced by these two different tests.

It is not surprising that the 200 hour/422K compatibility test was more destructive than the thermal cycling tests. What is surprising is that the thermal cycling test would produce as much degradation as it did. Polymer degradation is the result of chain scission versus chain crosslinking reactions. Both reactions are accelerated by higher temperatures. In the thermal cycling tests, the specimen is at the 422K (300F) temperature for only 1 to 2 minutes, and only above 366K (200F) for 12 to 15 minutes. The total 422K exposure, therefore, amounts to ~400 minutes or 6.7 hours. If we make the reasonable assumption that little or no degradation of Viton occurs at temperatures below 366K (i.e., 200F), the total time for degradation to occur will be 6.7 hours at 422K plus 50 hours at 366K to 420K. Little is known concerning either the nature of Viton degradation reactions or of the temperature coefficient of these reactions at elevated temperatures (Note 1). If, however, the old crude approximation is used that organic reaction rates often double for every 10K rise in temperature, then the degradation rate at 366K will be only $1/(2)^6$ or 1/64 of the rate at 422K. On this basis,

Note 1: In an analogous situation, Casgarea (Reference 3), found that the degradative mechanism of NBR O-rings changed markedly between 353K (176F) and 373K (212F).

the integrated effect of the 50 hours' residence time between 366K and 420K should produce approximately as much degradation as 2 hours at 422K. Obviously, the extent of degradation observed in these temperature cycling studies was far greater than would be obtained after less than 9 hours (i.e., ~6.7 hours plus 2 hours) immersion in MIL-H-83282 fluid at 422K (300F).

In the preceding discussion, decrease in tensile strength was used as a measure of degradation. In many degradative studies of seal rubbers, the ultimate elongation (i.e., elongation at break) has been found to be a truer measure of the degradation (References 3 and 4). On a percentage basis, the ultimate elongation of the two black Vitons did not suffer as great a decrease as did the tensile strengths. The measured elongations of all three candidate Vitons was about the same after the 200 thermal cycles as it was after 200 hours of continuous immersion at 422K.

From a practical point of view, modulus is probably more important than either the tensile strength or ultimate elongation. More rubber articles fail due to changes in modulus than fail due to changes in ultimate elongation and tensile strength combined. The E-60C (black) and the ECD-3234 (white) specimens decreased much more (~30% loss) under the constant 422K conditions than under thermal cycling conditions (-13% of M_{20} and -5% of M_{100}). It must be remembered that the ECD-3234 (black) specimens were thermal cycling in fluid produced by WADC, whereas the other two Vitons were thermal cycling in fluid produced by Royal Lubricants Inc.. It is also possible that changes in compatibility test conditions may not produce exactly the same degradative changes using the different MIL-H-83282 fluids.

3.1.2.3 Discussion

The results obtained in these thermal cycling experiments substantiates the earlier results obtained in the high temperature hydraulic fluid compatibility tests. Of the three Vitons tested to date, the non-carbon filled Viton, ECD-3234 (white), showed the best retention of properties under both the 200 hours at 422K exposure, and the thermal cycling exposure in MIL-H-83282 hydraulic fluid. The two filled (carbon black) Vitons, by contrast, suffered much greater losses of physical properties under the same conditions. In addition, the extent of degradation suffered by the black stocks varied widely from specimen to specimen under identical exposure conditions. Although all stocks degraded about twice as much during the 200 hour exposure to MIL-H-83282 hydraulic fluid at 422K (300F) than under 200 thermal cycles between 233K and 422K in the same hydraulic fluid, the extent of degradation occurring under the thermal cycling test is far greater than would be expected from a mere time/temperature phenomena. It is possible that the unexpectedly severe degradation occurring under thermal cycling conditions was due to a larger supply of atmospheric oxygen inside the specimen capsule. The test capsule was not hermetically sealed and the 1.8 mm diameter thermocouple hole permitted the capsule to "breathe" due to volume changes of the capsule atmosphere which accompanied the 189K temperature change during thermal cycling.

The amount of oxygen available to the fluid immersed rubber specimens could thus have been far greater than that available to the loosely stoppered high temperature compatibility specimens run at a constant temperature of 422K (300F).

3.1.3 Cyclic Load Deflection

Hydraulic system seal candidates were selected primarily for their oil resistance, creep resistance at 422K (300F), and resiliance/compliance at 233K (-40F). Actually, the most critical factor for sealability is stress decay. Stress decay is a complex function of viscoelasticity (i.e., viscous flow plus physical stress relaxation) at lower temperatures and chemical reactions (such as a combination of scission and crosslinking) at the higher temperatures. It will, therefore, be affected by both the geometry of the test specimen (which determines the stress distribution), the test temperature, the type of elastomer and its curing system, and upon the test conditions, whether static or dynamic. Since dynamic seal applications are not only numerous but historically have presented the most important failure modes, a large portion of this program involved dynamic testing of O-ring specimens. These dynamic tests include all or part of the following properties:

1. Cyclic load bearing properties
2. Cyclic work and hysteresis
3. Indicated modulus

3.1.3.1 Experimental Methods

Cyclic load deflection measurements were first performed using a military specification hydraulic, size -224 , O-ring face gland mounted on the compression/deflection test fixture shown in Figure 6. Load and readout were supplied by an Instron tester at zero chart speed. The O-ring was cycled successively from 1.81 Kg (4 lb.) to 68.7 Kg (170 lb.) load. This load produced 22% (0.032 in.) compression in the size -224 O-ring. Each compression/deflection cycle, with the exception of the first cycle, were precisely alike. The raw Instron cyclic load deflection measurements for the first 75 cycles of the first Viton E-60C O-ring at room temperature are shown in Figure 7. Since each successive trace contributed a finite pen width to the composite trace, the chart was advanced a short distance after each 5 cycles.

Although closed-loop hysteresis type curves shown in Figure 7 graphically illustrate the low and constant hysteresis as well as the absence of any significant compression set, it is difficult to obtain accurate quantitative measurements of either the compressive modulus or the hysteresis from them. Since these Instron stress-strain curves are the basis of all data generated from the cyclic load deflection experiments in this program, it was decided to magnify the stress component of the stress-strain curve by running the recording chart during the

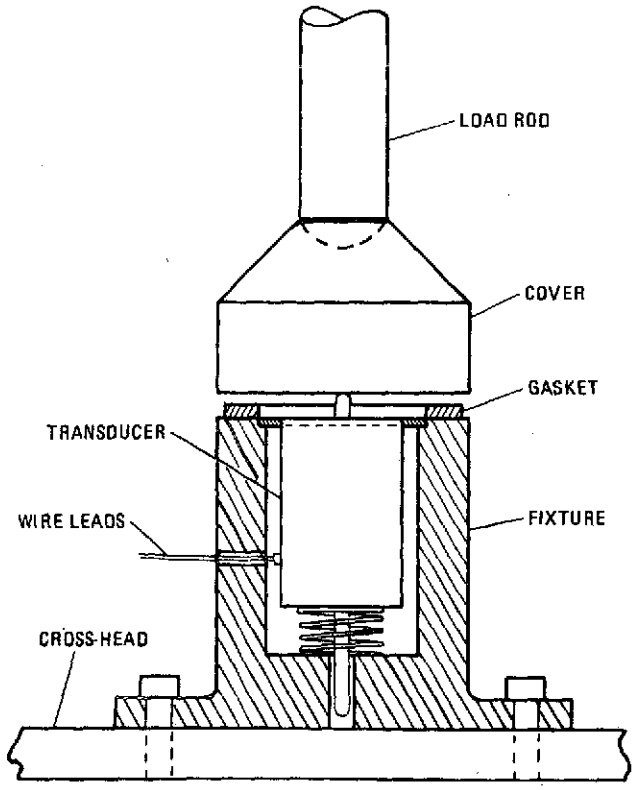

Figure 6. Compression vs. deflection test fixture.

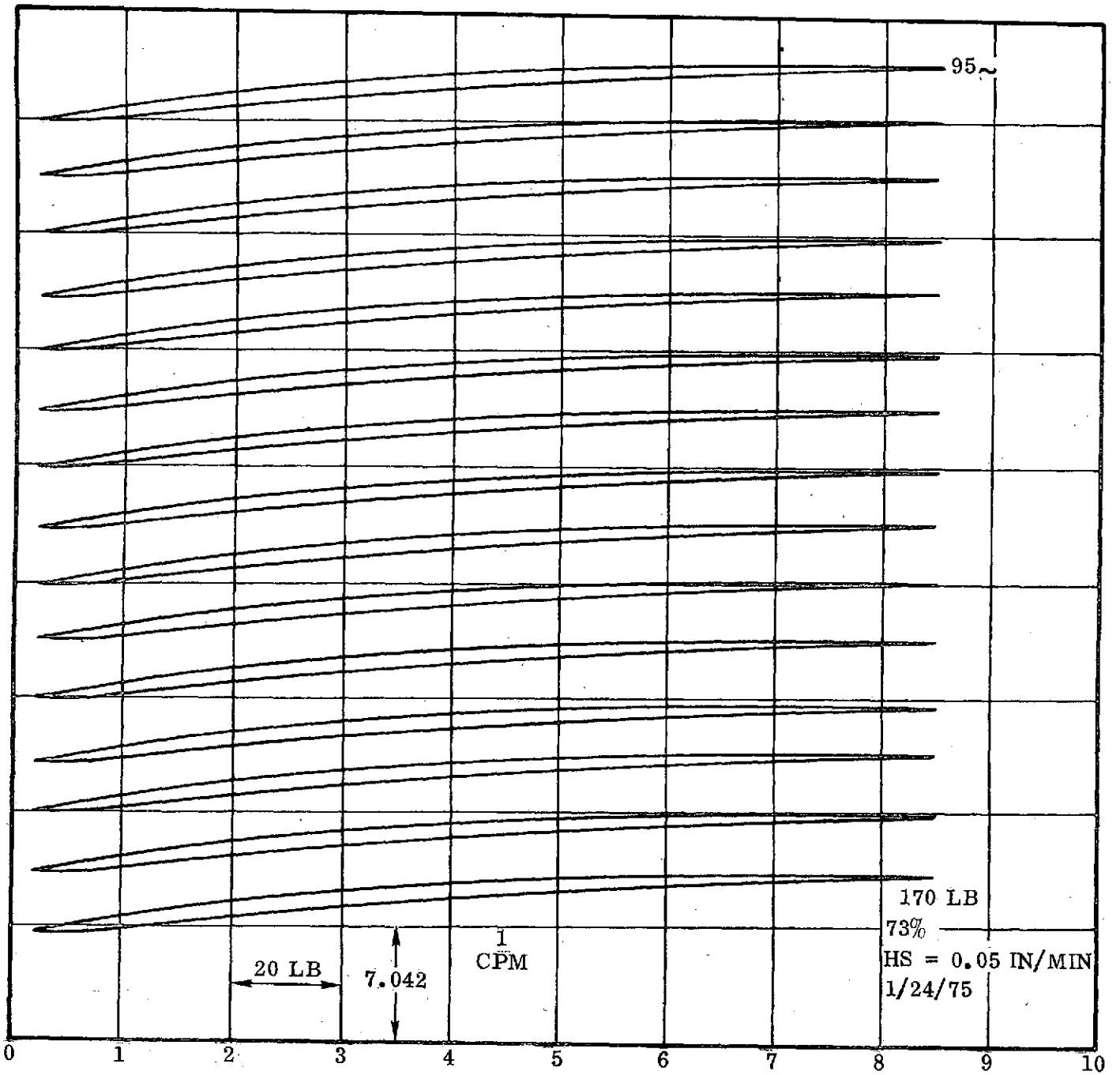

Figure 7. Instron Cyclic Load Deflection Curves at 296K (73F) on Viton E-60C, O-ring (Black) #2 Chart Speed = zero

compressive cycling. This changes the shape of the stress-strain curve from a closed-loop to an open cusp. Although the "cusp" shaped curve does not offer an obvious graphical representation of such features as the cyclic hysteresis which the closed-loop curve does, the "cusp" does permit accurate magnification of the entire stress-strain cycle through the simple expedient of increasing the chart speed. This is illustrated by Figures 8 through 10 which show stress-strain curves of Viton E-60C (black), size (-224) O-rings (under the same compressive cycles) with the chart speeds adjusted to 1.27 cm (0.5 in.)/min., 2.54 cm (1 in.)/min., and 12.7 cm (5 in.)/min., respectively. This last speed appeared to give optimum results, and this 5 in/min. chart speed was therefore employed as three O-rings of each of the three hydraulic seal candidate rubbers [Viton E-60C (black), Viton ECD-3234 (black), and Viton ECD-3234 (white)] were compression cycled 200 times at each of the following temperatures: 296K (73F), 422K (300F), and 233K (-40F). In each case, the 0.340 cm (0.134 inch) thick O-ring was compressed to 0.267 cm (0.105 inch), i.e., to 22 percent compression, by cycling the Instron compression head at the rate of 0.127 cm (0.05 inch) per minute, to within 0.0127 cm (.005 inch) of the (-224) military O-ring face seal gland.

Figure 10 is typical of the Instron stress-strain type curves obtained with all three different Viton rubber O-ringscompression cycled at 296K(70F). Moreover, very similar curves were obtained at 422K (300F). It was apparent from the shape of the curves and the height of the cusps at 296K and 422K that the dynamic-mechanical response of the various O-rings was unaffected by the amount of compressive cycling used in this program. However, this does not mean that these Viton O-rings do not exhibit "stress softening" (i.e., thixotropy) during the preliminary compression cycles, but rather that these O-ring specimens underwent sufficient compressive cycling during the preliminary manipulations so that the thixotropy initially present was reduced to negligible proportions before the first cycling measurements were started [the Instron head travel is adjusted so as to move downward to within exactly 5 mils (0.0127 cm) (as measured by "feeler gages") of the face of the O-ring gland. During these adjustments the O-ring is compressed several times]. See the first 10 stress-strain cycles of the Viton E-60C O-rings in Figures 8 and 9.

At 233K (-40F), compression cycled Vitons exhibit a radically different type of behavior. At 233K, all three types of Viton seal candidates are in the leatherby region rather than in the rubbery region. This leathery region is characterized by a great increase in all rheological parameters, including load bearing at 22% deflection, compressive work (energy) on both the loading and unloading cycles, cyclic hysteresis, and "indicated" modulus. The most striking manifestation of this fundamental change in rheological behavior is that the compressive force required to produce the desired 22% deflection decreases steadily during the compression cycling. Figure 11 shows typical stress-strain curves of the first 37 compression cycles at 233K of a typical Viton E-60C (Black) O-ring. The steady decay in maximum compressive forces (i.e., cusp height) is strikingly apparent.

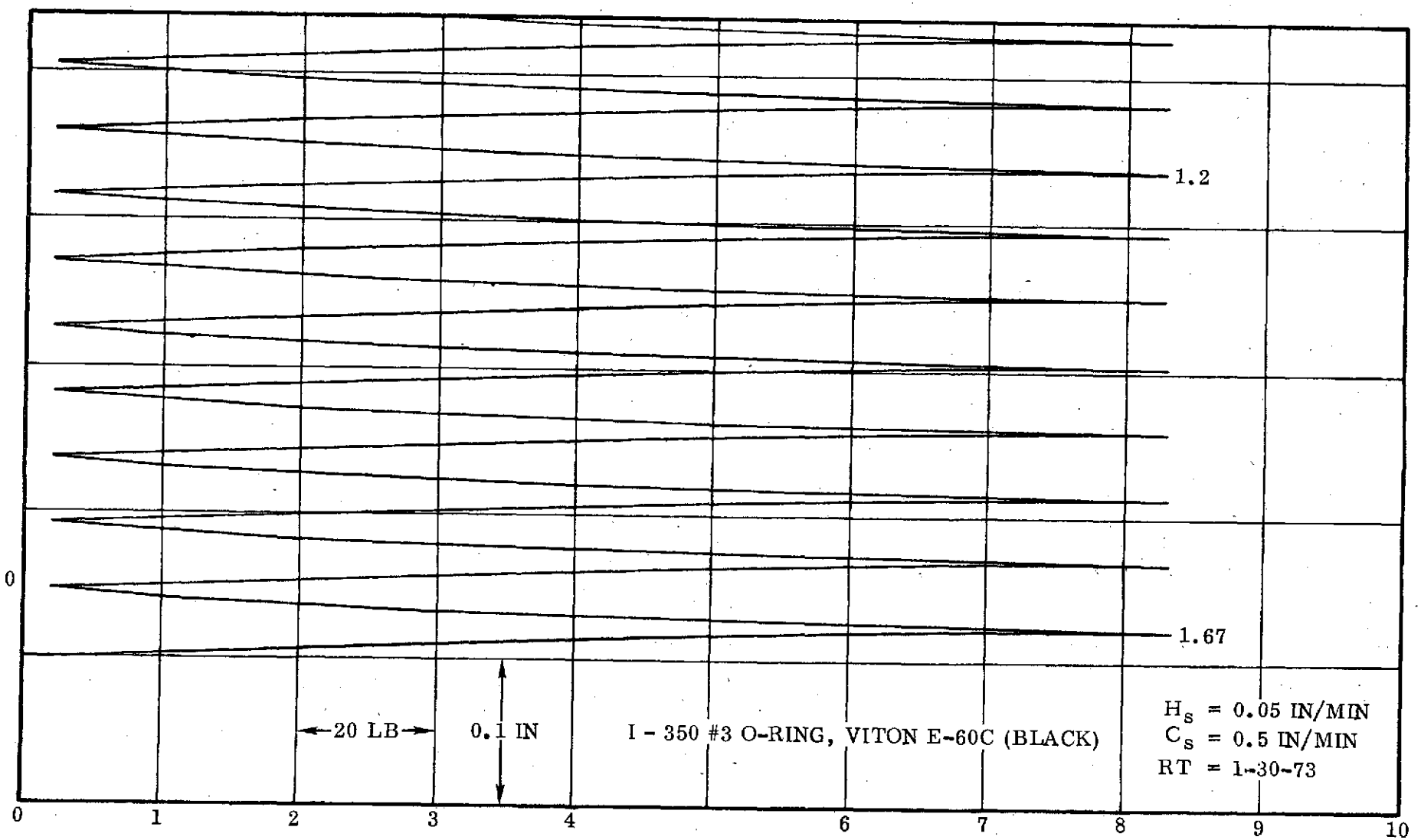

Figure 8. Instron Cyclic Load Deflection Curves at 296K (73F) on a Viton E-60C, O-ring
Chart Speed = 0.5 in./min.

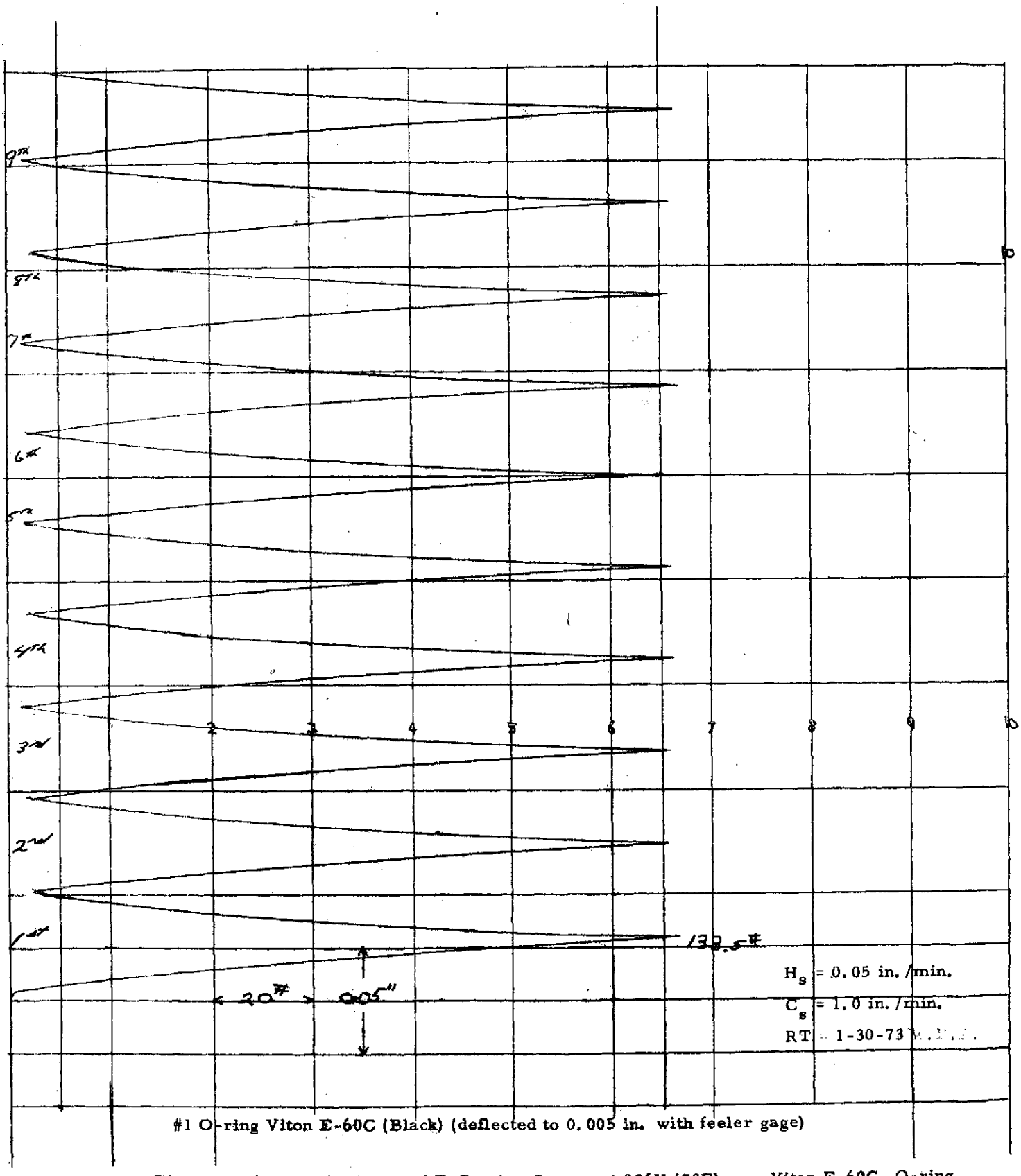

#1 O-ring Viton E-60C (Black) (deflected to 0.005 in. with feeler gage)

Figure 9. Instron Cyclic Load Deflection Curves at 296K (73F) on a Viton E-60C, O-ring
Chart Speed = 1.0 in./min.

Page intentionally left blank

Page intentionally left blank

3.1.3.2 Cyclic Load Bearing Properties

The load bearing stress of the subject Viton O-rings at 22% strain applied force (max.) is indicated by the height of the stress-strain cusps in the Instron cyclic load deflection curves. Any dynamic compression set (or creep), transient or permanent, which occurred during the dynamic compression cycling will be indicated as a decrease in the height of these stress-strain cusps. Although the individual cusp heights are readily determined, and although at 293K and 422K this height is consistent for almost every Viton O-ring throughout each complete 200 cycle run, checking results between different runs even on the same O-ring are often difficult to obtain. This is due to the shape factor. The force required to compress an O-ring increases exponentially with an increase in compression. A small variation in compression therefore, will produce large variations in the measured force. As previously mentioned in these experiments, the Instron compression head (anvil) was cycled to within 0.127 mm (0.005 inches) of the O-ring test gland using "feeler" gages to determine the distance. Since the Instron tester is a precise instrument, each series of successive compressions will be identical however, the initial compression adjustment will depend on the skill of the technician operating the Instron. For example, the 293K (73F) cyclic load deflections of three Viton E-60C O-rings shown in Table 7 was the result of measurements by two operators on three different days. Cycles 1 through 5 of O-ring specimens #1 and #2 were performed the same day by Operator #1. Cycles 25 through 100 on specimens #1 and #3 were produced by Operator #2 another day, as was cycles 1 through 5 on specimen #3. Operator #2 produced cycles 25 through 100 of specimen #2 on a third day. In spite of these operator variances, the average load per lineal length of these -224 size O-rings amounted to:

$$\frac{69.1 \text{ kg}}{15 \text{ cm}} = 4.6 \times 10^3 \text{ g/cm (25.8 ppi)}$$

with a range of: 4×10^3 to 5×10^3 g/cm (22.4 to 28.2 ppi)

Parker Seal Co. has published the results of similar studies on Buna-N O-rings. Parker found the load per lineal inch of seal ranged from 9.1 to 40 ppi for all O-ring compounds undergoing 20% compression, and a 18 to 92 ppi range for 30% compression. Interpolating between these values yields a load per lineal inch of 10.9 to 52 ppi for the 22% compression employed in this contract. Convair's results of 22.4 to 28.2 ppi lie in the center of this range.

Tables 8 and 9 tabulate similar room temperature cyclic load deflection studies of the Viton ECD-3234 O-rings, black and white stocks, respectively. As before, the first column of data, labeled Applied Force, Max., again displays an operator produced shift in values between the 5th and the 25th cycles. Once again, there was no real dynamic compression set, and this is indicated in the next column entitled "Compression Set."

TABLE 7

CYCLIC LOAD DEFLECTION MEASUREMENTS AT
293K (74F) OF VITON E-60C (BLACK) O-RINGS

Conditions:
1 Min. Cycle Time
22% Compression (max)
(-224) Size O-rings
Head Speed = 0.05"/Min

O-ring Spec	Cycle No.	Instron Data Characteristics	Applied Force, Max		"Compression Set"	ENERGY								
						Imposed			Recovered			Hysteresis		
			Kg	(lbs)		Planimeter	Squares	Joules	Planimeter	Squares	Joules	Planimeter	Squares	Joules
#1	1	1 square = 10^{-2} in lb or	60.5	(133)	-	-	117.0	0.132	-	82.25	0.093	-	34.75	0.039
	2	.113 x 10^{-2} joules	60.0	(132)	0	-	107.25	0.121	-	86.0	0.097	-	21.25	.024
	5	Chart speed 1.00"/min	60.0	(132)	0	-	97.5	0.110	-	102.50	0.116	-	-5	-.006
	25	1 sq = 2 x 10^{-3} in/lb or	72.7	(160)	-	0370.0	673.4	0.152	0311.3	566.5	0.128	58.7	106.8	0.024
	50	.226 x 10^{-3} joule	73.2	(161)	-	0360.0	655.2	0.148	0314.6	572.5	0.129	45.4	82.6	0.019
	100	Chart speed 5.00"/min	73.2	(161)	0	0367.0	667.9	0.151	0313.0	569.6	0.129	54.0	98.2	0.022
	200		73.2	(161)	0	0369.6	671.5	0.152	0313.0	569.6	0.129	56.0	101.9	0.023
	Ave.		67.5	(146)				.138			.117			.021
#2	1	1 sq = 10^{-2} in lb or	60.0	(132)	-	-	NA	-	-	NA	-	-	N/A	-
	2	.113 x 10^{-2} joules	60.9	(134)	0	-	104.75	0.118	-	77.5	0.088	-	27.25	0.031
	5	Chart speed 1.00"/min	60.0	(132)	0	-	89.75	0.101	-	87.0	0.098	-	2.75	0.003
	25	1 sq = 2 x 10^{-3} in lb or	67.3	(148)	-	0345	638.2	0.144	0282.5	522.6	0.118	62.5	115.6	0.026
	50	.226 x 10^{-3} joule	67.3	(148)	0	0340.5	629.9	0.142	0280	518	0.117	60.5	111.9	0.025
	100	Chart speed 5.00"/min	67.3	(148)	0	0338	625.4	0.141	0282	521.7	0.118	56.0	103.6	0.023
	200		67.3	(148)	0	0339.5	628	0.142	0280	518	0.117	59.5	110.0	0.025
	Ave.		64.2	(141)				.131			.108			.022
#3	1	1 sq = 2 x 10^{-2} in lb or	73.6	(162)	-	-	49	0.111	-	67.25	0.152	-	18.25	-0.041
	2	.226 x 10^{-2} joule	75.5	(166)	0	-	62	0.140	-	61.5	0.139	-	.5	.001
	5	Chart speed 0.50"/min	75.5	(166)	0	-	49.5	0.112	-	56.5	0.128	-	.7	-0.016
	25	1 sq = 2 x 10^{-3} in lb or	73.6	(162)	0	0368.3	670.3	0.151	0303	551.4	0.125	65.3	118.8	0.027
	50	.226 x 10^{-3} joules	73.6	(162)	0	0361.6	657.5	0.149	0295.3	537.4	0.121	66.3	120.6	0.027
	100	Chart speed 5.00"/min	73.6	(162)	0	0367	667.9	0.151	0285	518.7	0.117	82.0	149.2	0.034
	200		73.6	(162)	0	0356.3	648.4	0.147	0299	544.1	0.123	57.3	104.2	0.024
	Ave.		74.1	(163)				.137			.129			.008
		Grand Average	69.1	(152)										0.018
		Range:	60 to 75.5	(132 to				.135			.116		Range:	0.034 to -.041

Note: Energy for cycles 1-5 measured by area counting
Energy for cycles 25-100 measured by polarimeter

TABLE 8

CYCLIC LOAD DEFLECTION MEASUREMENTS OF VITON ECD-3234 (BLACK) O-RINGS
AT 293K (73F)

Conditions:
1 min. cycle time
22% compression (max)
(-224) size o-rings
(1 sq = .226 x 10^{-3} joules)

O-Ring Specimen	Cycle No.	Applied Force, max. Kg	(lb.)	"Compression Set"	ENERGY Imposed Planimeter	Imposed Squares	Imposed Joules	Recovered Planimeter	Recovered Squares	Recovered Joules	Hysteresis Planimeter	Hysteresis Squares	Hysteresis Joules
1	1	59.9	(132)	-	0310	561.1	.1268	0274	495.3	.1119	36.7	66.4	.0150
	2	59.9	(132)	0	0315	570.6	.1289	0276	499.5	.1128	39.3	71.3	.0161
	5	60.8	(134)	0	0298	539.9	.1220	0259	469.3	.1060	39.0	70.5	.0159
	25	63.1	(139)	-	0325	586.4	.1325	0284	514.0	.1164	40.5	73.3	.0166
	50	63.1	(139)	0	0311	562.9	.1272	0274	495.0	.1118	37.5	67.8	.0153
	100	63.1	(139)	0	0323	584.6	.1321	0272	492.0	.1111	51.0	92.3	.0208
	200	63.1	(139)	0	0217	573.7	.1296	0266	481.4	.1087	51.0	92.3	.0208
	Average	61.9	(136)	0			.1284			.1112			.0172
	Range	59.9- 63.1	132- 139				.1220- .1325			.1060- .1164			.0150- .0208
2	1	59.9	(132)	-	0336	621.6	.1404	0257	474.7	.1073	79.4	146.8	.0331
	2	59.9	(132)	0	0302	558.7	.1262	0246	455.1	.1028	56.0	103.6	.0234
	5	59.9	(132)	0	0309	571.6	.1291	0252	466.2	.1053	57.0	105.4	.0238
	25	62.6	(138)	-	0317	563.3	.1273	0276	490.3	.1108	41.0	72.9	.0164
	50	62.6	(138)	0	0318	566.0	.1279	0265	471.7	.1066	53.0	94.3	.0213
	100	62.5	(137.8)	0	0301	536.3	.1212	0282	498.4	.1126	21.3	37.9	.0085
	200	62.6	(138)	0	0310	551.8	.1247	0279	495.9	.1120	31.4	55.8	.0126
	Average	61.4	(135)	0			.1281			.1082			.0199
	Range	59.9- 62.5	132- 138				.1212- .1404			.1028- .1126			.0085- .0331
3	1	-	-	-	-	-	-	-	-	-	-	-	-
	2	59.9	(132)	-	0284	513.3	.1160	0241	436.2	.0985	42.6	77.1	.0174
	5	59.9	(132)	0	0300	543.0	.1227	0253	457.9	.1034	46.7	84.5	.0190
	25	63.1	(139)	0	0322	605.3	.1367	0281	528.1	.1193	41.0	77.0	.0174
	50	63.1	(139)	0	0322	605.3	.1367	0273	513.2	.1159	49.0	92.1	.0208
	100	63.1	(139)	0	0323	607.2	.1372	0273	513.2	.1159	50.0	94.0	.0212
	200	63.1	(139)	0	0321	603.4	.1363	0262	492.5	.1113	59.0	110.9	.0250
	Average	62.0	(137)	0			.1309			.1107			.0201
	Range	59.9- 63.1	132- 139				.1160- .1372			.0985- .1193			.0174- .0212
Grand Average		61.8	(136)				.1287			.1100			.0190

TABLE 9

CYCLIC LOAD DEFLECTION MEASUREMENTS OF VITON ECD-3234 (WHITE) O-RINGS
AT 293K (73F)

Conditions:
1 min. cycle time
22% compression (max)
(-224) size o-rings
(1 sq. = .226 x 10^{-3} joules)

O-Ring Specimen	Cycle No.	Applied Force, max. Kg	(lb.)	"Compression Set"	ENERGY Imposed Planimeter	Squares	Joules	Recovered Planimeter	Squares	Joules	Hysteresis Planimeter	Squares	Joules
1	1	48.8	(107.5)	-	0217	379.7	.0858	0194	339.5	.0767	23.0	40.2	.0090
	2	48.8	(107.5)	0	0222.3	389	.0879	0190.6	333.5	.0753	31.7	55.5	.0126
	5	48.8	(107.5)	0	0220.6	386	.0872	0191.6	335.3	.0753	29.0	50.7	.0119
	25	55.3	(122.0)	-	0267	483.2	.1092	0230	416.3	.0940	37.0	66.9	.0151
	50	55.3	(122.0)	0	0255	461.5	.0940	0232	419.9	.0948	23.0	41.6	.0094
	100	55.6	(122.5)	0	0263	476.0	.1076	0232	419.9	.0948	31.0	56.1	.0128
	200	55.6	(122.5)	0	0263	476.0	.1076	0241	436.2	.0985	22.0	39.8	.0091
	Average	52.6	(116)	0			.0970			.0871			.0100
2	1	49.0	(108)	-	0247.3	447.6	.1012	0208.3	377	.0852	39	70.6	.0159
	2	48.5	(107)	0	0233.6	422.8	.0956	02093	378.8	.0856	24.3	44	.0099
	5	49.0	(108)	0	0235.6	426.4	.0964	0205	371	.0838	30.6	55.4	.0125
	25	48.3	(106.5)	0	0229	407.6	.0921	0210	373.8	.0844	19	33.8	.0076
	50	48.3	(106.5)	0	0230	409.4	.0925	0206	366.6	.0828	24	42.8	.0096
	100	48.3	(106.5)	0	0229	407.6	.0921	0210	373.8	.0844	19	33.8	.0076
	200	48.3	(106.5)	0	0233	414	.0936	0211	375.0	.0847	22	39.0	.0088
	Average	48.5	(107)	0			.0948			.0844			.0103
3	1	46.5	(102.5)	-	0234	425.4	.0961	0202.6	360.6	.0814	36.4	64.8	.0146
	2	46.5	(102.5)	0	0230.6	410.4	.0928	0200	356	.0804	30.6	54.4	.0122
	5	48.8	(107.5)	0	0230.3	409.9	.0926	0205.6	365.9	.0826	24.7	53.0	.0119
	25	53.3	(117.5)	-	0253	442.7	.1001	0233	407.7	.0921	20	35.0	.0079
	50	53.5	(118)	0	0251	439.2	.0993	0232	406	.0917	19	33.2	.0075
	100	53.5	(118)	0	0255	446.2	.1008	0230	402.5	.0909	25	43.7	.0098
	200	53.3	(117.5)	0	0255	446.2	.1008	0233	407.7	.0921	22	38.5	.0087
	Average	50.7	(111.9)	0			.0975			.0872			.0103
Grand Average		50.6	(112)				.0964			.0862			.0102

The cyclic load bearing properties of all three Viton seal candidates at room temperature are summarized in Table 10. The load bearing capacity of these size -224 O-rings ranges from 69 kg. for the E-60C (black) stock to nearly 51 kg. for the ECD-3234 (white) stock. It will be observed that the load bearing properties of these Viton O-rings at 22% compression are roughly proportional to the tensile modulus at 100% elongation.

At the elevated temperature of 422K (300F) the load bearing properties of all three Viton rubbers increases markedly. Figures 12 and 13 are copies of the Instron stress-strain curves for the first five compression cycles, as well as the 25th, 50th, 100th, and 200th compression cycles. Figures 12 and 13 are representative of all the 422K load deflection curves obtained with the O-rings molded from either the E-60C (black) stock or the ECD-3234 (black) stock. Tables 11 and 12 summarize the 422K (300F) load deflection behavior of these two types of O-rings. It is apparent that the operator variances which plagued the room temperature load deflection experiments were overcome, and the "Applied Force, Max." values are now quite uniform. There was obviously no dynamic compression set, transient or permanent, during the 200 cycles. A small amount of dynamic compression set was, however, noted in the ECD-3234 (white) O-rings at 422K (300F). This is evident in Figures 14 and 15, which show the Instron curves the first 24 cycles, and the 25th, 50th, and 100th cycles, respectively. It will be noted that the cusp height was substantially unchanged for the first 13 cycles (Figure 14), and then slowly decreased. This same phenomenon is shown in the first two columns of Table 13 which summarizes all the load deflection measurements of the ECD-3234 (white) O-rings at 422K.

No dynamic compression set occurred in the first five cycles. The total amount of dynamic compression set or creep was relatively small, measuring 4% to 7% for the O-rings tested, and is probably technically unimportant. The delayed appearance of this compression set is, however, reminiscent of the induction period of a chemical reaction, and suggests that the phenomenon is probably not due to viscoelasticity, but rather to a chain/crosslink scission or oxidative reaction. It would be interesting to see whether the presence of antioxidant would suppress this dynamic compression set. The load bearing properties at 422K (300F) of all three Viton seal candidates are summarized in Table 14. Compared with the room temperature properties (Table 10), the load bearing properties at 422K have increased by 28% for the E-60C (black) stock, by 32% for the ECD-3234 (black) stock, and by 83% for the ECD-3234 (white) stock.

As already described in Section 3.1.3.1, 233K (-40F) is below the rubbery range of the above Vitons, and their dynamic behavior resembles that of leathery plastics rather than resilient rubbers. The steady decay in load bearing properties as the cycling continued was dramatically illustrated in Figure 11. The force required to produce the 22% O-ring deflection was successively lower for each successive compression cycle.

Table 10. Cyclic Load Bearing Properties of Three Vitron Seal Candidates at Room Temperature

Conditions: Room Temp. = 293K (73F)
Moduli are from Tensile Tests; 20"/min
Compression cycling - 2 cycles/min.
22% compression

Candidate	Specimen No.	Applied Force Max., (Cusp Height) Kg	(lb)	Avg. Load per Lineal Length g/lineal cm (lb/lineal inch)		Tensile Modulus 20% Newtons / m^2 x 10^6	(psi)	Tensile Modulus 100% Newtons / m^2 x 10^6	(psi)	Hardness Shore-A
Viton E-60C (Black)	1	67.5	(146)	4.5×10^3 g/cm	(24.75 ppi)					
	2	64.2	(141)	4.3×10^3	(23.9)					
	3	74.1	(163)	4.9×10^3	(27.6)	1.25	(167)	6.50	(937)	80
	Average	69.1	(152)	4.6×10^3	(25.8)					
Viton ECD-3234 (Black)	1	61.9	(136)	4.1×10^3 g/cm	(23.1 ppi)					
	2	61.4	(135)	4.1×10^3	(22.9)	1.16	(168)	5.86	(851)	78
	3	62.0	(137)	4.1×10^3	(23.2)					
	Average	61.8	(136)	4.1×10^3	(23.1)					
Viton ECD-3234 (White)	1	52.6	(116)	3.5×10^3 g/cm	(19.7 ppi)					
	2	48.5	(107)	3.2×10^3	(18.1)	1.24	(181)	5.25	(761)	75
	3	50.7	(112)	3.4×10^3	(19.0)					
	Average	50.6	(112)	3.4×10^3	(18.9)					

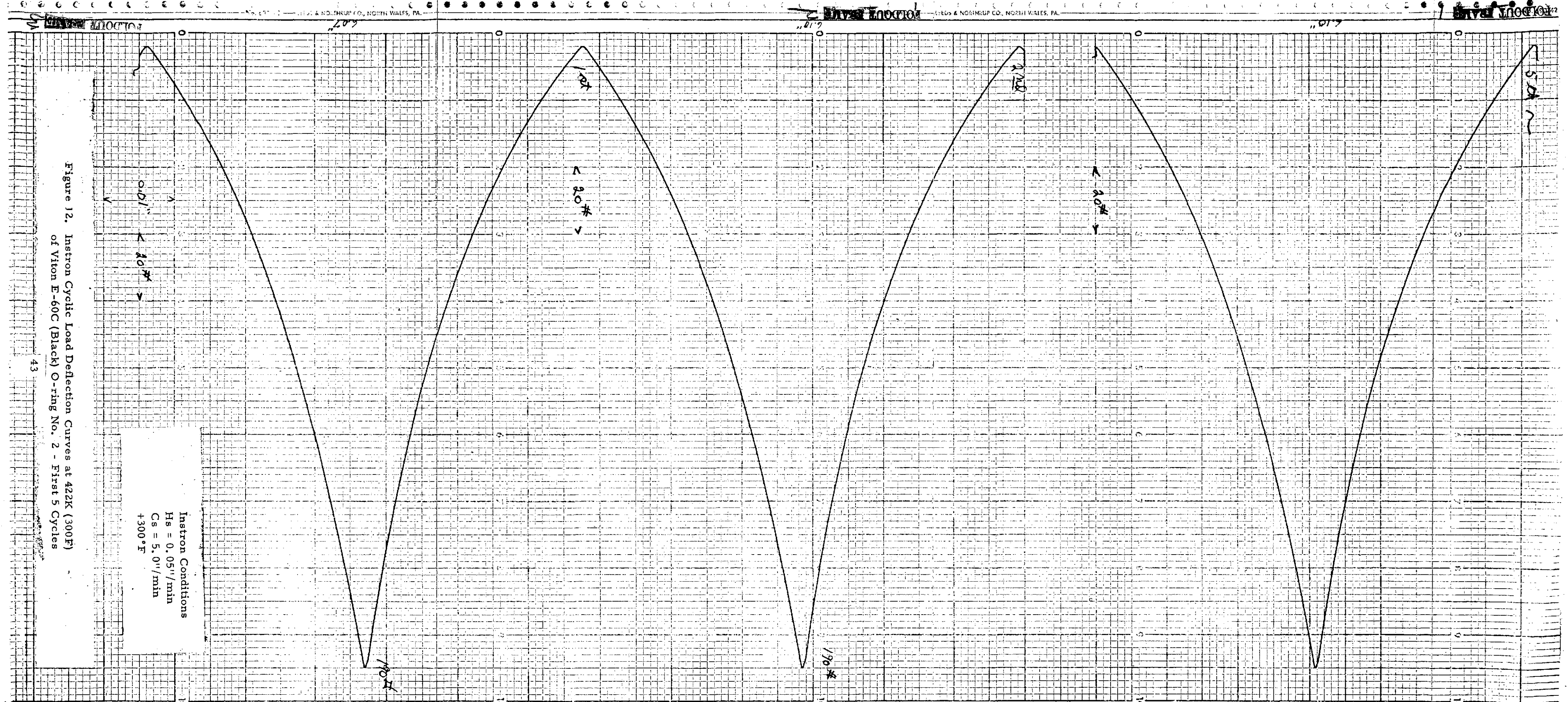

Figure 12. Instron Cyclic Load Deflection Curves at 422K (300F) of Viton E-60C (Black) O-ring No. 2 - First 5 Cycles

Page intentionally left blank

CYCLIC LOAD DEFLECTION MEASUREMENTS OF VITON E-60C (BLACK) O-RINGS
AT 422K (300F)

TABLE-11

Conditions:
1 min. cycle time
22% compression (max)
(-224) size o-rings
(1sq = .226 x 10^{-3} joules)

O-Ring Specimen	Cycle No.	Applied Force, max. Kg.	Applied Force, max. (lb.)	"Compression Set"	ENERGY Imposed Planimeter	Imposed Squares	Imposed Joules	Recovered Planimeter	Recovered Squares	Recovered Joules	Hysteresis Planimeter	Hysteresis Squares	Hysteresis Joules
4	1	82.1	(181)	-	0517.0	971.0	.2194	0495.3	931.1	.2104	21.7	39.9	.0090
	2	82.1	(181)	0	0511.6	961.8	.2173	0492.3	925.2	.2090	19.3	36.6	.0082
	5	82.1	(181)	0	0511.0	960.0	.2169	0500	940.0	.2124	11.0	20.0	.0045
	25	82.1	(181)	0	0519.3	960.7	.2171	0506.6	937.2	.2127	13.7	23.5	.0053
	50	82.1	(181)	0	0508.0	939.8	.2123	0486.6	900.2	.2034	21.4	39.6	.0089
	100	82.1	(181)	0	0506.3	936.6	.2116	0848.4	895.9	.2024	22.0	40.7	.0091
	200	82.1	(181)	0	0511.0	945.3	.2136	0496	917.6	.2073	15.0	27.7	.0062
	Average	82.1	(181)	0			.2155			.2082			.0073
	Range	-	-	-			.2116-.2197			.2024-.2127			.0045-.0091
2	1	86.2	(190)	-	0555	1043.4	.2358	0515	968.2	.2188	40	75.2	.0170
	2	86.2	(190)	0	0551	1035.8	.2340	0534	998.2	.2255	17	37.6	.0085
	5	86.2	(190)	0	0546	1026.4	.2319	0523	983.2	.2222	23	43.2	.0097
	25	86.2	(190)	0	0559	1050.9	.2375	0532	1000.1	.2260	27	50.8	.0115
	50	86.2	(190)	0	0559	1050.9	.2375	0535	1005.8	.2273	24	45.1	.0102
	100	86.2	(190)	0	0565	1062.2	.2400	0527	990.7	.2238	38	71.5	.0162
	200	86.2	(190)	0	0569	1069.7	.2417	0554	1041.5	.2354	15	27.6	.0064
	Average	86.2	(190)	0			.2369			.2256			.0114
	Range	-	-	-			.2319-.2417			.2188-.2354			.0064-.0170
3*	1	93.0	(205)	-	0205.6	359.8	.2033	0183	320.2	.1810	22.6	40.9	.0231
	2	93.0	(205)	0	0196.3	343.5	.1941	0184.3	322.5	.1822	12.0	16.3	.0092
	5	93.0	(205)	0	0199.3	348.8	.1971	0192	336.0	.1898	7.3	13.2	.0075
	25	93.0	(205)	0	0198.6	347.5	.1963	0191	334.2	.1888	7.6	13.3	.0075
	50	93.0	(205)	0	0200.0	350.0	.1978	0192	336.0	.1898	8.0	14.0	.0079
	100	93.0	(205)	0	0199.3	348.7	.1970	0199	348.2	.1967	0.3	0.52	.0003
	200	93.0	(205)	0	0203.6	356.3	.2013	0201	351.8	.1988	2.6	4.5	.0025
	Average	93.0	(205)	0			.1981			.1896			.0083
	Range	-	-	-			.1941-.2033			.1810-.1988			.0003-.0231
Grand Average		87.1	(192)				.2168			.2078			.0090

* 1 square = 5 x 10^{-3}; inch lbs. = .565 x 10^{-3} joules.

TABLE 12

CYCLIC LOAD DEFLECTION MEASUREMENTS OF ECD-3234 (BLACK) O-RINGS AT 422K (300F)

Conditions:

1 min. cycle time
22% compression (max)
(-224) size o-rings

O-Ring Specimen	Cyclic No.	Applied Force, max. Kg	(lb.)	"Compression Set"	ENERGY Imposed Planimeter	Squares	Joules	Recovered Planimeter	Squares	Joules	Hysteresis Planimeter	Squares	Joules
1	1	90.3	(199)	-	0193.0	349	.0788	0180.3	326.3	.0737	12.7	22.9	.00518
	2	90.3	(199)	0	0193.3	349.8	.0790	0180.3	326.3	.0737	13.0	23.5	.00531
	5	90.3	(199)	0	0188.0	340.2	.0768	0175.0	316.7	.0715	13.0	23.5	.00531
	25	90.3	(199)	0	0191.3	346.2	.0782	0183.3	340.8	.0770	8.0	14.4	.00325
	50	90.3	(199)	0	0191.0	345.7	.0781	0188.0	340.2	.0768	3.0	5.4	.00122
	100	90.3	(199)	0	0195.0	352.9	.0797	0188.0	340.2	.0768	7.0	12.6	.00285
	200	90.3	(199)	0	0195.0	352.9	.0797	0189.6	343.1	.0775	5.4	9.0	.00203
	Average	90.3	(100)	0			.0786			.0753			.0035
	Range	-	-	-			.0768-.0797			.0715-.0775			.0012-.0053
2	1	83.0	(183)	-	0159.3	269.2	.0594	0151.6	256.9	.0580	7.7	13.0	.00294
	2	83.0	(183)	0	0161.3	272.9	.0616	0153.0	258.5	.0584	8.3	14.0	.00316
	5	83.0	(183)	0	0161.3	272.5	.0615	0155.0	261.9	.0591	6.3	10.6	.00240
	25	83.0	(183)	0	0158.3	277.0	.0626	0158.3	277.0	.0626	0.0	0.0	.0000
	50	83.0	(183)	0	0159.3	277.8	.0627	0160.3	280.5	.0633	-1.0	-1.75	-.0004
	100	83.0	(183)	0	0164.0	287.0	.0648	0158.0	276.5	.0624	6.0	10.5	.00237
	200	83.0	(183)	0	0158.0	276.5	.0624	0158.0	276.5	.0624	0.0	0.0	.0000
	Average	83.0	(183)	0			.0621			.0607			.0015
	Range	-	-	-			.0594-.0648			.0580-.0633			-.0004-.0032
3	1	85.3	(188)	-	0201.3	372.4	.0841	0184.0	340.4	.0769	17.3	32.0	.00723
	2	85.3	(188)	0	0194.3	359.4	.0812	0184.3	340.9	.0770	10.3	19.0	.00429
	5	85.3	(188)	0	0196.0	362.6	.0819	0192.3	355.3	.0802	3.7	6.84	.00155
	25	91.6	(202)	-	0195.3	367.1	.0829	0186.6	350.8	.0792	8.7	16.3	.00368
	50	91.6	(202)	0	0196.3	369.0	.0833	0191.6	360.2	.0814	4.7	8.8	.00199
	100	91.6	(202)	0	0197.0	370.0	.0836	0189.3	355.8	.0804	7.7	14.4	.00325
	200	91.6	(202)	0	0199.0	374.1	.0845	0197.3	370.9	.0838	1.7	3.1	.00070
	Average	88.9	(196)	-			.0831			.0798			.0032
	Range	85.3-91.6					.0812-.0845			.0769-.0838			.0007-.0072
Grand Average		87.4	193				.0746			.0719			.0027

Page intentionally left blank

FOLDOUT FRAME 1

101 cycles

<50# x 0.01"

50th cycle

25th cycle

Instron Conditions

Head Speed = 0.05"/min.
Chart Speed = 5.0"/min.

Figure 15. Instron Cyclic Load Deflection Curves at 422K (300F) of Viton ECD-3234 (White). Cycles 25, 50, 101.

FOLDOUT FRAME 2

Table 13. Cyclic Load Deflection Measurements of ECD-3234 (White) O-Rings at 422K (300F)

Conditions:

1 min. cycle time
22% compression (max)
(-224) size O-rings
1 Square = 0.565×10^{-3} Joules

O-Ring Specimen	Cyclic No.	Applied Force, max. Kg	(lb)	"Compression Set %"	ENERGY Imposed Planimeter	Squares	Joules	Recovered Planimeter	Squares	Joules	Hysteresis Planimeter	Squares	Joules
1	1	97.1	(214)	-	0760.6	1376.6*	.3111	0669.6	1210.8*	.2736	91	165.8*	.0374
	2	97.5	(215)	0	0282.6	511.5	.2890	0265.6	480.7	.2716	17	30.8	.0174
	5	97.1	(214)	0	0281.6	509.6	.2879	0261.6	473.4	.2675	20	36.6	.0207
	25	93.9	(207)	3	0242.3	438.5	.2478	0223.6	404.7	.2287	18.7	33.8	.0191
	50	89.8	(198)	7	0233.4	422.4	.2387	0217.0	392.7	.2219	16.4	29.1	.0168
	100	86.2	(190)	11	0225.0	407.2	.2301	0203.3	367.9	.2079	21.7	39.3	.0222
	Average	90.3	199	—			.2675			.2452			.0223
	Range	86-97	(190-214)										
2	1	92.5	(204)	-	0291	529.6	.299	0267	485.9	.275	24	43.7	.025
	2	92.5	(204)	0	0280	509.6	.288	0260	473.5	.267	20	36.4	.021
	5	92.1	(203)	0	0285	518.7	.293	0266	484.1	.279	19	34.6	.020
	25	89.8	(198)	3	0270	491.4	.278	0245	445.9	.252	15	27.3	.015
	50	85.7	(189)	7	0253	460.5	.260	0272	495.0	.280	21	38.2	.022
	100	81.6	180	12	0237	431.3	.244	0219	398.6	.225	18	32.8	.019
	Average	89.0	(196)	-			.277			.263			.020
	Range	82-93	(180-204)										

* 1 Square = $.226 \times 10^{-3}$ Joules

TABLE 14
CYCLIC LOAD BEARING PROPERTIES OF
THREE VITON SEAL CANDIDATES AT 422K (300F)

Specimen	Cycles #1 - #5 Applied force, Max.		Cycles #25 - #200 Applied force, Max		Ave. Load/Lineal Length		
	Kg	(lb)	Kg	(lb)	g/lineal cm	(lb./lineal in.)	"Compression Set, %"
Viton E-60C (black)							
O-ring #2	86.2	(190)	86.2	(190)	5.75×10^3	(32.2)	0
O-ring #3	93.0	(205)	93.0	(205)	6.20×10^3	(34.8)	0
O-ring #4	82.1	(181)	82.1	(181)	5.47×10^3	(30.6)	0
Average	87.1	192	87.1	192	5.81×10^3	(32.5)	0
Viton ECD-3234 (black)							
O-ring #1	90.3	(199)	90.3	(199)	6.07×10^3	(33.8)	0
O-ring #2	83.0	(183)	83.0	(183)	5.54×10^3	(31.0)	0
O-ring #3	82.1	(181)	82.1	(181)	5.47×10^3	(30.6)	0
Average	81.9	188	81.9	188	5.68×10^3	(31.8)	0
Viton ECD-3234 (white)							
O-ring #8	97.1	(214)	90.3	(199)	6.02×10^3	(33.8)	7
O-ring #9	90.7	(200)	89.0	(196)	5.78×10^3	(32.4)	4
Average	93.9	(207)	98.6	(197)	5.90×10^3	(33.1)	5

It will be observed that the maximum applied force required to achieve the prescribed 22% compression of the O-ring is not only many times greater than the force required at room temperature (293K) or at 422K (300F), but this force steadily decreases from 762 kg (1680 lbs.) for the first cycle to 633 kg (1395 lbs.) for the 26th cycle. By the 200th cycle the maximum force decreased to 560 kg (1235 lbs.) for this particular Viton E-60C (black) O-ring. All of the other subject Viton O-rings, whether fabricated from the E-60C (black) stock or the ECD-3234 (black) or (white) stocks, showed the same type of decay of maximum force throughout the course of the compression cycling. The various cyclic load deflection measurements for the three types of Viton O-rings; E-60C (black), ECD-3234 (black), and ECD-3234 (white), are summarized in Tables 15, 16, and 17, respectively.

Review of the first two data columns (i. e. "Applied Force Max." and "Compression Set,")shows that all three Vitons lost approximately 28$\pm$2% of their initial applied force during the 200 compression cycles with the ECD-3234 (black) stock on the high side (31% and 28.2%), and the ECD-3234 (white) stock on the low side (25.5%).

It is tempting to ascribe this decay of the maximum applied force entirely to some type of compression set. Compression set is certainly involved in case of the ECD-3234 (black) stock. However, the present data does not offer any convincing proof of the existence of a true compression set in the case of the ECD-3234 (white) or the E-60C (black) stocks. In the latter two stocks, at least, the observed decay could be entirely a thixotropic effect, while the larger decay exhibited by the ECD-3234 (black) stock would be the result of a superposition of the already measured compression set on this thixotropic breakdown.

Surprisingly, the two Viton ECD-3234 stocks (which are designed for low temperature use) displayed no improvement over the E-60C stock. In fact, the ECD-3234 (black) stock not only displayed the greatest decrease in maximum applied force during the compression cycling at 233K (-40F), but was the only Viton stock which exhibited a true compression set when measured per ASTM D-395. Thus, the ECD-3234 (black) O-rings exhibited 2.7% to 3.9% compression set 30 minutes after removal from the 233K Conrad/Missimer test chamber. By comparison, the E-60C (black) and ECD-3234 (white) stocks exhibited no compression set when measured as little as 10 minutes after removal from the test chamber. The DuPont/Elastomer Chemicals Dept. reports that the ECD-3234 stocks have brittle points (per ASTM D-746) of about 236K (-35F) and TR-10 values (per ASTM D-1329) of 247K (-15F) compared with the corresponding values for the E-60C (black) stock of 244K (-20F) and 256K (+2F). It is probable that Convair's failure to detect the superior low temperature properties of the ECD-3234 stocks is simply due to the fact that the test temperature of 233K (-40F) is sufficiently below the "rubbery" phase of all three Viton stocks so that the measured 8K to 10K degree difference in brittle point and TR-10 values are not applicable. There is no fundamental reason for a close correlation between physical properties in the "leathery" region (at 233K) and physical properties at the border between the leathery and the rubbery regions.

Table 15

Cyclic Load Deflection Measurements of Viton E-60C (Black)
O-Rings at 233K (-40F)

Conditions:
1 min. cycle time
22% compression (max.)
(-224) size O-rings
1 square = 5.65×10^{-3} in. lb.

O-ring Spec.	Cycle No.	Applied Force, Max. Kg	(lb)	"Compression Set" Kg	(lb)	ENERGY Imposed Planimeter	Squares	Joules	Recovered Planimeter	Squares	Joules	Hysteresis Planimeter	Squares	Joules
#6	1	762	(1680)		-	0143.0	250.2	1.414	0107.0	187.2	1.029	36.0	63.0	0.356
	2	730	(1610)	32	(70)	0243.6	426.3	1.204	0213.0	372.7	1.053	30.6	53.6	0.151
	5	680	(1500)	82	(180)	0206.0	360.5	1.018	0184.0	322.0	0.910	22.0	38.5	0.109
	26	633	(1395)	129	(285)	0176.0	308.0	0.870	0154.3	270.0	0.763	21.7	38.0	0.107
	50	606	(1337)	156	(343)	0161.0	297.8	0.841	0147.3	272.5	0.770	13.7	25.3	0.071
	100	578	(1275)	184	(405)	0144.6	267.5	0.756	0133.0	246.0	0.695	11.6	21.5	0.061
	200	560	(1235)	202	(445)	0139.0	257.1	0.726	0125.0	231.2	0.653	14.0	25.9	0.073
#7	1	835	(1840)	-	-	0395.0	679.4	1.916	0286.0	491.9	1.387	10.9	187.5	0.529
	2	801	(1765)	34	(75)	-	-	-	-	-	-	-	-	-
	5	748	(1650)	52	(115)	0261	448.9	1.266	0233.6	401.7	1.133	27.4	47.2	0.133
	*	increased head loading through Instron cam adjustment												
	25	947	(2088)		-	0411.6	707.9	1.996	0369.6	635.7	1.793	42.0	72.2	0.204
	50	889	(1960)	58	(128)	0356.6	634.7	1.790	0319.3	568.3	1.603	37.3	66.4	0.187
	100	866	(1910)	81	(178)	0340.3	605.7	1.708	0310.6	552.8	1.559	29.7	52.9	0.149
	200	803	(1770)	144	(318)	0284.3	480.6	1.355	0270.3	456.8	1.288	14.0	23.8	0.067
#8	1	1309	(2885)		-	-	-	-	-	-	-	-	-	-
	2	1229	(2710)	79	(175)	0298.0	551.3	3.115	0233.0	431.0	2.435	65.0	120.3	0.680
	5	1154	(2545)	152	(340)	0259.0	479.0	2.706	0208.3	385.3	2.177	50.7	93.7	0.529
	25	1059	(2335)	249	(550)	0206.6	373.9	2.113	0187.0	338.4	1.912	19.6	35.5	0.201
	50	1016	(2240)	263	(580)	0185.0	334.8	1.892	0171.0	309.5	1.749	14.0	25.3	0.143
	100	924	(2037)	385	(848)	0160.0	289.6	1.636	0143.3	255.7	1.445	16.7	34.5	0.195
	200	945	(2083)	364	(802)	0166.3	296.0	1.672	0144.3	256.8	1.451	22.0	39.2	0.221

Table 16

Cyclic Load Deflection Measurements of Viton ECD-3234 (Black)
O-Rings at 233K (-40F)

Conditions:
1 min. cycle time, 22% compression (max.)
(-224) size O-rings

1 sq. = 5.65×10^{-3} Joules

O-ring Spec.	Cycle No.	Applied Force, Max. Kg	(lb)	"Compression Set" Kg	(lb)	ENERGY Imposed Planimeter	Squares	Joules	Recovered Planimeter	Squares	Joules	Hysteresis Planimeter	Squares	Joules
#7	1	1259	(2775)	–	–	0309.6	557.2	3.148	0238.6	429.4	2.426	71	127.8	0.722
	2	1202	(2650)	57	(125)	0271.3	488.3	2.759	0221.3	398.3	2.250	50	90.6	.509
	5	1134	(2500)	125	(275)	233	419.4	2.370	0200.3	360.5	2.037	32.7	58.9	.333
	25	1034	(2280)	222	(490)	0186.6	334.8	1.892	0171.6	308.8	1.745	14.4	26.0	.147
	50	1009	(2225)	249	(550)	0177	318.6	1.800	0158	284.4	1.607	19	34.2	.193
	100	907	(2000)	351	(775)	0139	250.0	1.413	0130	234.0	1.322	9	16.0	.090
	200	869	(1915)	390	(860)	0126	227.8	1.287	0116	208.8	1.180	10	19.0	.107
#8	1	1318	(2905)	–	–	0382.3	691.9	3.909	0292	528.5	2.986	91.2	163.4	.923
	2	1259	(2775)	59	(130)	0333.6	603.8	3.411	0271	490.5	2.771	62.6	113.3	.640
	5	1188	(2620)	129	(285)	0291.3	529	2.989	0240.6	435.4	2.460	50.7	93.6	.529
	27	1111	(2450)	206	(455)	0216	399.6	2.258	0187.3	346.5	1.958	28.7	53.1	.300
	50	1077	(2375)	240	(530)	0197	364.4	2.059	0178.6	330.4	1.867	18.4	34	.192
	100	1007	(2220)	311	(685)	0167.6	303.3	1.714	0154.6	279.8	1.581	13.0	23.5	.133
	200	946	(2085)	372	(820)	0150.3	272	1.537	0135	244.3	1.380	15.3	27.7	.157

Table 17

Cyclic Load Deflection Measurements of Viton ECD-3234 (White)
O-Rings at 233K (-40F)

Conditions:

1 min. cycle time
22% compression (max.)
(-224) size O-rings

1 square = 5.65×10^{-3} in. lb.

O-ring Spec.	Cycle No.	Applied Force, Max. Kg	(lb)	"Compression Set" Kg	(lb)	ENERGY Imposed Planimeter	Squares	Joules	Recovered Planimeter	Squares	Joules	Hysteresis Planimeter	Squares	Joules
#7	1	930	(2050)		-	0190.3	344.4	1.946	0153.8	277.4	1.567	37.0	67.0	0.379
	2	870	(1980)	32	(70)	0171.0	309.5	1.749	0142.6	258.1	1.458	28.0	51.4	.290
	5	871	(1920)	59	(130)	0151.0	273.3	1.542	0137.6	249.0	1.407	13.4	24.3	.137
	*	Increased head loading through adjustment of Instron cam												
	25	1098	(2420)	-	-	0234.0	423.5	2.393	0213.6	386.6	2.184	21.4	38.7	.218
	50	1055	(2325)	43	(95)	0214.3	387.8	2.191	0189.3	342.6	1.936	25.0	45.2	.255
	100	1022	(2255)	75	(165)	0194.3	351.6	1.987	0172.6	312.4	1.765	21.7	39.2	.221
	200	-	-	-	-	-	-	-	-	-	-	-	-	-
#8	1	1175	(2590)		-	0306.3	542.2	3.062	0222.6	393.2	2.222	0083.2	149.0	0.842
	2	1107	(2440)	68	(150)	0243.0	430.5	2.430	0203.6	360.4	2.036	0039.4	70.1	.396
	5	1039	(2290)	136	(300)	0202.3	358.0	2.023	0184.3	326.2	1.843	0018.0	32.0	.181
	25	954	(2104)	220	(486)	0164.3	297.4	1.680	0151.0	273.3	1.544	0013.3	24.0	.136
	50	948	(2090)	227	(500)	0154.3	279.3	1.578	0148.0	267.8	1.513	0006.3	11.4	.064
	100	948	(2090)	227	(500)	0159.0	287.8	1.626	0145.0	262.4	1.483	0014.0	25.3	.143
	200	875	(1930)	299	(660)	0131.0	237.1	1.340	0125.4	228.7	1.281	0005.6	10.4	.059

3.1.3.3 Cyclic Work and Hysteresis

The Instron stress-strain curves obtained when the three hydraulic seal candidates Viton E-60C (black), Viton ECD-3234 (black) and Viton ECD-3234 (white) are compression cycled at three test temperatures [422K (300F), 293K (73F), and 233K (-40F)] were described in the previous sections. Since the elastic hysteresis is the internal friction (energy loss) occurring in the O-ring specimen when it is compression cycled, it should be readily obtained by measuring the difference in area between the loading and unloading portion of each stress-strain cycle (or cusp). Unfortunately, this seemingly simple operation is difficult to perform rapidly and accurately, and this difficulty is aggravated in the case of high modulus, low hysteresis Viton rubbers where one is attempting to accurately measure a small difference between two large quantities, i.e., (large area under loading half of cycle) - (large area under unloading half cycle) = small hysteresis. In addition, such measurements must be convenient, since these parameters were to be determined at three different temperatures on the 1st, 2nd, 5th, 50th, 100th, and 200th cycles for every seal candidate of this program. Because of its importance, four different methods of measuring this hysteresis area was investigated. These four methods are:

1. Manually cutting out and weighing the curves. Splitting each "cusp" into the loading and unloading portion by dropping a perpendicular from the cusp peak to the base and then weighing the two halves. This method is very accurate, but since several other pertinent measurements (such as the effective dynamic modulus) must also be determined later on, it is obviously undesirable to sacrifice the original Instron curves to this cutting procedure. Accordingly, an attempt was made to utilize Xerox type copies of the curves for the cutting-and-weighing. Office copying machines used at Convair Aerospace give good duplication of surface areas, i.e., neither shrinkage or enlargement occurs. An effort was made to determine whether the output of these copying machines is consistent in weight as well as they are dimensionally. Five, 2.34 by 25.4 cm (0.92 by 10.0 in.), strips of the original and of copies produced by two radically different copying machines (a Brunning, "Revalute 880" and a "Copystat 500") were weighed. As expected, the strips cut from the original Instron chart paper were very uniform. By comparison, the strips from the two copying machines varied widely. The "Copystat 500" yielded strips having an average weight of 0.5759g $\pm$ .0030g., i.e., $\pm$0.573% variation. The Brunning (ammonia) copying machine was even worse, yielding a weight average of 0.4791g $\pm \begin{matrix} .0169g \\ .0069g \end{matrix}$, i.e., +3.3% to -1.6% variation.

   This amount of variation was considered unacceptable. It was thought that the variation might be due to uneven retention of moisture, and, therefore, could be minimized by conditioning the paper in a constant humidity chamber

prior to weighing. Strips from the "Copystat 500" (a "wet type" copying machine) were equilibrated in various humidity chambers before weighing. Although the "Copystat" strips equilibrated rapidly and consistently, the variation in weight/unit area was not decreased by this conditioning. For these reasons, the manual cutting and weighing procedure was abandoned.

2. Direct counting of the squares (i. e. area) under the curves, although obvious, is tedius and time-consuming. However, since Xerox-type copies can be used, it was convenient to determine the area of some of the small load deflection cusps of this contract by direct counting. For example, the cyclic hysteresis of the 1st, 2nd, and 5th cycles of all three Viton E-60C (black) O-rings (which were recorded at the low chart speed of 1. 27 cm (0. 50 inches)/ min.) were measured by direct counting. These results are contained in Table 7. To insure accuracy, each "half" of each cusp was counted until checking results were obtained. Attempts to extend direct counting to the "magnified" cusps produced by the higher chart speed of 12. 7 cm (5. 0 inches) per minute, however, proved impractical. For example, the 25th cycle cusp of O-ring of Viton E-60C (black) O-ring #1 was counted half a dozen times by two different people before a valid "average" value of 114 squares (i. e., 0. 258 joules or 0. 019 ft lb) was determined for the hysteresis.

3. A combination of methods 1 and 2 was attempted next. The cusps were cut out of the Xerox-type copies and the two halves of the cusp superimposed on each other to get a closed-loop hysteresis type curve identical with those described in Section 3. 1. 3. 1, and shown in Figure 7, but larger and consequently more accurate. Although practical, this method was discarded in favor of the planimeter method described below.

4. The area of each half of the compression deflection cusp was measured by running the tracer point of a Keuffel and Esser #4242 compensating polar planimeter around the periphery of the cusp half and reading the distance traversed by the measuring wheel of the planimeter. Each area measurement is repeated until checking results are obtained. This usually requires about three runs, however, operation of the planimeter is rapid and the time required per cusp is quite reasonable. The planimeter values are converted to energy units (joules/foot pounds) by simply running the planimeter trace point around a 400 square block of the Instron chart paper which represents, for example (40 lbs) x (0. 020 inches) = 0. 800 inch pounds which is equivalent to 0. 0667 foot lbs. or 0. 09044 joules.

Results of the cyclic load deflection measurements for the three Viton E-60C specimens at room temperature are summarized in Table 7. The average hysteresis amounted to 17 x 10^{-3} joules (12. 5 x 10^{3} foot pounds) with a wide range of 34 x 10^{-3} to -41 x 10^{-3} joules. The greater part of this scatter, however,

is contributed by the 1st, 2nd, and 5th cycles which were the least sensitive curves run at low chart speeds. If only the more accurately measured values of the 25th through 200th cycles are considered, then hysteresis values of the three specimen O-rings amounts to:

Specimen No.	Average	Hysteresis	Range
1	22×10^{-3} joules	(16×10^{-3} ft. lb)	19 to 24×10^{-3} joules
2	25×10^{-3} joules	(18.5×10^{-3} ft. lb)	23 to 26×10^{-3} joules
3	28×10^{-3} joules	(20.6×10^{-3} ft. lb)	24 to 34×10^{-3} joules
Overall Average	25×10^{-3} joules	(18.4×10^{-3} ft. lb)	

and the consistency within each O-ring and between the different O-rings is quite satisfactory. This average hysteresis value of 25×10^{-3} joules (19×10^{-3} ft. lb) is believed to be the most nearly correct value for the Viton E-60C (black) O-rings at room temperature.

Tables 8 and 9 summarize the room temperature cyclic load deflection measurements of the Viton ECD-3234 (black) and (white) O-rings, respectively. It is apparent that the elastic hysteresis of the ECD-3234 Vitons is significantly less than that of the E-60C Viton. For example, although load bearing properties of the ECD-3234 (black) O-rings are 90% of those of the E-60C (black) O-rings, and the Imposed Cyclic Energy is 95% of that exhibited by the E-60C (black) O-rings, the hysteresis is only 76% of the latter. This pertinent data is summarized for all three Viton candidates in Table 18. It will be observed that the single non-carbon-black-reinforced seal candidate tested in this program, the ECD-3234 (white) stock, is far superior to both of the black-reinforced Vitons. The elastic hysteresis of the ECD-3234 (white) stock is only 10×10^{-3} joules. This is only 40% of the hysteresis exhibited by the E-60C (black) stock. In spite of this, the load bearing properties of the ECD-3234 (white) stock were still about 71% to 73% of those of the E-60C (black) stock.

Based on these room temperature results, the ECD-3234 (white) stock appears to be dynamically superior to either of the black Viton stocks. As noted previously, the white stock also showed the best retention of properties under both the 200 hour/422K compatibility test and the thermal cycling testing in MIL-H-83282 fluid.

The 422K (300F) cyclic load deflection measurements of the three subject Vitons are tabulated in Tables 11, 12 and 13. It will be noted that although both the "Imposed" and "Recovered Energy" of the compression cycles was much greater at 422K than it had been at room temperature, the cyclic hysteresis was about the

TABLE 18

CYCLIC LOAD DEFLECTION PROPERTIES OF THREE VITON SEAL CANDIDATES AT ROOM TEMPERATURE

Candidate	Specimen No.	Avg. Load per Lineal Length g/lineal, cm	(lb/lineal, inch)	Avg. Cyclic Energy in Joules x 10^{-3} Imposed	Recovered	Avg. Elastic Hystersis in Joules x 10^{-3} +	*
Viton E-60C (Black)	1	4.5×10^3 g/cm	(24.75 ppi)	138	117	22	(21)
	2	4.3×10^3	(23.9)	131	108	25	(22)
	3	4.9×10^3	(27.6)	137	129	28	(8)
	Average	4.6×10^3	(25.8)	135	115	25	(17)
Viton ECD-3234 (Black)	1	4.1×10^3 g/cm	(23.4 ppi)	128	111	17	
	2	4.1×10^3	(22.9)	128	108	20	
	3	4.1×10^3	(23.2)	131	110	20	
	Average	4.1×10^3	(23.2)	129	110	19	
Viton ECD-3234 (White)	1	3.5×10^3 g/cm	(19.7 ppi)	97	87	10	
	2	3.2×10^3	(18.1)	95	84	10	
	3	3.4×10^3	(19.1)	98	87	10	
	Average	3.4×10^3	(19.0)	96	86	10	

+ Avg. excluding inaccurate 1-5 cycles.

* Actual "raw" average.

same at 422K as what it had been at 296K. This is best illustrated in Table 19, which summarizes results of the load deflection measurements on the three types of Viton O-rings at all three temperatures.

It was expected that both the load bearing properties and the cyclic work would increase or decrease concurrently. The disproportionally greater increase in cyclic work at 422K as compared to load bearing properties was unexpected. Also unexpected was the 600% increase in cyclic energy of the ECD-3234 O-rings, compared with the 70% increase exhibited by the E-60C (black) O-rings, when the temperature was raised from 298K to 422K.

In general, the subject Viton O-ring candidates are significantly better rubbers at elevated temperatures than at room temperatures. By contrast, at low temperatures such as 233K (-40F), the subject Viton O-ring candidates are terrible rubbers. As previously mentioned in Sections 3.1.3.1 and 3.1.3.2, the compressive force/energy/hysteresis of the subject compressive Viton O-rings is about 20 times greater at 233K (-40F) than it was at 296K (73F) or 422K (300F). Unfortunately, a direct comparison of the 233K (-40F) data with the 293K/422K data is complicated by a steady decay in the stress-strain constants as the compression cycling continued at 233 K(-40F). This steady decay was extensively discussed in connection with the load bearing properties, however, examination of Tables 15, 16 and 17 disclose that the imposed and the recovered energy of each cycle also show an even greater decrease as the cycling proceeds than the "Applied Force Max." values. For example, although the "Applied Force, Max." decreases to 70% of its initial value within 200 cycles, and the recovered and imposed energy values per cycle decrease to less than half of their initial values, the cyclic hysteresis decreases to only $\sim$ 14% of the initial value. In fact, the amount of heat evolved per cycle (i.e., the cyclic hysteresis) decreased 50% in the first five cycles. This rapid decrease in the value of cyclic hysteresis per cycle obviously precludes any possibility that the observed decay is simply due to a temperature buildup within the compression cycled O-ring. If either the maximum applied force or the recovered energy are plotted against the log of the number of cycles, fairly straight lines are obtained for all three Viton candidates. By contrast, when the elastic hystresis is plotted in the same way, strongly curved lines are obtained, i.e., the hysteresis decays at a much faster rate than any other parameters.

To summarize, the dynamic behavior of the subject Viton O-rings at 233K (-40F) were not only poor, but uniformly poor. Differences in the cyclic load deflection properties which exist between the three different subject Vitons at higher temperatures simply has been "frozen-out" at 233K (-40F). The data of Table 19 illustrates this clearly.

Table 19. Summary of Cyclic Load Deflection Measurements on Viton Seal Candidates

Seal Candidate	Temp.	Max Force	"Compression Set "	Avg. Energy in Joules x 10^{-3}		
				Imposed	Recovered	Hysteresis
Viton E-60C (Black)	422K (300F)	87.1 Kg (192 lb)	None	216.8	207.8	9
	293K (73F)	69.1 Kg (152 lb)	None	135.0	116.0	25 †
	233K (-40F)	1,300 to 550 Kg (2,900 to 1,235 lb)	Substantial at 233K. Complete recovery upon warming.	3,100 to 725	2,435 to 653	680 to 67
Viton ECD-3234 (Black)	422K (300F)	87.4 Kg (193 lb)	None	74.6	71.9	2.7
	293K (73F)	61.9 Kg (137 lb)	None	127.8	110.0	17.8
	233K (-40K)	1,318 to 907 Kg (2,905 to 2,000 lb)	Substantial at 233K. Measured,* 30 min. after removal, 2.7% to 3.9%	3,909 to 1,287	2,986 to 1,180	722 to 90
Viton ECD-3234 (White)	422K (300F)	95 Kg to 83 Kg (209 to 185 lb)	Slight	272.	254.	21
	293K (73F)	51.2 Kg (112 lb)	None	96.4	86.2	10.2
	233K (-40F)	1,175 to 871 Kg (2,590 to 1,920 lb)	Substantial at 233K. Complete recovery upon warming	3,062 to 1,340	2,222 to 1,281	842 to 59

* per ASTM D-395

† overage of 25 to 200 cycles only

3.1.3.4 Indicated Modulus

For most materials exhibiting reversible strain the elastic modulus is simply elastic stress per unit of elastic strain, and can be calculated from the slope of the stress-strain curve. Unfortunately, although elastomers exhibit reversible strain, their stress-strain curves are never linear and, when carried through the entire elastic range to rupture, exhibit the famous rubber "S" curve. For this reason the modulus of rubbers is usually taken as simply "stress at indicated strain." The present contract, however, was not concerned with rubbers per se, but with O-ring seals which are being compression cycled to ~22 percent compression. Although this compression strain is essentially reversible the resulting load-deflection curves include a very large shape factor. Therefore, the slope of the subject load deflection curves do not correspond to a true "modulus." In fact, since the load bearing area of the O-ring changes radically as the O-ring is compressed, this slope (called an "Indicated Modulus") does not even have the usual modulus units (i.e. Newtons/m^2, or psi), but rather the units: Kg/cm (or ppi).

In this program the Indicated Modulus was measured at 50 percent of the maximum applied load as determined by construction of a tangent at this 50 percent point both on the loading and unloading portions of the load-deflection cusp. Due to the significant, although regular, change in slope of the stress-strain cusp, this tangent cannot be geometrically constructed. An alternative method of drawing a tangent by inspection alone proved inaccurate. Construction of a co-tangent via a scribed mirror also proved unsatisfactory even when the parallax error was minimized.

A better method was finally devised which is based on the fact that it is easier to correctly "fit" one curved line to a similarly curved line at any precise point than it is to "fit" a straight line to a curved line (which is what is done when a tangent is drawn by simple inspection). If the measuring curve bears a true tangent (or co-tangent), then this tangent (or co-tangent) will, of course, be applicable for any unknown curve to which the measuring curve is fitted. A simple engineering drafting device called a Radius Template satisfies all these requirements. A straight edge is fastened on one edge, parallel to the center line, of a transparent Radius Template. This template assembly is then superimposed on the subject Instron load-deflection curves so that the 50 percent load point of the Instron curve is directly below the intersection of the "center line" with the best matching arc of the template. The slope of the template's "center line" is, of course, equal to the co-tangent of the subject load-deflection curve. It is more convenient, however, to slide a right triangle along the straight edge and draw the desired tangent at any convenient place on the Instron chart and calculate the modulus from this tangent directly.

Figure 16 shows a typical modulus measurement. The transparent Radius Template with an attached ruler-straight edge has been placed over the 100 and 200 cycle cusps of an Instron load-deflection curve for a typical Viton E-60C (black) O-ring. The 15" arc appears to conform most closely to the curvature of the 100th cycle load deflection cusp at the 50 percent of maximum load point. The intersection of the 15" arc and the centerline of the template has, therefore, been superimposed over the 50 percent maximum load point of the 100th cycle cusp and the desired tangent drawn, with the help of the right triangle.

The measured Indicated Modulus (50 percent) is: $\frac{14.96 \text{ Kg}}{.0127 \text{ cm}} = 1,157 \text{ Kg/cm.}$

The consistency of indicated moduli obtainable via this "Radius Template" method is illustrated by the analysis of the room temperature cyclic load-deflection curves of two Viton ECD-3234 (black) O-rings summarized in Table 20. As might be expected for rubbers exhibiting a small but definite hysteresis at room temperature, the 296K indicated moduli of the load (i.e., "imposed") portion of each cycle is measurably less than that exhibited upon unloading (i.e., during "recovery").

At higher temperatures (i.e., 422K) this difference between the "imposed" and "recovered" indicated moduli decreases to within the limits of experimental error. This is in accord with the substantial decreased hysteresis observed at elevated temperatures (see Table 19).

At the low temperature of 233K (-40F), all three Viton seal candidates are in the leathery region, which is characterized by great increases in the various rheological parameters. As might be expected, the corresponding indicated moduli also increased greatly upon moving from the rubbery to the leathery range. However, unlike the cyclic load deflection properties described above (i.e., the maximum applied force, the imposed and recovered energies, etc.), the indicated modulus does not decay but remains constant throughout the compression cycling. Table 21, which summarizes the indicated modulus of two Viton ECD-3234 (black) O-rings at 233K, illustrates the consistency of the indicated modulus throughout the 200 compression cycles. This consistency absolutely excludes any possibility that the previously discussed decay in the stress-strain constants during compressive cycling was due to a temperature buildup. The modulus in the leathery region is extremely thermo-sensitive. In addition, the complete absence of modulus decay by all three Viton rubber stocks suggests that the decay observed for the maximum load, hysteresis, etc. may indeed be due entirely to a transient compression set, since it is difficult to conceive of a thixotropic breakdown which would not effect the modulus. Direct evidence for such a compression set was, however, obtained in only one of the three Viton seal candidates. The indicated modulus measurements for the three subject Viton rubbers at the three test temperatures of this contract are summarized in Table 22. It will be observed that the 233K (-40F) moduli are from 16 fold for the Viton E-60C (black) to 24 fold for the ECD-3234 (white) greater than the modulus at either 296K or 422K. Once again at 233K, these Vitons show a significantly lower modulus on loading than on unloading.

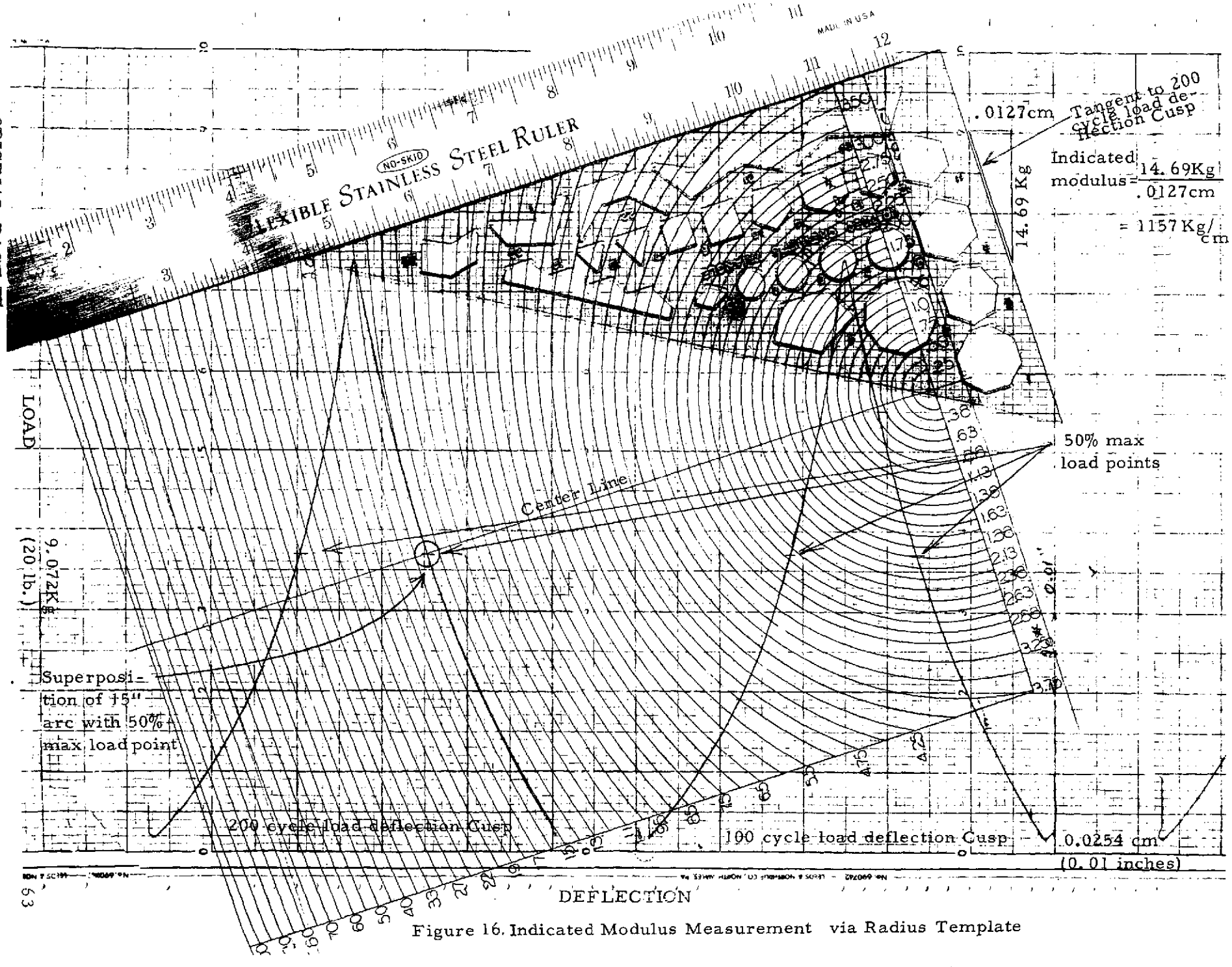

Figure 16. Indicated Modulus Measurement via Radius Template

Table 20

Indicated Modulus of Viton ECD-3234 (Black)
O-rings at Room Temperature

O-ring Specimen	Cycle No.	Indicated Modulus x 10^3 Imposed Kg/cm	Imposed (ppi)	Recovered Kg/cm	Recovered (ppi)
1	1	1.05	(5.88)	1.13	(6.31)
	2	1.06	(5.94)	1.15	(6.45)
	5	1.06	(5.94)	1.14	(6.38)
	25	1.03	(5.82)	1.15	(6.45)
	50	1.05	(5.88)	1.18	(6.5)
	100	1.18	(6.59)	1.32	(7.40)
	200	1.18	(6.59)	1.29	(7.22)
	Average	1.09	(6.09)	1.19	(6.69)
2	1	1.00	(5.60)	1.13	(6.31)
	2	1.05	(5.88)	1.15	(6.45)
	5	1.05	(5.88)	1.14	(6.38)
	25	1.07	(6.00)	1.13	(6.31)
	50	1.05	(5.88)	1.16	(6.51)
	100	1.07	(6.00)	1.13	(6.31)
	200	1.07	(6.00)	1.13	(6.31)
	Average	1.05	(5.89)	1.14	(6.37)

Table 21

Indicated Modulus of Viton ECD-3234 (Black) O-rings at 233K (-40°F)

O-Ring Specimen	Cycle No.	Indicated Modulus x 10^3			
		Imposed Cycle		Recovered Cycle	
		Kg/cm	(ppi)	Kg/cm	(ppi)
#7	1	22.0	(123)	25.2	(141)
	2	22.0	(123)	24.8	(139)
	5	22.9	(128)	23.8	(133)
	25	22.7	(127)	24.5	(137)
	50	23.2	(130)	24.5	(137)
	100	22.9	(128)	23.6	(132)
	200	22.9	(128)	24.1	(135)
	Avg.	22.7	(127)	24.3	(136)
#8	1	22.1	(124)	24.8	(139)
	2	22.3	(125)	24.5	(137)
	5	22.5	(126)	24.8	(139)
	25	23.2	(130)	24.5	(137)
	50	23.9	(134)	24.8	(139)
	100	24.6	(138)	24.8	(139)
	200	24.5	(137)	24.3	(136)
	Avg.	23.4	(131)	24.6	(138)

Table 22

Indicated Modulus of the Subject Various Viton O-rings from 233K to 422K

Conditions: Avg. of 1-200 cycles - Cycle load deflection to 22% compression

Seal Candidate		Temperature	Indicated Modulus x 10^3 Imposed Kg/cm	Imposed (ppi)	Recovered Kg/cm	Recovered (ppi)
Viton E-60C(Black)	1	422K (300F)	1.16	(6.51)	1.13	(6.36)
	2		1.19	(6.69)	1.21	(6.78)
	3		1.27	(7.12)	1.29	(7.21)
	Avg.		1.21	(6.77)	1.21	(6.78)
	1	296K (73F)	1.19	(6.69)	1.33	(7.49)
	2		1.16	(6.50)	1.31	(7.36)
	3		1.43	(8.01)	1.50	(8.45)
	Avg.		1.26	(7.07)	1.38	(7.77)
	1	233K (-40F)	18.9	(106)	19.2	(108)
	2		22.3	(125)	24.7	(138)
	Avg.		20.6	(115)	22.4	(123)
Viton ECD-3234(Black)						
	1	422K (300F)	1.29	(7.27)	1.29	(7.24)
	2		1.23	(6.92)	1.21	(6.82)
	3		1.28	(7.22)	1.27	(7.13)
	Avg.		1.27	(7.14)	1.26	(7.06)
	1	296K (73F)	1.09	(6.09)	1.19	(6.69)
	2		1.05	(5.89)	1.14	(6.37)
	3		1.09	(6.09)	1.17	(6.57)
	Avg.		1.08	(6.04)	1.17	(6.54)
	1	233K (-40F)	22.7	(127)	24.3	(136)
	2		23.4	(131)	24.6	(138)
	Avg.		23.0	(129)	24.5	(137)
Viton ECD-3234(White)						
	1	422K (300F)	1.36	(7.64)	1.30	(7.28)
	2		1.34	(7.50)	1.29	(7.22)
	Avg.		1.35	(7.57)	1.30	(7.25)
	1	296K (73F)	0.954	(5.34)	1.02	(5.70)
	2		0.834	(4.67)	0.87	(5.02)
	3		0.902	(5.05)	0.97	(5.45)
	Avg.		0.897	(5.02)	0.95	(5.39)
	1	233K (-40F)	20.7	(116)	22.5	(126)
	2		22.8	(128)	24.5	(137)
	Avg.		21.7	(122)	23.5	(131)

c - 2

3.1.4 Stress Relaxation Measurements of Hydraulic Seal Candidates

There are two basic types of stress-relaxation measurements: continuous stress relaxation and intermittent or repeated stress relaxations. Either of these may be for small deformations or for large deformations. The intermittent measurements may be at various cyclic or interval patterns, either uniform or non-uniform in loading and/or time.

Each of these basic measurements are usually strongly affected by time, temperature, initial strain, strain rate, cyclic number, cycling rate, and the material itself. Most of the effects are non-linear and often cannot be transposed into equivalent functions for dissimilar materials or conditions. Relationships between time and temperature is one of the rare exceptions, and several approximations that are good for limited ranges have been established for some of the other relationships. However, most relationships are still established by extensive testing.

Stress relaxation can be due to several causes, usually each with a different external effect. Some of these causes which have been identified are:

1. Chemical Reactions - These types of stress relaxations may involve a study of curing processes, oxidation processes, crosslinking processes, chain scission processes, or various other chemical exchange reaction rates. In general, these chemical stress relaxation measurements, in linear type tests, result in an exponential equation such as:

$$\frac{\sigma}{\sigma_o} = e^{-Kt} \quad \text{or} \quad \frac{\sigma}{\sigma_o} = e^{-\frac{t}{\lambda}}$$

   where λ = relaxation time of Maxwellian decay. Chemical stress relaxation was not encountered in this contract largely because thermally unstable and/or oxidatively susceptible materials were deliberately excluded during the seal candidate selection.

2. Irrecoverable viscous flow due to translation of whole molecules - Uncured rubber represents this type of relaxation and, as a process, it never entirely disappears for any type of rubber.

3. Physical Relaxation - This involves equilibrium within the crosslinked network. This is the basic mechanics of rubber-like materials and, for linear type tests, results in a log t type equation such as:

$$\sigma_t = \sigma_{(t=1)} - K \log t$$

When a particular rubber is involved with two different chemical reactions with different chemical rates, and these effects are combined with viscous flow and physical relaxation functions, one can begin to appreciate how complicated the stress relaxation equation can become. Some of these complications are discussed in detail in Appendix D.

In the O-ring tests performed in this program, the approach would be close to a continuous type test, although non-time controlled cyclic or repeat tests were often accomplished. The O-rings were linearly loaded but this was significantly compromised by being confined in an O-ring groove.

3.1.4.1 Test Results

Room temperature stress relaxation measurements were performed on the three Viton seal candidates. The subject O-ring was mounted in the same military (-224) size O-ring face seal which was used for the cyclic load deflection measurements of Section 3.1.3. The O-ring was compression cycled ten times to the usual 22% squeeze to minimize the usual rubber thixotropy. On the 10th cycle, the Instron head was stopped at maximum compression and the change in load recorded over a 2-hour period. The relaxation in all cases could be described by the relationship:

$\sigma = \sigma_1 - K \log t$, where σ_1 = stress when t is unity
σ = stress at time, t
K = constant

and the stress plotted against the log of time gave good straight lines.

A typical raw Instron stress relaxation curve obtained by this method is shown in Figure 17. The subject O-ring under this relaxation test was molded from Viton ECD-3234 (black). In the interest of accuracy the first minute of each relaxation was recorded at 12.7 cm (5 inches)/min. Once this initial rapid stress relaxation phase was over, the chart speed was reduced to 0.5 cm (0.2 inches)/min. in order to keep the Instron chart length within reasonable limits. This change in speed is responsible for the anomalous "break" in the otherwise smooth relaxation track of Figure 17.

Since the data indicated that all of the necessary information could be extracted from the first few minutes of relaxation, the stress relaxation period was shortened from 120 minutes to 30 minutes in the interest of economy. The slope, "K", of these O-ring relaxation curves (with the stress measured in Kg) varied from:

$1.9^{+.00}_{-.16}$ for the ECD-3234 (black) Viton to $2.77^{+.8}_{-.5}$ for the E-60C (black) Viton.

Page intentionally left blank

Reproducibility ranged from good for the ECD-3234 (black) to poor for the ECD-3234 (white) stock. Reproducibility was undoubtedly affected by the normal variation in O-ring thickness and the data could be improved by "normalizing."

Attempts to extend the Instron stress relaxation methods described above to elevated temperatures failed to yield consistent and reproducible results. These difficulties were finally traced to variable expansion and/or contraction occurring in the 30 cm. long tie rods which connect the hot (422K) O-ring test gland anvil with the Instron load cell operating at room temperature. It was calculated that as little as a 25×10^{-4} cm. contraction or expansion in the 30 cm. long tie rods will cause ~a 25% error in a stress relaxation measurement. It was apparrent, therefore, that this problem is inherent in the Instron equipment and its solution would necessitate a complete change in apparatus. The problem was finally solved by building an entirely new stress relaxation apparatus (shown in Figure 18). This apparatus consists of a Kistler Model 902 piezoelectric load washer mounted directly under the O-ring. This entire unit is loaded by a hydraulic press and can be heated to test temperatures by a clamshell oven which extends beyond the contacts to the load ram of the hydraulic press. Measuring the relaxation loads directly in the vicinity of the O-ring removes the thermal expansion problem which existed as a result of the long load arms of the Instron tester.

Using this new piezoelectric compression/stress relaxation cell, accurate stress relaxation measurements at 422K (300F) were obtained for the three Viton seal candidates. Representative checking stress relaxation curves for two Viton ECD-3234 (black) and two Viton ECD-3234 (white) O-rings are shown in Figures 19 and 20. It will be noted that although the data is invariably linear after the first minute of applied stress, the data sometimes deviates from linearity during the first few seconds of applied stress. This deviation from linearity is not associated with any particular temperature or instrumentation (it also occurred in some of the room temperature stress relaxation measurements run in the Instron tester), nor is it associated with any particular Viton compound.[1]

This apparent anomaly was finally traced to selection of the correct zero time, i.e., knowledge of when the full stress is actually applied to the specimen. If the true zero time is actually earlier than assumed, the plot will curve to the left. If the true zero time is actually later than assumed, the plot will curve to the right. This is illustrated in Figure 21. The false curves on either side of the "correct zero time" line are only 6 seconds and 12 seconds later (left) or earlier (right) than assumed. Since the stress cannot be applied instantaneously in either the hydraulically loaded piezoelectric system or the Instron tester, some uncertainty in selecting the zero time is inevitable. One added difficulty, associated

(1) Note the pronounced divergence at $t < 2$ min. for Run E, but not for Run G of Figure 20.

FIGURE 18

GENERAL DYNAMICS
Convair Division

HIGH TEMPERATURE O-RING STRESS RELAXATION APPARATUS

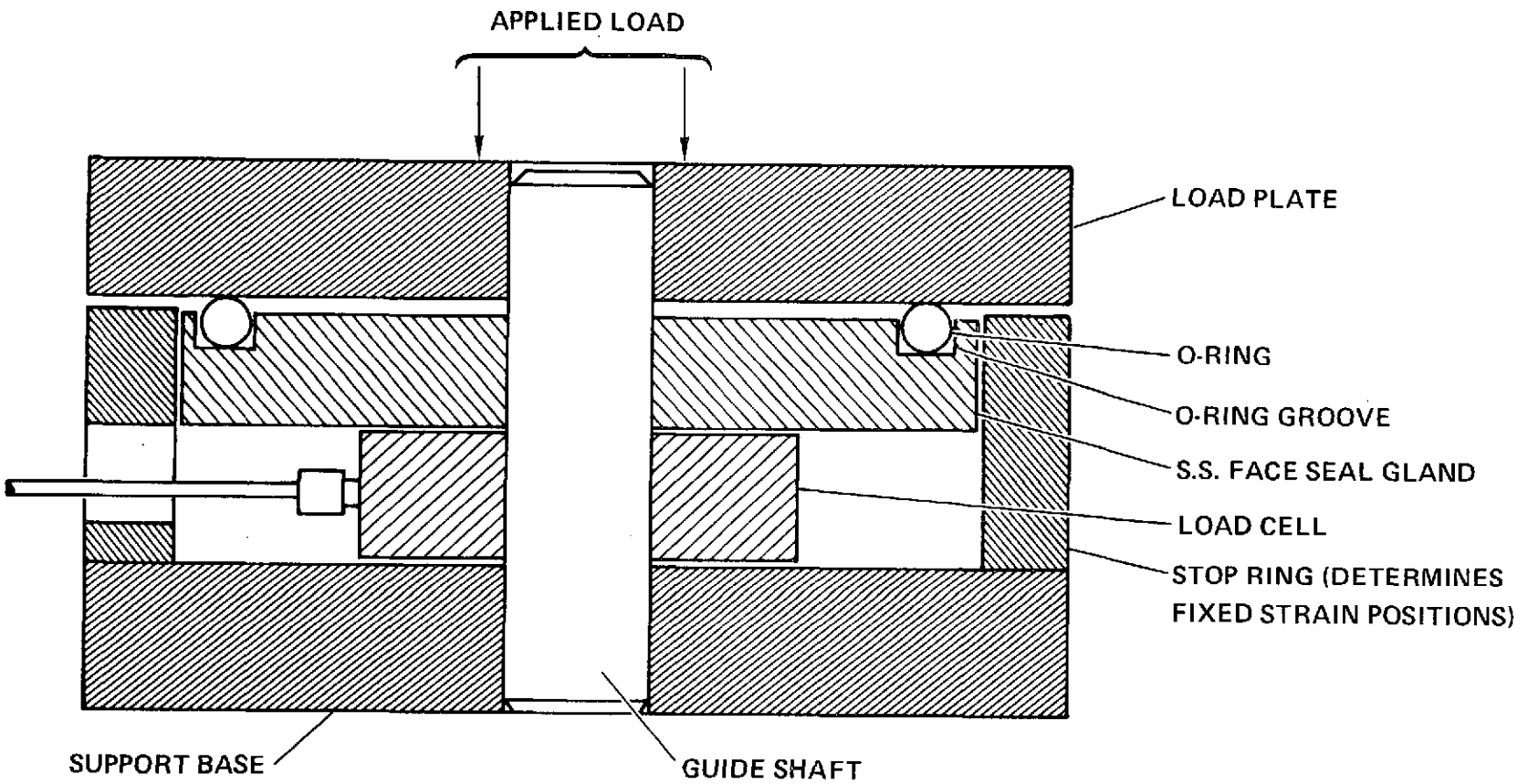

21054CVE5356

Figure 19.

GENERAL DYNAMICS
Convair Division

STRESS RELAXATION OF VITON ECD-3234 (BLACK) O-RINGS AT 422K (300F)

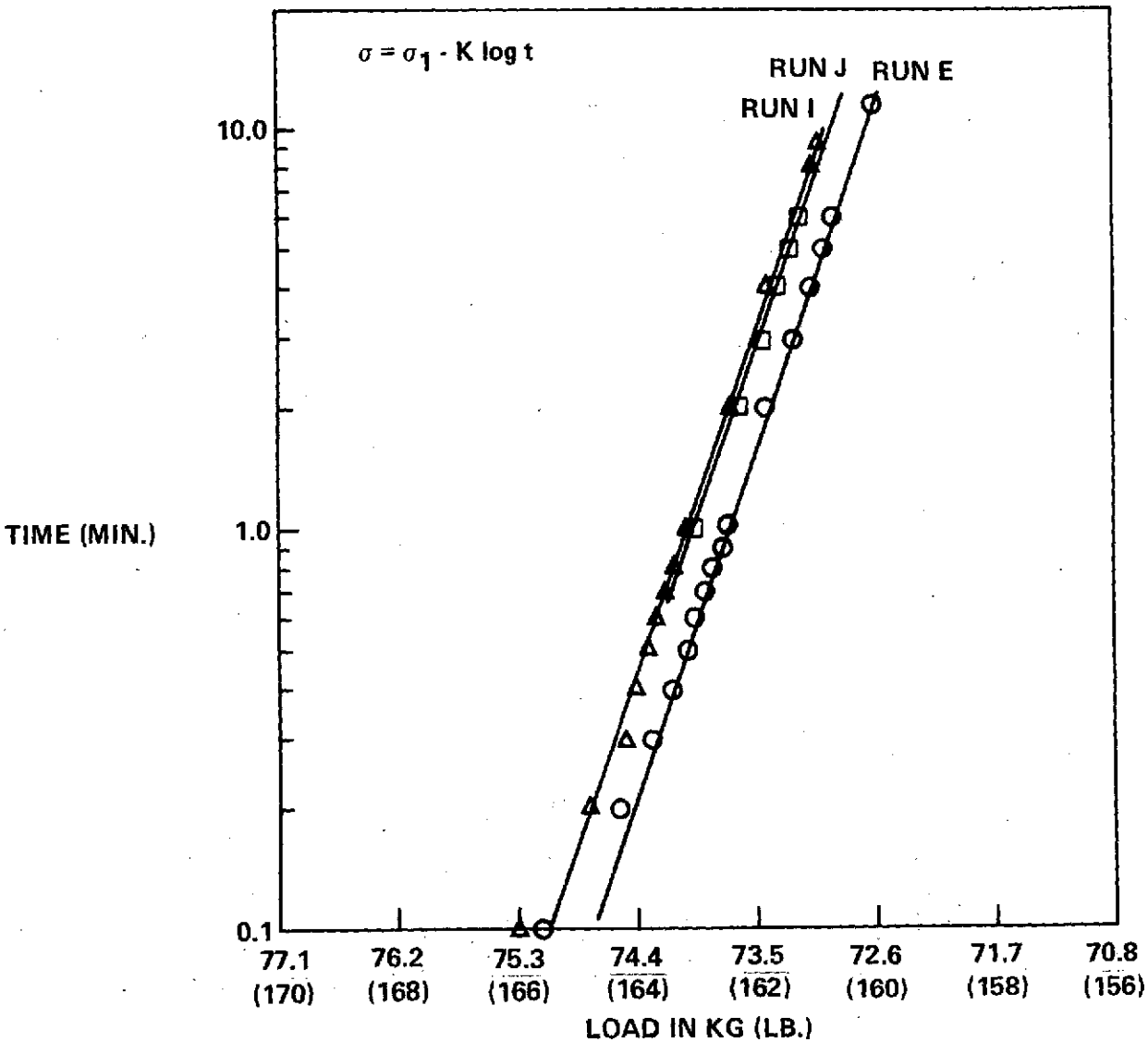

30074CVE5761

Figure 20.

GENERAL DYNAMICS
Convair Division

STRESS RELAXATION OF VITON ECD-3234 (WHITE) O-RINGS AT 422K (300F)

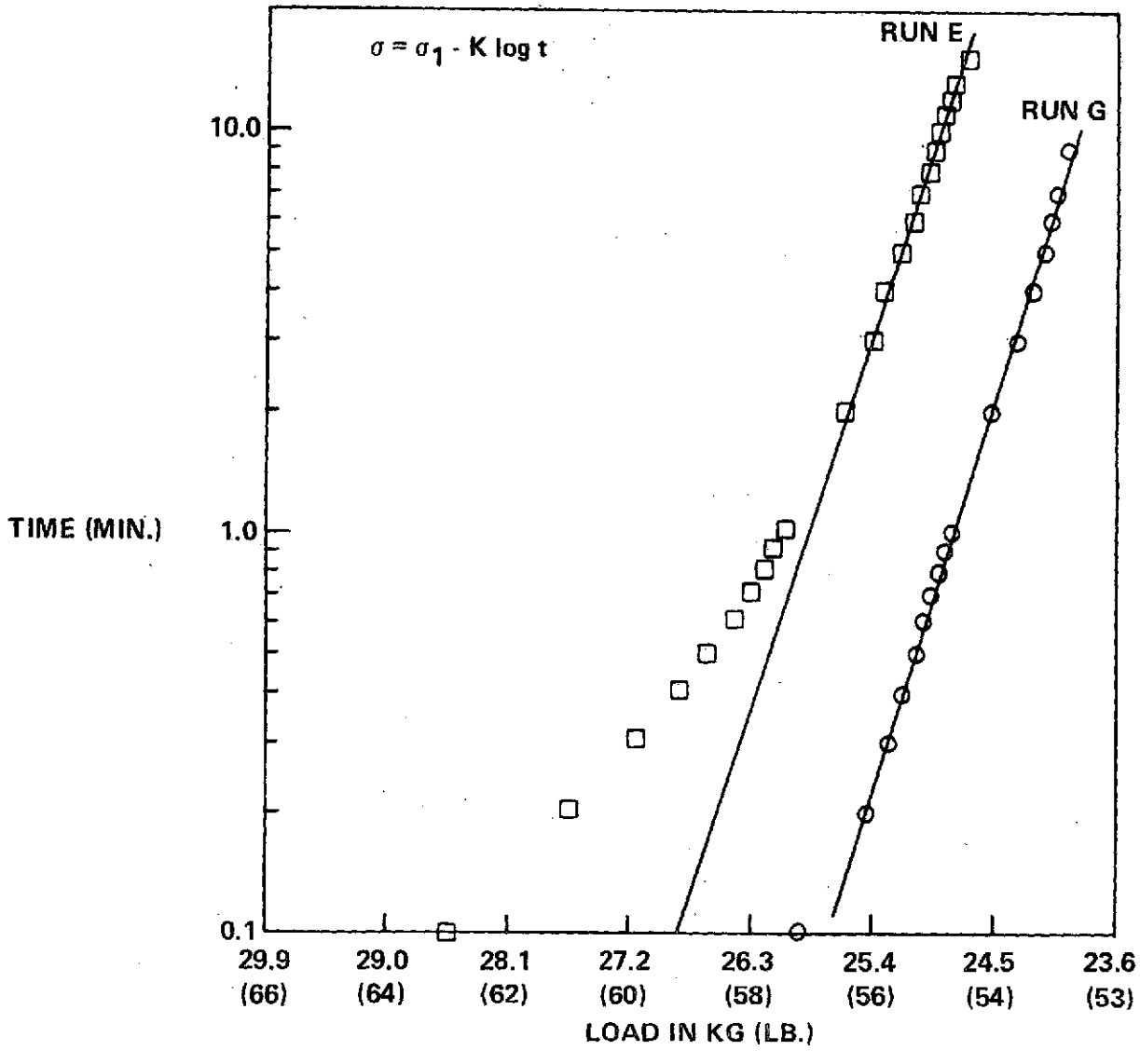

30074CVE5762

Figure 21.

GENERAL DYNAMICS
Convair Division

EFFECTS OF ERRORS IN ZERO POINT TIME SELECTION ON STRESS RELAXATION MEASUREMENTS

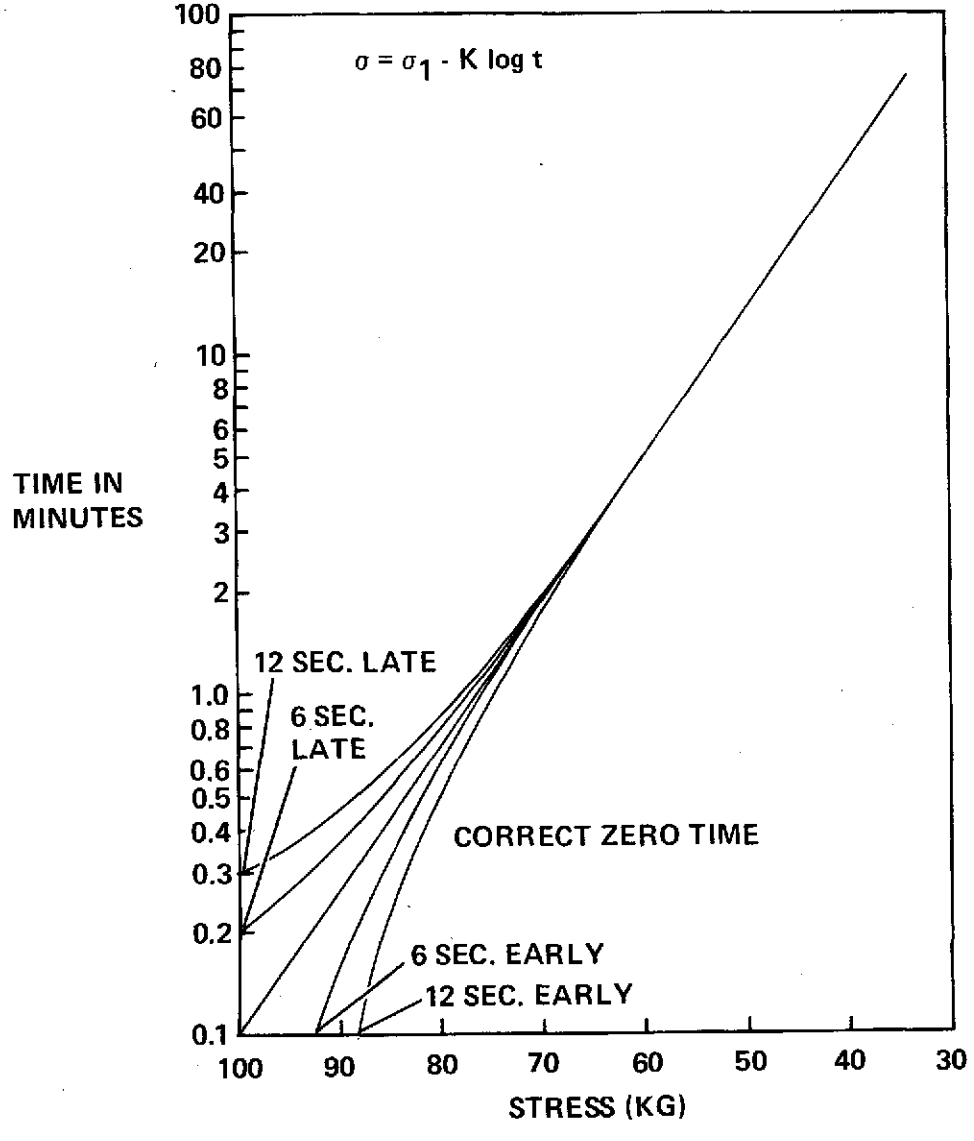

30074CVE5763

only with the higher temperature runs, is that of precise temperature control. In order to avoid the addition of elaborate temperature controls which would have unduly delayed the program, the length of time for measurement was shortened from 30 to 10 minutes. The 10 minute relaxation time was more than ample to accurately determine the relaxation constant "K" for the usual equation: $\sigma = \sigma_1 - K \log t$.

The complete stress relaxation data for the three hydraulic seal candidates at 296K (73F) and 422K (300F) are summarized in Table 23. It is apparent that there is relatively little change in stress relaxation on going from room temperature to 422K (300F). This is particularly noticeable when the data is normalized for the initial stress, i.e., when the equation is put in the form:

$$\sigma/\sigma_1 = 1 - K/\sigma_1 \log t$$

The normalized relaxation constant, K/σ_1 is tabulated at the last column of Table 23. It will be noted that, in the case of the two carbon-black filled Vitons, the rate of relaxation at 422K (300F) is actually less than it is at room temperature. Apparently, the very strong thermally stable crosslinking (i.e., curing) system employed with these three modern Vitons, coupled with the inherent oxidation resistance of the perfluoropropylene/vinylidine fluoride copolymer itself, effectively suppresses any oxidative or chemical relaxation. As a result, the stress relaxation of these well-cured Viton rubbers are relatively temperature insensitive. Moreover, since stress relaxation is the result of viscous flow by the load-bearing, molecular segments, lower temperatures can only decrease this molecular flow (and, therefore, the rate of stress relaxation) still further. Accordingly, the stress relaxation measurements originally planned for 233K (-40F) were cancelled.

Table 23

Stress Relaxation of Viton Hydraulic Seal Candidates,
At 296K and 422K; $\sigma = \sigma_1 - K \log t$

Seal Candidate	Run No.	Temperature °K	Temperature (°F)	Stress at 1 min, "σ_1" Kg	Stress at 1 min, "σ_1" (lb.)	Relaxation Constant, "K" Kg	Relaxation Constant, "K" (lb)	Nomalized Relaxation Const. "K/σ_1"
Viton E-60C	350	296	(73)	67.6	(149)	3.6	$(8.0 \pm .5)$	.054
(Black)	352	296	(73)	54.0	(119)	2.3	$(5.0 \pm .2)$	.042
	C	422	(300)	69.72	(153.7)	0.91	$(2.0 \pm .1)$	.013
	D	422	(300)	68.68	(151.4)	0.85	$(1.87 \pm .15)$	.012
Viton ECD-	553	296	(73)	55.8	(123)	1.95	$(4.3 \pm .3)$	.035
3234 (Black)	554	296	(73)	51.7	(114)	1.72	$(3.8 \pm .5)$	.033
	I	422	(300)	73.98	(163.1)	1.06	(2.34)	.0143
	J	422	(300)	73.94	(163.0)	1.05	(2.31)	.0142
	E	422	(300)	73.66	(162.4)	1.07	(2.35)	.0143
Viton ECD-	359	296	(73)	47.2	(104)	1.50	$(3.3 \pm .2)$	.032
3234 (White)	356	296	(73)	44.9	(99)	0.95	$(2.1 \pm .3)$	.021
	357	296	(73)	44.9	(99)	0.95	$(2.1 \pm .3)$	.021
	F	422	(300)	25.9	(57.0)	0.95	(2.10)	.037
	G	422	(300)	24.8	(54.6)	0.95	(2.10)	.038

3.1.5 Cyclic Compression Sealability Tests

Sealability-leak tests were performed on O-rings molded from the three Viton rubber seal candidates, Viton E-60C (black), Viton ECD-3234 (black), and Viton ECD-3234 (white) from 233K (-40F) to 422K (300F) using the following cyclic test procedure. The O-ring specimen is placed in a size (-224) stainless steel O-ring face seal gland which is mounted on the Instron tester via a self-leveling ball joint. An Instron sealing anvil containing a 0.15 cm (.063 in.) I.D. gas inlet tube is brought down on the O-ring, thus producing a small pressure cell. The inlet tube carries 500 cc of helium gas per minute under a pressure of 1.35 MN/m^2 (~196 psi). Due to the small 2 cm^3 (.122 in^3) volume of the system and the low gas flow rate, any O-ring leakage is easily detectable using an ordinary 2.06 MN/m^2 (300 psi) pressure gage.

At 296K (73F) all three types of Viton O-rings started to seal with as little as 13.6 Kg (30 lbs.) and 10% compression. Once sealing action has occurred, an elastic O-ring (pressurized on one side) will continue to seal long after the flange loading has been reduced to zero. The Instron curve of a typical dynamic sealability test is shown in Figure 22. It can be seen that this particular O-ring [(size (-224))Viton ECD-3234 (black), W = .1350 in.] started to seal (i.e., the internal helium gas pressure started to build up) when the O-ring had been compressed to the extent of 0.10 mm (0.004 in.) i.e. 10%, and had achieved complete sealing (as indicated by the internal pressure reaching 1.35 MN/m^2 (196 lb)) when the O-ring had been compressed to the extent of 0.228 mm (0.009 in.), i.e., 26%. Once complete sealability had been achieved, the internal helium pressure remained constant at 1.35 MN/m^2 regardless of compression or decompression of the O-ring. The height of the Instron curve, i.e., the recorded load will, therefore, be a sum of the Instron head loading on the O-ring plus the force generated by the internal pressurization.

As can be seen, the Instron loading was increased at the rate of 0.508 mm/min. (.02 in/min.) until the O-ring was completely compressed into the O-ring gland and metal-to-metal, anvil-to-gland contact was established. This required 372 kg. (820 lbs) and the measured head travel was 0.89 mm (.035 in.). The head travel was then reversed and the O-ring unloaded at the same steady rate of 0.508 mm/min. Unlike the compression portion of this test, the decompression portion of the curve did not fall off rapidly as the O-ring was unloaded. In fact, the sealing anvil was raised the full 0.89 mm (0.035 in.) above the gland surface without the recorded Instron load falling below 296 kg (655 lbs.). With a 0.89 mm gap, the O-ring theoretically should have been completely unloaded and leaking. Actually, the Instron sealing anvil was raised another 0.127 mm (0.050 in.) before the O-ring leaked leaking occurring by a catastrophic blow-out of the O-ring from the test gland.

FOLDOUT FRAME 1

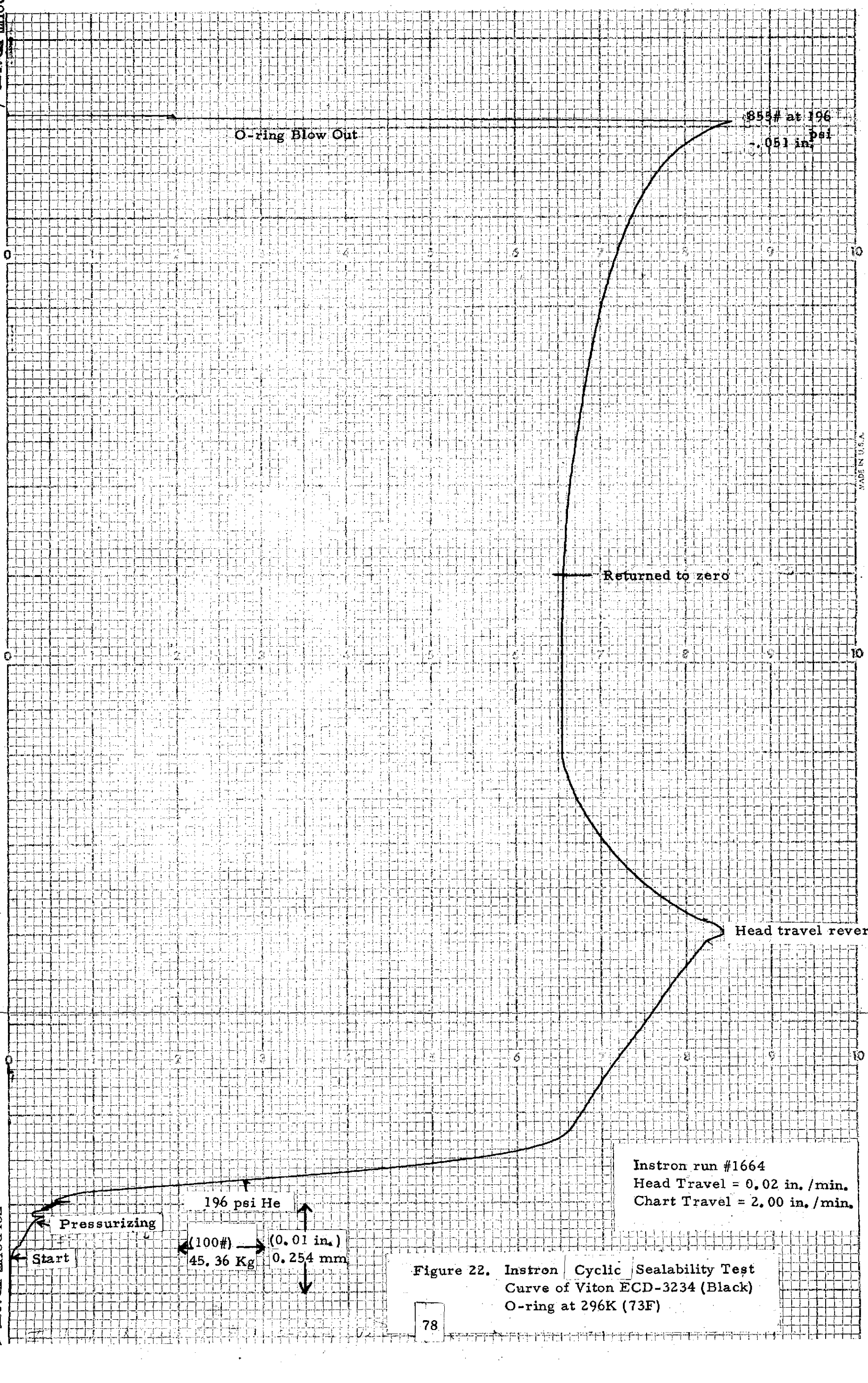

Figure 22. Instron Cyclic Sealability Test Curve of Viton ECD-3234 (Black) O-ring at 296K (73F)

FOLDOUT FRAME 2

It is apparent that as the face seal gland was "opened," the internally pressurized elastic O-ring moved out against the gland shoulder and finally extruded between the gland shoulder and sealing anvil. This mechanism also accounts for the surprising rise in the Instron recorded load during the later part of the test while the sealing anvil was raising from 0.89 mm to 1.37 mm above the gland face. Obviously, not only would the O-ring wedged between the gland shoulder and the sealing anvil exert a very real force, but the pressurized area on the anvil would also increase. The net result of this outward extrusion of the elastic O-ring into the clearance between the gland shoulder and the anvil sealing surface was that sealing action was maintained until the clearance amounted to as much as 40% of the thickness of the O-ring. All three types of the subject Viton O-rings gave nearly identical Instron sealability test curves, and it is likely that any elastic O-ring, regardless of composition, will behave similarly. Failure occurred by complete extrusion (blowout) of the O-ring from between the gland shoulder and the sealing surface surface. These "blowouts" do not appear to damage the O-ring, and they could be, and were, remounted and reused immediately. The sealability test curves obtained from these "reused" O-rings were essentially identical to those obtained with the virgin O-rings.

Sealability characteristics at 422K (300F) are similar to those exhibited at room temperature, however, the data is more erratic and the terminating "blowout" often requires a significantly larger clearance between the gland shoulder and the sealing anvil, particularly in the case of the Viton ECD-3234 (white) O-rings. In addition, at 422K many of these Viton O-rings ruptured (i.e., broke) during the blowout. A typical 422K Instron cyclic sealability test curve is shown in Figure 23.

At 233K (-40F), where the Viton O-rings are in the leathery region and have lost virtually all their high elasticity, the subject O-rings started to seal even more readily (i.e., at 3% compression and 4.54 Kg (10 lbs.) flange loading). High anvil loading of ~454 kg (~1000 lb), however, are required to achieve complete sealing. In addition, the Viton rubber modulus is much too high at 233K to allow the O-ring specimens to extrude into the clearance between the gland shoulder and the anvil sealing surface (at least under the 1.35 MN/m^2 (196 psi) gas pressure utilized in these tests). As a result, at 233K the Instron sealability test curves no longer have the unusual saddle shape peculiar to elastic O-rings, but instead have a more normal leakage curve. A representative curve, for a Viton ECD-3234 (black) O-ring is shown in Figure 24.

In order to minimize the considerable "cyclic compression set" exhibited by the subject O-rings at 233K,[1] the O-rings were completely compressed (i.e., to ~28% squeeze) during the first cycle. The loadings required to achieve complete

(1) This "cyclic compression set" phenomena was extensively discussed in Section 3.1.3.2 of this report.

FOLDOUT FRAME 1

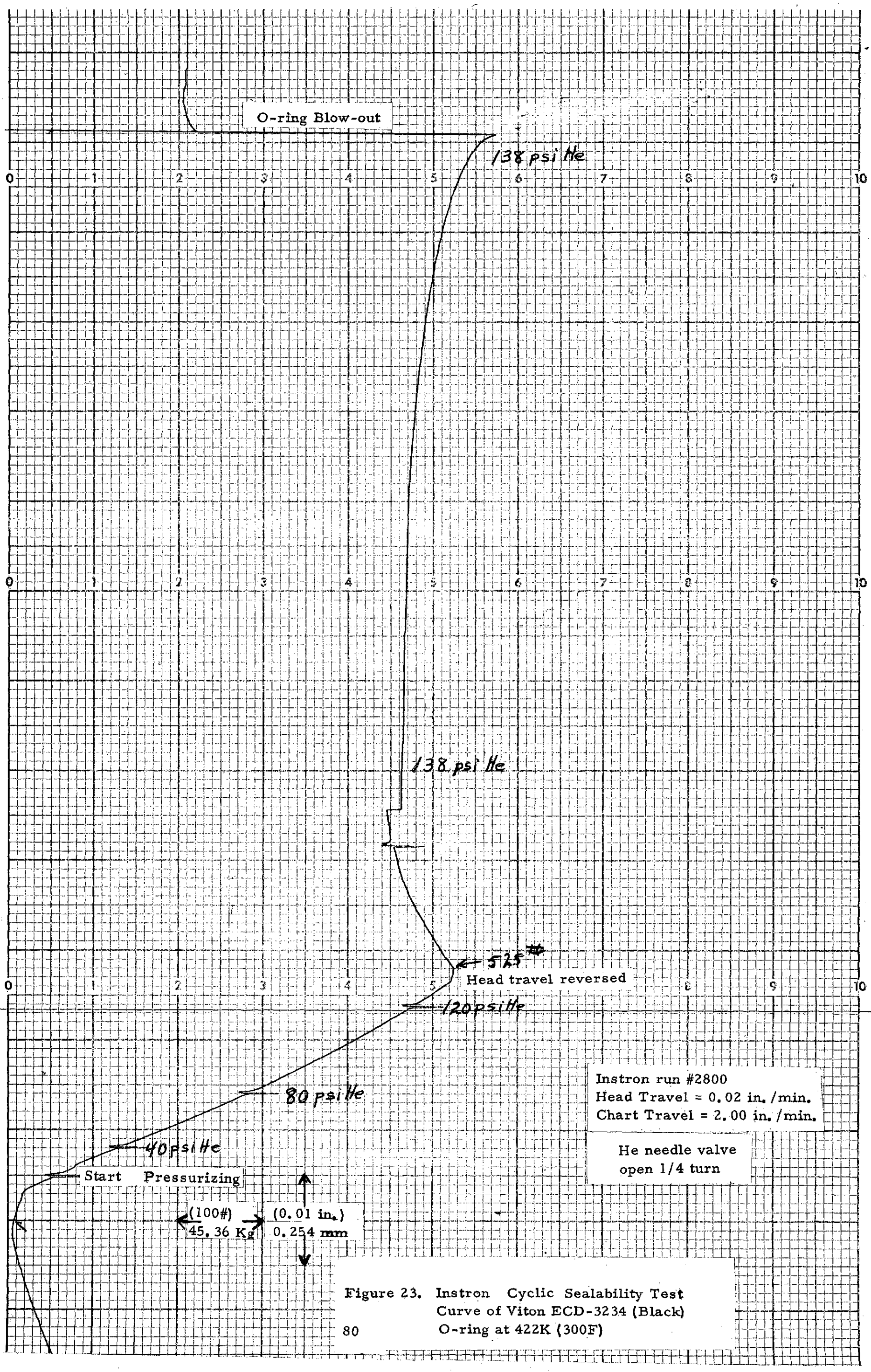

Figure 23. Instron Cyclic Sealability Test Curve of Viton ECD-3234 (Black) O-ring at 422K (300F)

FOLDOUT FRAME 2

Page intentionally left blank

sealability on both the loading and the unloading portion of this first cycle was noted. On all subsequent leak test cycles, the O-ring was loaded to approximately halfway between these two loadings. In Figure 24 for example, in the first cycle the O-ring was completely compressed by applying 1,588 kg (3,500 lb). Complete sealing (196 psi internal pressurization) required 520 kg (1,150 lb) on the initial loading. The first leakage appeared at 300 kg (660 lb) on the initial unloading. An intermediate maximum loading of 454 kg (1,000 lb) was therefore employed in the subsequent compression sealing cycles. Following this initial cycle, the system became stable and the sealing/loading cycles quite reproducible. Complete sealability in the next five cycles ranged from 413 kg (910 lb) to 431 kg (950 lb), and the first detectable leakage appeared between 259 kg (570 lb) and 272 kg (600 lb).

The complete sealability behavior from 233K (-40F) to 422K (300F) of each of the three subject Viton seal candidates is shown in Tables 24 to 26. Since these three tables are rather voluminous, the average data for the three types of O-rings at the three subject temperatures is summarized in Table 27. If the first high loading cycle of the 233K (-40F) sealability test (which is non-reproducible) is disregarded, the sealability data is reasonably consistent. It should be noted that this first non-reproducible sealability cycle of the 233K (-40F) tests (shown in Tables 24 to 26) is not included in the average values listed in Table 27.

The following conclusions are clearly indicated by Table 27:

1. At low temperature (i.e., 233K), the forces and compressions required to obtain both initial and complete sealing are almost identical for all three types of Vitons.

2. As the test temperature is raised to 296K and 422K, the amount of compression required to achieve complete sealability increases significantly while the required loading force decreases sharply. This is to be expected, since the "indicated" modulus of the subject Vitons increases $\sim$20 fold on moving from the high temperature rubbery region to the low temperature leathery region (see Section 3.1.3.4 and Table 22).

3. Within each test temperature the three types of Vitons show very similar sealing properties, both on the loading and the unloading portion of the cycle.

TABLE 24

THE SEALABILITY BEHAVIOR OF VITON E-60C (BLACK) O-RINGS FROM 233K (-40F) TO 422K (300F)

Conditions: Instron Head Speed = .509 mm/min. (.02 in/min.)
Internal Pressurization = 1.34 MN/m^2 (195 psi)
He at 500 ml/min.

		Instron Loading Cycle								Instron Unloading Cycle							
		Initial Sealing				Complete Sealing				Initial Leak				Complete Loss of Sealing			
		Load		Compression		Load		Compression		Load		Compression		Load		Compression	
Temp.	O-ring Specimens	Kg	(lb)	mm	inches	Kg	(lb)	mm	(inches)	Kg	(lb)	mm	(inches)	Kg	(lb)	mm	(inches)
233K (-40F)	O-ring #1, Initial Run	4.54	(10)	.15	(.006)	771	(1700)	.53	(.021)	295	(650)	.58	(.023)	< 4.5	(< 10)	.41	(.016)
	1st rerun	*15.9	(35)	.10	(.004)	-	-	-	-	349	(770)	.33	(.013)	9.1	(20)	.13	(.005)
	2nd rerun	18.1	(40)	.10	(.004)	445	(980)	.41	(.016)	308	(680)	.41	(.016)	9.1	(20)	.23	(.09)
	3rd rerun	20.4	(45)	.08	(.003)	431	(950)	.33	(.013)	277	(610)	.10	(.009)	6.8	(15)	.28	(.011)
	4th rerun	9.1	(20)	.08	(.003)	435	(960)	.30	(.012)	281	(620)	.23	(.009)	6.8	(15)	.25	(.010)
	O-ring #2, Initial Run	*113	(250)	.15	(.006)	975	(2150)	.51	(.020)	261	(575)	.46	(.018)	~4.5	(~10)	.25	(.010)
	1st rerun	9.1	(20)	.10	(.004)	445	(980)	.33	(.013)	272	(600)	.23	(.009)	< 4.5	(< 10)	.08	(.003)
	2nd rerun	6.8	(15)	.08	(.003)	454	(1000)	.30	(.012)	272	(600)	.20	(.008)	< 4.5	(< 10)	.05	(.002)
	3rd rerun	4.5	(10)	.08	(.003)	454	(1000)	.30	(.012)	286	(630)	.20	(.008)	< 4.5	(< 10)	.03	(.001)
296K (73F)	O-ring #1, Initial Run	17.2	(38)	.15	(.006)	297	(655)	.36	(.014)	None, "Blow out"				372	(820)	-1.45	(-.057)
	rerun	13.6	(30)	.18	(.007)	299	(660)	.41	(.016)	None, "Blow out"				361	(796)	-1.32	(-.052)
	O-ring #2, Initial Run	18.1	(40)	.17	(.0065)	295	(650)	.38	(.015)	None, "Blow out"				374	(825)	-1.37	(-.054)
	rerun	13.6	(30)	.18	(.007)	295	(650)	.41	(.016)	None, "Blow out"				378	(834)	-1.30	(-.051)
422K (300F)	O-ring #1	18.1	(40)	.13	(.005)	252	(555)	.74	(.029)	None, "Blow out" (O-ring broke)				259	(570)	-1.78	(-.070)

* Erroneous values caused by presence of ice crystals on anvil face.

TABLE 25

THE SEALABILITY BEHAVIOR OF VITON ECD-3234 (BLACK) O-RINGS
FROM 233K (-40F) TO 422K (300F)

Conditions: Instron Head Speed = .509 mm/min. (.02 in/min.)
Internal Pressurization = 1.34 MN/m^2 (195 *psi*)
He at 500 ml/min.

		Instron Loading Cycle								Instron Unloading Cycle							
		Initial Sealing				Complete Sealing				Initial Leak				Complete Loss of Sealing			
		Load		Compression		Load		Compression		Load		Compression		Load		Compression	
Temp.	O-ring Specimens	Kg	(lb)	mm	(inches)	Kg	(lb)	mm	(inches)	Kg	(lb)	mm	(inches)	Kg	(lb)	mm	(inches)
233K	O-ring #2, Initial Run	>9.1	(<20)	.04	(.0015)	521.6	(1150)	.33	(.013)	363	(800)	.46	(.018)	< 4.5	(<10)	.29	(.0114)
(-40F)	1st rerun	~9.1	(~20)	.05	(.002)	408.2	(900)	.25	(.010)	272	(600)	.18	(.007)	< 4.5	(<10)	.02	(.001)
	2nd rerun	~9.1	(~20)	.05	(.002)	417.3	(920)	.28	(.011)	263	(580)	.18	(.007)	< 4.5	(<10)	.02	(.001)
	3rd rerun	~9.1	(~20)	.05	(.002)	422	(930)	.28	(.011)	263	(580)	.20	(.008)	< 4.5	(<10)	.02	(.001)
	4th rerun	~9.1	(~20)	.08	(.003)	431	(950)	.29	(.0115)	~263	~(580)	.19	(.0075)	< 4.5	(<10)	.02	(.001)
	5th rerun	~9.1	(~20)	.05	(.002)	431	(950)	.28	(.011)	~259	~(570)	.18	(.007)	< 4.5	(<10)	.02	(.001)
	O-ring #1, Initial Run	~18.1	(~40)	.09	(.0035)	578	(1275)	.38	(.015)	286	(630)	.56	(.022)	< 4.5	(<10)	.36	(.014)
	1st rerun	13.6	(30)	.05	(.002)	431	(950)	.25	(.010)	299	(660)	.15	(.006)	< 4.5	(<10)	.01	(.0005)
	2nd rerun	4.5	(10)	.05	(.002)	435	(960)	.28	(.011)	295	(650)	.18	(.007)	< 4.5	(<10)	.01	(.0005)
	3rd rerun	9.1	(20)	.08	(.003)	431	(950)	.28	(.011)	304	(670)	.19	(.0075)	< 4.5	(<10)	.02	(.001)
	4th rerun	4.5	(10)	.08	(.003)	445	(980)	.29	(.0115)	304	(670)	.23	(.009)	< 4.5	(<10)	.05	(.002)
	5th rerun	13.6	(30)	.10	(.004)	435	(960)	.29	(.0115)	295	(650)	.23	(.009)	< 4.5	(<10)	.05	(.002)
296K	O-ring #2, Initial Run	9.1	(20)	.10	(.004)	299	(660)	.41	(.016)	None, "Blow out"				381	(840)	-1.35	(-.053)
(73F)	rerun	6.8	(15)	.13	(.005)	304	(670)	.41	(.016)	None, "Blow out"				410	(903)	-1.32	(-.052)
	O-ring #1, Initial Run	13.6	(30)	.33	(.013)	299	(660)	.56	(.022)	None, "Blow out"				365	(805)	-1.19	(-.047)
	rerun	13.6	(30)	.20	(.008)	295	(650)	.43	(.017)	None, "Blow out"				388	(855)	-1.30	(-.051)
422K	O-ring #8	9.98	(22)	.08	(.003)	227	(500)	.76	(.030)	None, "Blow out"		(O-ring broke)		272	(600)	-3.81	(-.150)
(300F)	O-ring #9	18.1	(40)	.10	(.004)	237	(522)	.66	(.026)	None, "Blow out"				260	(573)	-1.73	(-.068)

TABLE 26

THE SEALABILITY BEHAVIOR OF VITON ECD-3234 (WHITE) O-RINGS
FROM 233K (-40F) TO 422K (300F)

Conditions: Instron Head Speed = .509 mm/min. (.02 inches/min.)
Internal Pressurization = 1.34 MN/m^2 (195 psi)
He at 500 ml/min.

		Instron Loading Cycle								Instron Unloading Cycle							
		Initial Sealing				Complete Sealing				Initial Leak				Complete Loss of Sealing			
		Load		Compression		Load		Compression		Load		Compression		Load		Compression	
Temp.	O-ring Specimens	Kg	(lb)	mm	(inches)	Kg	(lb)	mm	(inches)	Kg	(lb)	mm	(lb)	Kg	(lb)	mm	(inches)
233K	O-ring #1, Initial Run	32	(70)	.10	(.004)	771	(1700)	.56	(.022)	286	(630)	.56	(.022)	<4.5	(<10)	.28	(.011)
(-40F)	1st rerun	11	(25)	.10	(.004)	~454	~(1000)	.33	(.013)	299	(660)	.23	(.009)	<4.5	(<10)	.05	(.002)
	2nd rerun	9.1	(20)	.08	(.003)	~454	~(1000)	.30	(.012)	299	(660)	.22	(.0085)	<4.5	(<10)	.03	(.001)
	3rd rerun	9.1	(20)	.08	(.003)	~454	~(1000)	.30	(.012)	295	(650)	.20	(.008)	<4.5	(<10)	.03	(.001)
	4th rerun	5.9	(13)	.08	(.003)	~454	~(1000)	.30	(.012)	295	(650)	.18	(.007)	<4.5	(<10)	.05	(.002)
	5th rerun	5.9	(13)	.06	(.0025)	~454	~(1000)	.28	(.011)	286	(630)	.18	(.007)	<4.5	(<10)	.00	(.000)
	O-ring #2, Initial Run	~11	(~25)	.08	(.003)	544	(1200)	.33	(.013)	295	(650)	.56	(.022)	<4.5	(<10)	.33	(.013)
	1st rerun	6.8	(15)	.08	(.003)	431	(950)	.30	(.012)	240	(530)	.18	(.007)	<4.5	(<10)	.05	(.002)
	2nd rerun	-	-	.05	(.002)	431	(950)	.28	(.011)	245	(540)	.18	(.007)	<4.5	(<10)	.05	(.002)
	5th rerun	2.3	(5)	.03	(.001)	435	(960)	.25	(.010)	272	(600)	.15	(.006)	<4.5	(<10)	.00	(.000)
296K	O-ring #1, Initial Run	13.6	(30)	.13	(.005)	209	(460)	.23	(.009)	None, "Blow out"				365	(805)	-1.50	(-.059)
(73F)	1st rerun	9.1	(20)	.15	(.006)	297	(655)	.38	(.015)	None, "Blow out"				345	(760)	-1.42	(-.056)
	2nd rerun	7.3	(16)	.13	(.005)	297	(655)	.36	(.014)	None, "Blow out"				369	(814)	-1.04	(-.041)
	O-ring #2, Initial Run	4.5	(10)	.15	(.006)	295	(650)	.38	(.015)	None, "Blow out"				396	(874)	-1.37	(-.054)
	1st rerun	9.1	(20)	.15	(.006)	299	(660)	.36	(.014)	None, "Blow out"				364	(802)	-1.12	(-.044)
422K	O-ring #8	10.4	(23)	.15	(.006)	245	(540)	.74	(.029)	*None, "Blow out"				286	(630)	-1.09	(-.043)
(300F)	O-ring #9	4.5	(10)	.10	(.004)	186	(410)	.99	(.039)	+None, failed by massive leak on 7th cycle				197	(435)	-.13	(-.005)

* Due to operator error, this O-ring was subjected to 4 complete compression/relaxation cycles in which the clearance between the gland shoulder and the anvil mating surface ranged from 0.0127 cm (.005 in.) to 0.076 cm (.030 in.) prior to the final "blow out" cycle.

\+ Due to operator error, this O-ring was subjected to 6 complete compression/relaxation cycles in which the gland/anvil clearance cycled from .0127 cm to .076 cm. Failure occurred by formation of a crack completely around the O-ring on the 7th cycle.

TABLE 27

SUMMARY OF THE SEALABILITY BEHAVIOR OF THE THREE TYPES OF VITON O-RINGS FROM 233K (-40F) TO 422K (300F)

Conditions: Instron Head Speed = .509 mm/min. (.02 in./min.)
Internal Pressurization = 1.34 MN/m^2 (195 psi)
He at 500 ml/min.

Temp.		Instron Loading Cycle				Instron Unloading Cycle			
		Initial Sealing		Complete Sealing		Initial Leak		Complete Loss of Sealing	
		Load Kg	Compression (mm)	Load Kg	Compression (mm)	Load Kg	Compression (mm)	Load Kg	Compression (mm)
	E-60C (Black)								
233K		*12	.09	444	.33	283	.30	6	+.19
296K		16	.17	297	.39	Blow Out		371	-1.36
422K		18	.13	252	.74	Blow Out with rupturing		259	-1.78
	ECD-3234 (B)								
233K		*10	.07	430	.28	300	.20	4.5	+.03
296K		11	.19	299	.45	Blow Out		386	-1.3
422K		14	.09	232	.70	Blow Out with rupturing		265	-2.7
	ECD-3234 (W)								
233K		* 7	.07	446	.29	279	.19	4	+.03
296K		9	.14	280	.36	Blow Out		368	-1.32
422K		7	.13	215	.86	Cracked or ruptured		241	-.60

* 1st cycle disregarded

3.1.6 Static Thermal Cycling Leak Tests

Viton ECD-3234 (white) was selected as the most promising hydraulic seal candidate on the basis of its superior high temperature resistance to MIL-H-83282 hydraulic fluid (see Sections 3.1.1.2 and .3).

The essential parts of the static thermal cycling leak test assembly is shown in Figure 25. The subject O-ring is mounted in the stainless steel military face seal gland, size (-224), and compressed by means of a stainless steel loading anvil. 0.203mm (0.008 in.) thick shims were placed between the gland shoulders and the anvil to insure a constant 20% compression of the O-ring. The assembly was vertically loaded by three "C" clamps arranged uniformly around the periphery. In order to prevent these "C" clamps from loosening during the nearly 200K range of thermal cycling, the assembly was spring loaded with two heavy Belleville-type National Disc Springs (P/N AM804150) stacked in series. The gland was internally pressurized with 1.35 MN/m^2 (196 psi) of gaseous helium by means of a 0.203 mm (0.008 in.) I.D. introduction tube silver soldered through the anvil. Due to the small volume of the system, any leakage was readily detectable. Full sealability was defined as no observable loss in pressure measured via a conventional 2.06 MN/m^2 (300 psi) pressure gage over five minutes time at zero inlet flow rate.

This test fixture containing the Viton ECD-3234 (white) O-ring was thermocoupled and manually placed successively in a 296K (73F) water bath, a 422K (300F) constant temperature oven, and a 233K (-40F) cold reservoir. A refrigerated tank of Freon MF (i.e. chlorotrifluoromethane) maintained at 230K served as the cold reservoir. In order to prevent the Freon MF from solvating the Viton O-ring, the entire test fixture was encased in a polyethylene bag before immersion in the refrigerated Freon. After coming to each designated temperature, the fixture was held at that temperature for a minimum of thirty minutes before passing on to the next thermal environment. The following successive temperature stages comprised one complete thermal cycle:

296K(73F)	→	422K(300F)	→	296K(73F)	→	233K(-40F)	→	296K(73F)
Full Sealability		Full Sealability		Full Sealability		Slow leak which gradually increased with time		Full Sealability

Each O-ring was subjected to three complete thermal cycles. As indicated by the inscription shown under each stage, leakage only occurred at the lowest temperature (i.e. at 233K), and full sealability was regained upon warming.

FIGURE 25

STATIC THERMOCYCLING O-RING LEAK-TEST FIXTURE

GENERAL DYNAMICS
Convair Division

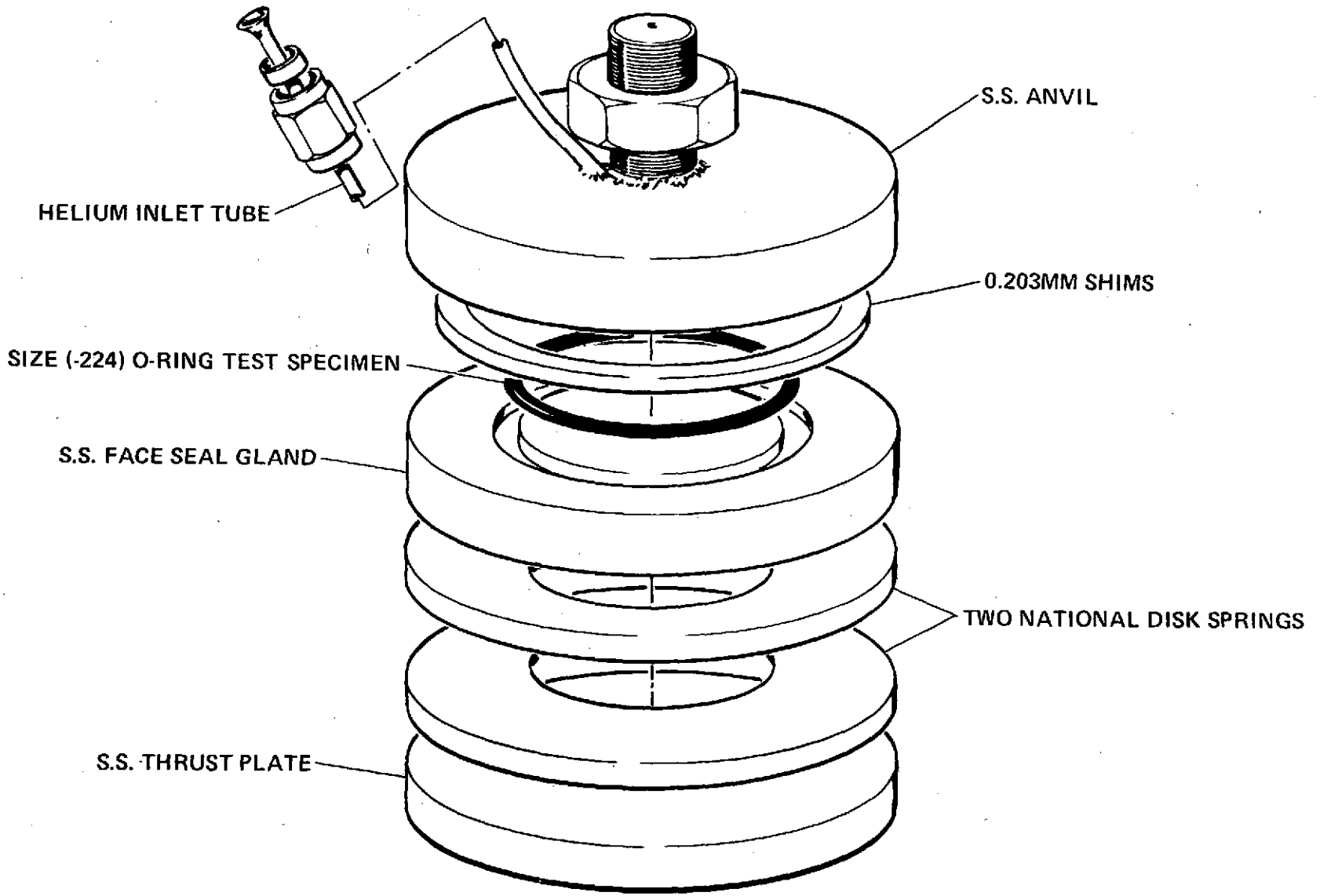

21054CVE5357

The indicated behavior was completely reproducible with all of the O-rings tested regardless of the particular cycle or the length of time the O-ring is held in the various stages, except in the low temperature stage. Absolutely no leakage was ever detected on the cooling cycle until the gland temperature fell below 243K (-22F). At lower temperatures, the rate of leakage depended on the rate of cooling and/or dwell time. At the cooling rate of 0.5 K/min. the rate of leakage gradually increased until at 236K (-35F) the Viton ECD-3234 (white) O-ring was leaking at the rate of~200cc He/min. (estimated), and at 233K (-40F) the leakage rate had increased to~400cc He/min. Surprisingly, still further cooling to 230K (-46F) increased the leakage rate only slightly.

On the warm-up cycle, leakage decreased sharply. By the time the gland temperature had risen to 236K (-35F), the leak rate had dropped to~300 cc/min., and full sealability was recovered by the time the gland temperature had risen to 243K (-22F). It is entirely probable that much of the erratic behavior in the low temperature stage may simply reflect a failure of the O-ring specimen (an insulator) to come to thermal equilibrium with the metallic test fixture within the 0.5K/min. heating and cooling rates employed. It should also be emphasized that the particular low temperature leakage behavior observed in the subject Viton O-rings is probably related to the 20% compression employed. In the preceeding section (3.1.5), it was shown that at low temperature leakage is indeed a function of squeeze.

3.2 Main Propellant Seals

3.2.1 Cryogenic Soak Testing of Main Propellent Seal Candidates

It was originally proposed to test those seal candidates intended for liquid hydrogen use in LH_2 (20K/423F), and to test those seal candidates intented for liquid oxygen use in LN_2 (76K/-320F). Since any seal candidate which could survive the 20K temperature soak would certainly survive the 76K temperature, it was decided to dispense with the LN_2 soak and subject all seal candidates to the more severe LH_2 soak. Accordingly, tensile specimens of the four candidate elastomers:

phosphazine fluoroelastomer #1884-34 (A)
Viton ECD-3234 (white)
Viton E60-C (white)
perfluoroelastomer AF-E-124D

and of the three fluoroplastics:

linear Halar
crosslinked Halar
linear Tefzel

were subjected to a one-hour soak in LH_2. After warming back to room temperature, the elastomers were tensile tested (via Instron tester) at the usual 20 in/min. and the fluoroplastics at 0.2 in/min.

Results are summarized in Tables 28 and 29. For comparison, virgin specimens (both GD/C molded and vendor molded), are included. Both the 20% and 100% rubber modulus* are listed for the elastomer seal candidates. Since the fluoroplastic seal candidates exhibit clearly defined tensile yield points (see Figure 26), two tensile strengths (at "yield" and at "break") and two elongations (also at yield and at break) are required to define each candidate. The hardness of the elastomers was measured via a Shore-A durometer, the fluoroplastics via a Shore-D durometer.

It is apparent that the one-hour cryogenic exposure had little or no effect on the physical properties of these seal candidates. Section 3.2.3 which involves the thermal cycling of these same seal materials 200 times from 76K (-320F) to 344K (160F) will, of course, present much more exacting service conditions. The actual mechanical behavior of these seal candidates at cryogenic conditions is even more important, but unfortunately was outside the scope of the present program.

* rubber modulus = stress at indicated strain

Table 28

Effect of Cryogenic Temperatures on Elastomeric Seal Candidates for the Main Propellent System

Conditions: 1 hour soak in LH_2
Tested - R. T., 20 in/min. head speed

Rubber Compound	Instron Run No.	Tensile Strength Newtons/m^2 in millions	(PSI)	% Elongation at Break	Rubber Modulus (*) at 20% Newtons/m^2 in millions	(PSI)	at 100% Newtons/m^2 in millions	(PSI)	Shore A Hardness
Phosphazine Fluoroelastomer #1884-34(A)									
vendor slab "as is"	4424	5.8	(843)	200	0.16	(23)	1.45	(211)	66
after 1 hr/LH_2	4450	7.44	(1,079)	170	0.10	(15)	2.31	(335)	65
after 1 hr/LH_2	4451	7.75	(775)	170	.30	(43)	2.00	(291)	65
Average		7.00	(899)	173	.19	(27)	1.92	(279)	65
Viton ECD-3234 (White)									
GD/C slab "as is"	4398	9.5	(1,377)	200	1.20	(175)	5.4	(787)	75
GD/C slab "as is"	4399	10.0	(1,458)	200	1.31	(191)	5.77	(838)	75
GD/C slab "as is"	4400	8.1	(1,178)	190	1.22	(177)	4.53	(657)	75
Average		9.2	(1,784)	197	1.245	(181)	5.25	(761)	75
after 1 hr/LH_2	4441	9.3	(1,349)	190	0.75	(109)	4.85	(704)	78
after 1 hr/LH_2	4442	9.95	(1,444)	180	1.07	(156)	6.82	(991)	78
after 1 hr/LH_2	4443	9.05	(1,315)	180	0.92	(133)	5.20	(755)	78
Average		9.42	(1,369)	183	0.90	(133)	5.63	(817)	78
DuPont slab "as is"	4401	7.71	(1,120)	180	1.34	(194)	4.96	(721)	75
DuPont slab "as is"	4402	8.21	(1,192)	170	1.62	(236)	5.96	(866)	75
DuPont slab "as is"	4403	7.7	(1,119)	160	0.94	(136)	5.60	(814)	75
Average		7.9	(1,144)	170	1.30	(189)	5.51	(800)	75
Viton E60-C (White)									
GD/C slab "as is"	4761	10.65	(1,546)	170	1.11	(162)	6.95	(1,010)	74
GD/C slab "as is"	4762	11.4	(1,654)	180	1.23	(179)	7.44	(1,080)	75
GD/C slab "as is"	4763	10.9	(1,586)	180	1.17	(170)	7.06	(1,025)	76
Average		11.0	(1,595)	177	1.17	(170)	7.14	(1,038)	75
after 1 hr/LH_2	4444	10.4	(1,507)	170	0.99	(144)	6.4	(933)	78
after 1 hr/LH_2	4445	11.0	(1,602)	180	.98	(143)	6.45	(938)	78
after 1 hr/LH_2	4446	11.1	(1,612)	170	1.00	(145)	6.70	(972)	78
Average		10.8	(1,575)	173	.99	(144)	6.53	(948)	78
DuPont slab "as is"	4764	9.7	(1,407)	210	1.33	(194)	6.11	(887)	77
DuPont slab "as is"	4765	8.8	(1,279)	220	1.05	(152)	4.78	(694)	77
DuPont slab "as is"	4766	8.95	(1,297)	200	1.27	(184)	5.7	(827)	77
Average		9.13	(1,328)	210	1.22	(177)	5.53	(801)	77

Table 28 - Continued

Rubber Compound	Instron Run No.	Tensile Strength Newtons/m^2 in millions	(PSI)	% Elongation at Break	Rubber Modulus (*) at 20% Newtons/m^2 in millions	(PSI)	at 100% Newtons/m^2 in millions	(PSI)	Shore A Hardness
Perfluoroelastomer AF-E-124D									
GD/C slab "as is"	4758	13.2	(1,920)	180	.83	(120)	3.79	(550)	75
GD/C slab "as is"	4759	9.16	(1,330)	180	.82	(119)	4.26	(619)	75
GD/C slab "as is"	4760	15.2	(2,210)	160	.89	(130)	3.76	(545)	75
Average		12.5	(1,840)	173	.85	(123)	3.94	(571)	75
after 1 hr/LH_2	4447	16.5	(2,388)	190	.77	(112)	3.70	(538)	72
after 1 hr/LH_2	4448	14.5	(2,105)	190	.46	(68)	3.56	(517)	72
after 1 hr/LH_2	4449	15.8	(2,286)	200	.52	(75)	3.16	(459)	72
Average		15.6	(2,260)	193	.59	(85)	3.6	(505)	72

* rubber modulus = stress at indicated strain

Table 29

Effect of Cryogenic Temperature on Fluoroplastic Seal Candidates for the Main Propellant System

Conditions: 1 hour soak in LH_2
Tested - RT, 0.2 in/min. head speed

Fluoroplastic	Instron Run No.	Tensile strength at yield (PSI)	Tensile strength at yield Newtons/m^2 in millions	Tensile Strength at Break (PSI)	Tensile Strength at Break Newtons/m^2 in millions	% Elongation at Yield	% Elongation at Break	Shore-D Hardness
Linear Halar-Grade #302								
As Is	4464	(4,878)	33.6	(10,476)	72.1	3.0%	122%	76
As Is	4465	(4,740)	32.6	(10,881)	74.9	2.8%	126%	76
As Is	4466	(4,788)	33.0	(11,105)	76.5	2.8%	128%	76
Average		(4,802)	33.1	(10,821)	74.6	2.9%	125%	
after 1 hr/LH_2	4455	(4,891)	33.6	(10,883)	74.9	2.5%	132%	75
after 1 hr/LH_2	4456	(4,776)	32.9	(11,544)	79.5	2.7%	146%	75
after 1 hr/LH_2	4457	(4,859)	33.5	(10,074)	69.4	3.2%	130%	76
Average		(4,842)	33.3	(10,834)	74.6	2.8	136%	75
Vendor published data - Allied Chemical	-	(5,500)	37.8	(7,000)	48.2	-	100-250%	-
Crosslinked Halar-5 Megarads, Cobalt60, Grade #302								
As Is	4467	(4,404)	30.3	(8,505)	58.6	3.6%	236%	75
As Is	4468	(4,308)	29.7	(8,542)	59.0	3.2%	242%	75
As Is	4469	(4,396)	30.2	(8,619)	59.4	3.8%	254%	76
Average		(4,369)	3.01	(8,555)	59.0	3.5%	244%	75
after 1 hr/LH_2	4458	(4,156)	28.6	(8,638)	59.5	3.8%	272%	75
	4459	(4,101)	28.2	(7,887)	54.3	3.8%	240%	75
	4460	(4,115)	28.4	(8,360)	57.6	3.8%	260%	75
Average		(4,124)	28.4	(8,295)	57.1	3.8%	257%	75
Vendor published data - Allied Chemical		(4,750)	32.7	(7,450)	51.3	-	185%	-
Linear Tefzel								
As Is	4461	(4,045)	27.8	(6,448)	44.4	11.5%	338%	75
	4462	(4,039)	27.8	(4,721)	32.6	15.3	196%	75
	4463	(4,009)	27.6	(5,743)	39.5	13.7	314%	75
Average		(4,031)	27.7	(5,637)	38.8	13.5	283	75
after 1 hr/LH_2	4452	(2,930)	20.2	(5,082)	35.0	20.0%	268%	72
	4453	(4,162)	28.6	(5,440)	37.4	14.7%	242%	72
	4454	(4,118)	28.4	(5,983)	41.2	12.6%	294%	72
Average		(3,737)	25.7	(5,502)	37.9	15.8%	268%	72
Vendor published data - Du Pont	-	(4,000)	27.7	(6,500)	44.7	-	100-300%	75

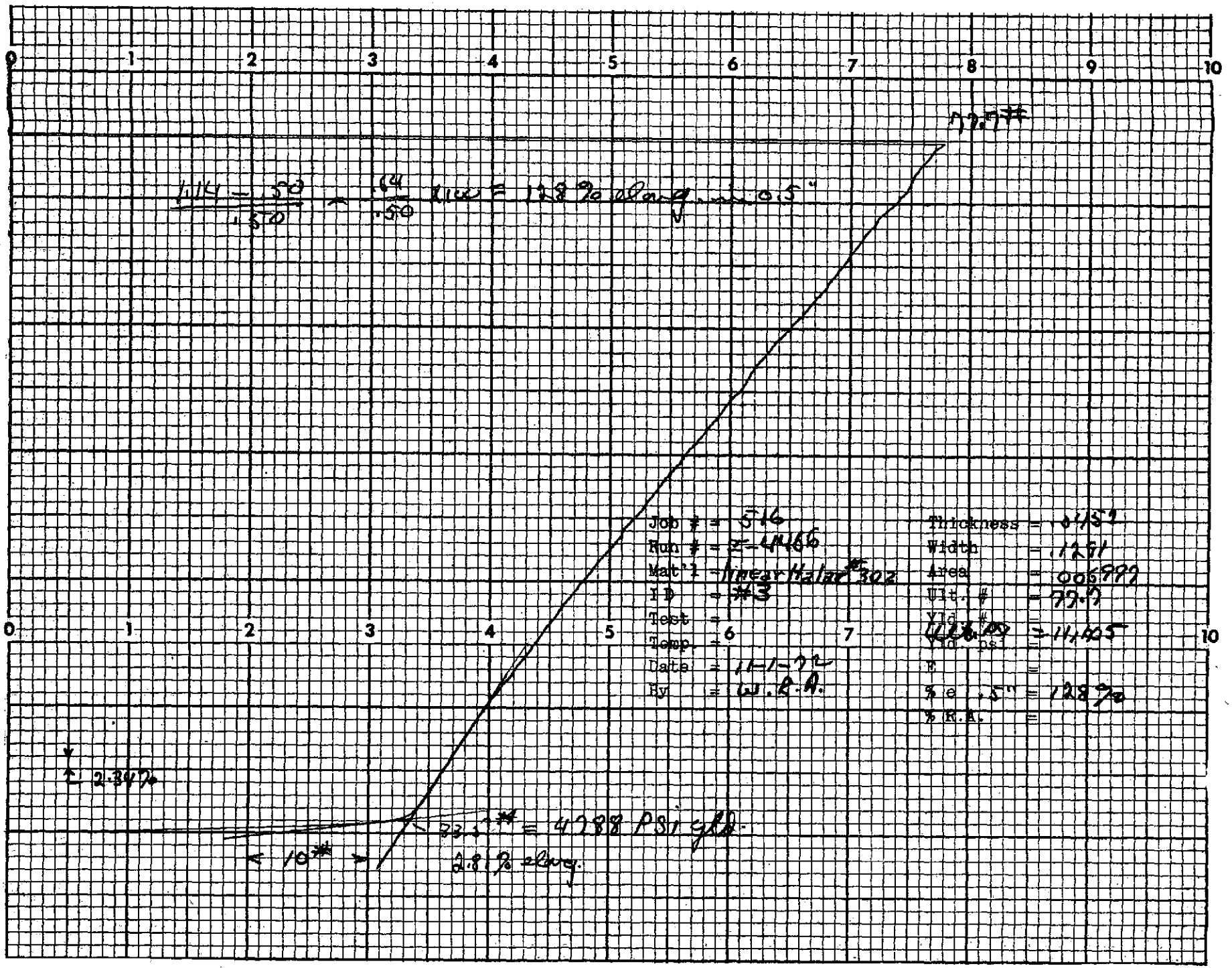

Figure 26. Instron Stress/Strain Curve of Linear Halar #302

Tables 28 and 29 are also of interest since they include the first mechanical property data on the three fluoroplastics and on the perfluoroelastomer, AF-E-124D. The latter is indeed a good strong rubber although of lower modulus than the subject Viton rubbers. The mechanical properties of both the Halar and Tefzel fluoroplastics as measured at Convair agrees fairly well with the published vendor data. The sole exception is the tensile strength at break of the linear Halar, which is ~50% greater than the published data, and is also significantly greater than that exhibited by the radiation crosslinked Halar tensile specimens. The ultimate elongation of Convair's sample of radiation crosslinked Halar is, however, nearly twice that of the uncured Halar.

3.2.2 LO_2 Impact Sensitivity Tests

Four elastomers:	phosphazine fluoroelastomer, #1884-39A Viton ECD-3234 (white) Viton E60-C (white) perfluoroelastomer AF-E-124D
and three fluoroplastics:	linear Halar crosslinked Halar linear Tefzel

were the prime candidates. As noted above, all seven of these candidates were tested and survived the one hour soak in liquid hydrogen (LH_2). Since it is highly desirable to develop main propellant seals which are applicable both to the LO_2 oxidizer as well as the LH_2 fuel, LO_2-impact compatibility is a prime requisite of these seal candidates.

Only one of the four elastomers, the perfluoroelastomer AF-E-124D, was known to be LO_2 compatible (Ref. 6). One of the fluoroplastic candidates, the linear Halar, was also known to be LO_2 compatible as measured by NASA's MSFC-SPEC -106B (Ref. 7). Since radiation crosslinking the linear Halar would certainly not decrease (and might even increase) the LO_2-impact sensitivity, only the four remaining seal candidates required LO_2-impact testing.

Discs, 1.27 cm (0.5 inches) in diameter, were cut from 0.127 mm (0.050 inch) thick sheets of these seal candidates. These discs were subjected to the standard liquid oxygen impact sensitivity test, MSF-106B. A drop height of 43.3 inches was employed and the discs were tested in the "as is" condition without any special cleaning of the surfaces. Results are summarized in Table 30. Even though all four candidates failed to pass, it was thought that the situation was not as discouraging as it appeared. For example, only one out of the 20 disc specimens of Viton ECD-3234 (white) detonated, and this was a moderate explosion on rebound. It was quite possible that this single failure was due to surface contamination since none of these specimens were specially cleaned for LO_2 use prior to testing.

At any rate, it seemed worthwhile to repeat these LO_2-impact tests with specially cleaned specimens for the two Viton rubbers and Tefzel. Due to the tacky nature of the phosphazine fluoroelastomer, 1884-34A, surface cleaning was impractical, and it was therefore not retested. It should be remembered that this tacky surface is not an inherent property of phosphazine fluoroelastomers, but merely of this particular specimen (#1884-34A), which was an obsolete vulcanizate with much lower physical properties and stability than the current vulcanizates (see Appendix C).

Table 30

LO_2 Impact Tests of Main Propellant Seal Candidates

Conditions: per MSFC-106B
drop height = 110 cm (43.3 in.)
sample condition: "as is"

Laboratory Number	Seal Candidate	Results in Reactions/Test Specimens	Type of Reaction
3C-2408	phosphazine fluroelastomer	2/18	Moderate on rebound
3C-2409	Viton ECD-3234 (white)	1/20	Moderate on rebound
3C-2410	Viton E-60C (white)	2/20	1 extreme, 1 moderate, on rebound
3C-2411	Linear Tefzel	2/6	Both moderate, 1 on rebound

The results of this second series of LO_2-impact tests, using specially cleaned specimens, are shown in Table 31. It is apparent that although special cleaning for the LO_2 service did reduce the impact sensitivity of two of the seal candidates (i.e., of Viton E-60C and linear Tefzel), none of these candidates meet the requirements for use in liquid oxygen systems. Thus, the number of seal candidates for the main propellent system was drastically reduced from six candidates to two; crosslinked Halar and the perfluoroelastomer, AF-E-124D. The most disappointing result of these LO_2 impact tests was the highly sensitive behavior of the Tefzel. It had been assumed that since the ethylene/chlorotrifluoroethyline copolymer,

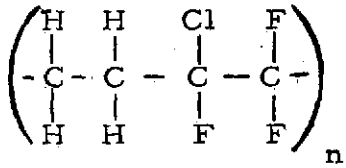

called Halar, was LOX-compatible, surely the ethylene/tetrafluoroethylene copolymer,

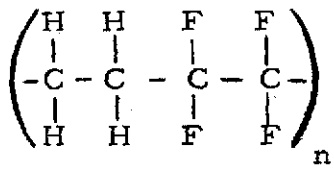

called Tefzel, would also be LO_2 compatible. In general, any fluorocarbon is significantly more stable than the corresponding chlorocarbon because the strength of the C-F bond = 116 kcal/g. mole, whereas the strength of the C-Cl bond = 70 kcal/g. mole. The surprising chemical resistance of Halar may be due to some unique stereoregularity which is not shared by Tefzel. It is interesting in this respect that Halar is also much more flame resistant than Tefzel (O_2-Index Test Values of 60 vs. 30). LO_2-sensitivity, however, does not usually correlate with flame resistance.

Table 31

Second Series of LO_2 Impact Tests on Main Propellant Seal Candidates

Conditions: per MSFC 106B
drop height = 110 cm (43.3 in.)
sample condition: LO_2 cleaned

Laboratory Number	Seal Candidate	Results in Reactions/Test Specimens	Type of Reaction
3C-2436	Viton ECD-3234 (white)	1/20	Moderate on rebound
3C-2437	Viton E-60C (white)	3/20	No detonations but specimens charred
3C-2435	Linear Tefzel	3/20	1 moderate 2 faint

3.2.3 Thermal Cycling Tests

LO_2-impact testing described in the preceeding Section (3.2.2) eliminated four of the six candidates for this Main Propellant System. The surviving two seal candidates, the fluoroplastic crosslinked Halar and the perfluoroelastomer AF-E-124D, were therefore subjected to thermal cycling between 76K (-320F) and 344K (160F). The same programmed dipping machine described in Section 3.1.2 was utilized. However, unlike the thermal cycling tests of the hydraulic seal candidates the subject tensile dumbells of this phase were not encased in pyrex envolopes. Rather, the bare tensile specimens were plunged from the 342K furnace directly into a large LN_2 filled dewar in less than five seconds. The LN_2 dwell time was 10 minutes. The furnace dwell time was 30 minutes. After 200 of these thermal-shock cycles none of the specimens displayed any evidence of cracking or warping. Subsequent tensile tests showed only minor changes in physical properties. The detailed subject tensile data is summarized in Table 32.

3.2.4 Cyclic Load Deflection Measurements

3.2.4.1 Experimental Methods

Cyclic load deflection measurements were performed on the two surviving seal candidates for the Main Propellant System (crosslinked Halar and the perfluoroelastomer AF-E-124D utilizing the same military specification O-ring face gland/Instron tester arrangement previously described in Section 3.1.3.1. Since it was impractical to impose the same 22% compression on the hard crosslinked Halar O-rings which had been imposed on the highly elastic Viton O-rings of Section 3.1, the former were subjected to cyclic load deflections somewhat greater than that required to produce a gas-tight seal. The Instron load required to achieve complete sealing was determined in the cyclic sealability measurements of Section 3.2.6 concurrently with the cyclic load deflection measurements of this section. In view of the failure of the AF-E-124D O-rings to seal properly at cryogenic temperatures (83K), the costly time-consuming calculations of indicated modulus, load bearing properties, cyclic work, and hysteresis were limited to the much more promising crosslinked Halar.

3.2.4.2 Cyclic Load Bearing Properties

The sealability tests of Section 3.2.6 disclosed that the preferred crosslinked Halar O-rings required minimum sealing loads ranging from 500 Kg at 296F and 344K to ~1,000 Kg at 83K. As a result, 635 Kg (1,400 bs.) of compressive force was utilized for the 296K/344K load deflection cycles, and 2,250 Kg (5,000 lbs.) of force for the cryogenic cycle. Representative Instron cyclic load deflection curves of these crosslinked Halar O-rings at 344K (160F), 296K (73F), and 83K (-310F) are shown in Figures 27 to 29, respectively. Only the important 1st,

Table 32

Thermal Cycling of Main Propellant Seal Candidates from 76K to 344K

Conditions: Bare dumbell specimens
200 cycles, 10 minutes at 76K (-320F)
30 minutes at 344K (160F)
Entire cycle time = 40 minutes
Tested: R.T., 0.2 in/min. head speed - Halar
20 in/min. head speed - AF-E-124D

Fluoroplastic	Instron Run No.	Tensile Strength at Yield Newtons/m^2 in millions	(PSI)	Tensile Strength at Break Newtons/m^2 in millions	(PSI)	% Elongation at Yield	% Elongation at Break	Shore D Hardness
Crosslinked Halar-5 Megarads, Cobalt 60, Grade #302								
As Is	4467	30.3	(4,404)	58.6	(8,505)	3.6	236	75
	4468	29.7	(4,308)	59.0	(8,542)	3.2	242	75
	4469	30.2	(4,396)	59.4	(8,619)	3.8	254	76
Average		30.1	(4,369)	59.0	(8,555)	3.5	244	75
200 cycles/76K to 344K	1737	31.6	(4,587)	52.7	(7,642)	3.0	266	75
	1738	30.6	(4,445)	54.2	(7,854)	4.0	266	73
	1739	30.4	(4,408)	52.6	(7,632)	4.5	266	74
Average		30.9	(4,480)	53.2	(7,709)	3.8	266	74
Average Change		+0.8	+111	-5.8	-846	+.3	+22	negligible
Average % Change		+2.6	+2.5	-10	-10	+8	+8	-

Rubber Compound	Instron Run No.	Tensile Strength Newtons/m^2 in millions	(PSI)	% Elongation at Break	Rubber Modulus at 20% Newtons/m^2 in millions	(PSI)	Rubber Modulus at 100% Newtons/m^2 in millions	(PSI)	Shore A Hardness
Perfluoroelastomer AF-E-124D									
GDCA slab "as is"	4758	13.2	(1,920)	180	.83	(120)	3.79	(550)	75
	4758	9.16	(1,330)	180	.82	(119)	4.26	(619)	75
	4760	15.2	(2,210)	160	.89	(130)	3.76	(545)	75
Average		12.5	(1,820)	173	.85	(123)	3.94	(571)	75
200 cycles/80K to 344K	1734	13.4	(1,946)	170	.71	(103.0)	3.90	(566)	72
	1735	12.3	(1,791)	165	.69	(99.5)	3.91	(567)	70
	1736	16.2	(2,355)	183	.69	(99.8)	3.72	(539)	68
Average		14.0	(2,031)	173	.70	(100.7)	3.84	(557)	70
Average Change		+1.5	+210	0	-.15	-22.3	-.10	-14	-5
Average % Change		+12	+12	0	-18	-18	-2.5	-2.5	-7

Page intentionally left blank

Page intentionally left blank

Page intentionally left blank

2nd, 5th, 25th, 50th, and 100th cycles are shown. It will be noted that the stress-strain cusps of the 83K experiments do not come to a point, but instead have a wide apex. This wide apex was also produced by the AF-E-124D O-rings at 83K (-310F), so it may be a characteristic of the cryogenic load deflection measurements rather than of a true rheological response of an extremely high modulus, plastic O-ring.

As before (see Section 3.1.3.2), the load bearing stress is indicated by the height of the stress-strain cusp, and any compression set which occurred during the dynamic compression cycling will result in a decrease in the height of these stress-strain cusps. The cusp heights are tabulated under the columns "Applied Force, Max." of Tables 33 to 35 which summarize the cyclic load deflection measurements of the subject crosslinked Halar O-rings at 344K (160F), 296K (73F), and 83K (-310F), respectively. After 200 cycles of sealing to a compressive force of $\sim$635 Kg (i.e., $\sim$1,400 lbs.), there was significant compression set amounting to between 100 to 139 Kg (i.e., $\sim$19%) at 344K. At 296K (73F), these Halar O-rings exhibited negligible compression set under this same sealing force. This very low compression set was confirmed by micrometer measurements; the W-dimension suffering $<$1% compression set (.0016 in.).

As might be expected, the compression set will be proportional to the loading force. Thus, when the sealing force imposed on crosslinked Halar O-ring #5 was approximately doubled to about 1,400 Kg (3,100 lbs.), then even the 296K compression set becomes appreciable. In the case of O-ring #5 (Table 34) under 1,400 Kg force at 296K, the "compression set" amounted to 136 Kg or approximately 10%. This greater, sealing force would, of course, be required to insure sealability at cryogenic temperatures. At 83K (-310F), the even greater compressive force of 2,300 Kg ($\sim$5,000 lbs.) produced little or no compression set (see Table 35). The data suggested that the Halar O-rings which were supposedly crosslinked by exposure to 5 Megarads of radiation (see Appendix A) are still considerably more thermoplastic than had been anticipated.

The average required load per lineal length at 344K and 296K amounted to:

at 344K; $\frac{600 \text{ Kg}}{15 \text{ cm}} = 40 \times 10^3$ g/cm (224 ppi),

and at 83K; $\frac{1,400 \text{ Kg}}{15 \text{ cm}} = 93 \times 10^3$ g/cm (521 ppi).

Representative cyclic load deflection curves of the AF-E-124D O-rings at 344K (160F), at 296K (73F), and 83K (-310F) are shown in Figures 30, 31, 32, and 33. As usual, only the important 1st, 2nd, 5th, 25th, 50th, and 100th cycles are shown. The most striking characteristic of these load deflection curves is the great dependence of load bearing properties on temperature even in the rubbery

Table 33

Cyclic Load Deflection Measurements of Crosslinked Halar O-rings at 344K (160F)

Conditions: 1 min. cycle time
(-224) size O-rings
(1 sq = 2.26 x 10^{-3} joules)

O-Ring Specimen	Cycle No.	Applied Force, max. Kg	Applied Force, max. (lb)	Compression Set Kg	Compression Set (lb)	ENERGY Imposed Planimeter	Imposed Squares	Imposed Joules	Recovered Planimeter	Recovered Squares	Recovered Joules	Hysteresis Planimeter	Hysteresis Squares	Hysteresis Joules
I-2717														
8	1	608	(1,340)*	-	-	-	-		-	-	-	-	-	-
	2	644	(1,420)	-	-	0395	731	1.65	0267	495	1.12	128	236	0.53
	5	606	(1,335)	39	(85)	0293	542	1.22	0244	451	1.02	49	91	0.20
	25	556	(1,225)	50	(110)	0235	435	0.98	0227	420	0.95	8	15	0.03
	50	531	(1,170)	25	(55)	0205	380	0.86	0192	356	0.80	13	24	0.06
	100	506	(1,115)	25	(55)	0176	326	0.74	0179	332	0.75	-3	-6	-.01
	Total	-	-	139	(305)									
	Average	569	(1,253)	-	-			1.09			0.93			0.16
I-2716														
7	1	649	(1,430)	-	-	0438	795	1.80	0271	492	1.11	157	303	0.69
	2	631	(1,390)	18	(40)	0330	600	1.36	0256	465	1.05	74	135	0.31
	5	608	(1,340)	23	(50)	0285	517	1.17	0244	444	1.00	41	73	0.17
	25	582	(1,283)	26	(57)	0239	435	0.98	0220	400	0.90	19	35	0.08
	50	567	(1,250)	10	(23)	0230	417	0.94	0219	398	0.90	11	6	0.04
	100	544	(1,200)	23	(50)	0233	423	0.96	0220	400	0.90	13	3	0.06
	Total	-	-	100	(220)									
	Average	597	(1,316)	-	-			1.20			0.98			0.23

* Believed to be erroneous value - disregard.

Table 34

Cyclic Load Deflection Measurements of Crosslinked Hala- O-rings at 296K (73F)

Conditions: 1 min. cycle time
(-224) size O-rings
(1 sq = 5.65×10^{-3} joules)

O-Ring Specimen	Cycle No.	Applied Force, max. Kg	(lb)	Compression Set Kg	(lb)	ENERGY Imposed Planimeter	Squares	Joules	Recovered Planimeter	Squares	Joules	Hysteresis Planimeter	Squares	Joules
I-2673														
5	1	1,406	(3,100)	-	-	0600⊛	1062⊛	6.00⊛	0298	527	2.98	402⊛	712⊛	4.02⊛
	2	1,363	(3,005)	43	(95)	0374	662	3.74	0279	494	2.79	95	168	0.95
	5	1,338	(2,950)	25	(55)	0341	604	3.41	0207	366	2.07	134	237	1.34
	25	1,293	(2,850)	45	(100)	0294	520	2.94	0243	430	2.43	51	90	0.51
	50	1,270	(2,800)	23	(50)	0276	488	2.76	0232	411	2.32	44	78	0.44
	100	1,270	(2,800)	0	(0)	0030 (low accuracy-disregard)								
	Total	-	-	136	(300)									
	Average	1,323	(2,918)	-	-			3.21			2.52			0.81
	Range													
I-2689												(1 sq = 2.26×10^{-3} joules)		
6	1	621	(1,370)	-	-	0226	410	0.93	0210	382	0.86	16	28	0.06
	2	621	(1,370)	0	(0)	0203	369	0.83	0208	378	0.85	-5	-9	0
	5	618	(1,363)	3	(7)	0203	369	0.83	0209	380	0.86	-6	-11	0
	25	615	(1,355)	4	(8)	0212	386	0.87	0187	340	0.77	25	46	0.10
	50	608	(1,340)	7	(15)	0205	373	0.84	0187	340	0.77	18	33	0.07
	100	617	(1,360)	+9	(+20)	0199	362	0.82	0193	351	0.79	6	11	0.02
	Total	-	-	5*	(10)									
	Average	617	(1,360)	-	-			0.85			0.82			0.04
	Range													

* Micrometer measurements of the O-ring cross section disclosed a compression set of .1418 - .0016 or ~1%.

⊛ Anomalous loading cycle - disregard.

Table 35

Cyclic Load Deflection Measurements of Crosslinked Halar O-rings at 83K (-310F)

Conditions: ¼ min. cycle time
(-224) size O-rings

O-Ring Specimen	Cycle No.	Applied Force, max. Kg	(lb)	Compression Set	ENERGY Imposed Planimeter	Squares	Joules	Recovered Planimeter	Squares	Joules	Hysteresis Planimeter	Squares	Joules
											(1 sq = 1.13×10^{-3} joules)		
I-2285													
4	1	2,359	(5,200)	-	0458	832	9.40	0406	739	8.36	52	93	1.04
	2	2,359	(5,200)	0	0461	839	9.48	0430	782	8.84	31	57	0.64
	5	2,390	(5,270)	0	0465	846	9.56	0428	779	8.80	37	67	0.76
	25	2,449	(5,400)	0	0465	846	9.56	0414	753	8.50	51	93	1.06
	50	2,354	(5,190)	0	0467	850	9.60	0412	750	8.48	55	100	1.12
	100	2,313	(5,100)	0	0460	837	9.46	0415	755	8.54	45	82	0.92
	Average	2,371	(5,227)	0			9.51			8.59			0.92
											(1 sq = 5.65×10^{-3} joules)		
I-2286													
2	1	2,291	(5,050)	-	0885	1610	9.10	0815	1482	8.37	70	128	0.73
	2	2,263	(4,990)	0	0877	1595	9.01	0800	1455	8.22	77	140	0.79
	4*	2,268	(5,000)	0	0874	1590	8.98	0800	1455	8.22	74	135	0.76
	25	2,268	(5,000)	0	0885	1610	9.10	0790	1440	8.14	95	170	0.96
	50	2,268	(5,000)	0	0871	1589	8.98	0795	1448	8.18	76	141	0.80
	Average	2,272	(5,008)	0			9.03			8.22			0.81

*5th cycle lost.

Page intentionally left blank

Page intentionally left blank

Page intentionally left blank

Page intentionally left blank

region. For example, when the test temperature was increased from room temperature to 344K (166F) (an increase of only 48K), the load bearing properties of the AF-E-124D O-rings decreased nearly 50%. By comparison, all three types of Viton O-rings discussed carlier in this report (see Section 3. 1. 3) actually increased their load bearing properties when tested at elevated temperatures (i. e. , at 422K (300F)), and this increase in load bearing properties encompassed a 126 K change in temperature.

In addition, at the temperatures tested in the rubbery region (i. e. , 296K and 344K), the AF-E-124D O-rings exhibited a small but very real compression set. This is shown by the progressive decrease in the cusp height of Figures 30 and 31, and was confirmed by measurements of the O-ring thickness before and after the cyclic load deflection operation. These measured compression sets are expressed as percentage of the 22% original deflection. All of these cyclic load bearing properties are summarized in Table 36.

As indicated in Table 36, the load bearing properties of the subject AF-E-124D O-rings are nearly 100 fold greater at cryogenic temperatures than at room temperature. Surprisingly, the cyclic load deflection cusps gave no indication of compression set at 83K (-310F). Although there was indeed some fluctuation in cusp height during the 200 impressed compression cycles, there was no consistent decay. The random fluctuations are possibly due to thermal effects. This is suggested by the changes in cusp height during cycles #40 to #50, as shown in Figure 33. Unfortunately, because of difficulties of performing precise mechanical measurements at LN_2 temperatures, this absence of compression set was not confirmed by actual measurements of the subject O-rings themselves.

3. 2. 4. 3 Cyclic Work and Hysteresis of Crosslinked Halar O-rings

Crosslinked Halar is the sole main propellant seal candidate to have survived all the preceding tests of this section in general, and the LO_2 Impact Test (Section 3. 2. 2) and the Dynamic Sealability Test (Section 3. 2. 6) in particular. The Instron stress-strain curves obtained when these crosslinked Halar O-rings were compression cycled at 344K (160F), 296K (73F), and 83K (-310F) are shown in Figures 27, 28 and 29, respectively. The pertinent characteristics of these curves have already been fully discussed in the preceding Section.

The cyclic work and hysteresis of these compression cycled O-rings were measured by means of the compensating polar planimeter as described previously in Section 3. 1. 3. 3. Results of these measurements are summarized in Tables 33, 34 and 35. It is instructive to compare these cyclic work and hysteresis values obtained from the hard, plastic, crosslinked Halar O-rings with

Table 36

Cyclic Load Bearing Properties of Perfluoroelastomer AF-E-124D O-rings from 344K (160F) to 83K (-310F)

Temp.	O-ring Spec.	Instron Run	Cycles #1 - #5 Applied Force, max. Kg	(lb)	Cycles #25 - #200 Applied Force, max. Kg	(lb)	Avg. Load/Lineal Length (Kg/lineal cm.)	(lb/lineal in.)	"Compression Set," %, from Cusp Height	Compression Set from O-ring Thickness	Compression Set as % of Orig. Deflection
344K	7	2738	15.1-14.8	(33.3-32.7)	14.7-14.5	(32.5-32.0)	0.99	(5.55 ppi)	4	(.0025 in.)	13
(160F)	8	2756	16.4-15.4	(36 -34)	14.5-14.1	(32 -31)	1.02	(5.72 ppi)	13	(.0017 in.)	8
296K	9	2757	29.9-28.6	(66 -63)	28.1-26.8	(62 -59)	1.90	(10.7 ppi)	10	(.0024 in.)	12
(73F)	7	2775	26.8-25.7	(59 -56.6)	25.2-25.0	(55.5-55.0)	1.74	(9.8 ppi)	7	(.0010 in.)	5
83K	4	2306	2,386-2,436	(5,260-5,370)	2,461-2,415	(5,425-5,325)	161.2	(904.3 ppi)	nil	-	-
(-310F)	5	2308	2,273-2,322	(5,010-5,120)	2,361-2,318	(5,205-5,110)	147.5	(827.5 ppi)	nil	-	-

analogious values obtained from the soft Viton O-rings of Section 3.1.3.3. With a glass transition temperature (T_g) of 413K (284F), the subject Halar O-rings are in the glassy state in all three test temperatures of this program. By contrast, the Viton O-rings of this program were in the rubbery state in two out of three of the test temperatures. Only at the 233K (-40F) test temperature were the Viton O-rings below their Tg of 243K (-22F), and even at 233K they were in the leathery rather than the glassy state. Since this pertinent data is scattered in a number of different places throughout this report summary Table No. 37 was prepared. For conciseness, Table 37 contains only average values rounded to one or two places. The reference number of the various tables from which these average values were extracted is listed alongside each set of data.

It can be seen that, as the Viton O-rings are cooled to 233K (-40F) and the O-rings pass from the rubbery to the glassy state, the indicated modulus, the cyclic work of compression, and the hysteresis all increase by a factor of approximately 20. The indicated modulus of the crosslinked Halar O-rings at room temperature are also about equal to that of the Viton at 233K; i.e., about 21 kg/cm; however, both the cyclic work and the hysteresis are significantly less; i.e., 1 Joule and 0.04 Joules, respectively, vs. 2.2 Joules and 0.7 to 0.1 Joule for the 233K (-40F) Viton. Ostensibly, the crosslinked Halar is a better O-ring material at 296K (in its glassy state) than the Viton is in its "leathery" state. Actually, the above two materials are not in "corresponding temperatures"(Ref. 8) at 296K and 233K, respectively. In addition, judging from the extensive compression set displayed by the Viton rubbers in the 233K compression cycles (see Section 3.1.3.2), the 22% deflection employed on all the Viton deflection tests, although correct for Viton O-rings in the rubbery state, is probably excessive for the O-rings in the leathery state. Probably the sealing behavior of different kinds of O-rings should be compared not only at their corresponding temperatures, but also at equivalent minimum sealing loads. The dynamic sealability/cyclic load deflection tests of this program are probably useful if applied with these two constraints in mind.

This concept is supported by the data of Tables 33 and 34. Of the two crosslinked Halar O-rings tested at 296K (73F), one (O-ring No. 5) was compression cycled from 1400 to 1270 Kg of force, which is ~2-1/2 times the 500 to 550 Kg of force required to achieve complete sealing at 296K (see Table 40 and Figure 38). The result of this excessive loading produced a compression set >10%, a cyclic work of 3.2 Joules (loading cycle) to 2.5 Joules (unloading cycle), and a hysteresis of 0.81 Joules. The two cyclic work values are three to four times, and the hysteresis twenty times that exhibited by O-ring No. 6, which was compression cycled at the more realistic load of ~600 kg. Similarly, when these crosslinked Halar O-rings were compression cycled at 344K (160F) under a 600 to 650 kg load, they again displayed excessive compression set and larger hysteresis, although the cyclic work was satisfactorily low.

Table 37

Comparison of Some Cyclic Load Deflection Measurements of Carbon Black-Filled Viton O-rings vs. Crosslinked Halar O-rings

	Carbon-Filled Viton O-rings						Crosslinked Halar O-rings					
	At 296K (73F)			At 233K (-40F)			At 296K (73F)			At 344K (160F)		
Property	Loading	Unloading	Reference	Loading	Unloading	Reference	Loading	Unloading	Reference	Loading	Unloading	Reference
Indicated Modulus x 10^3, in Kg/cm	~1.1	~1.	Table 22	~21	~23	Table 22	~20	~21	Table 39	~15	~19	Table 39
Cyclic Work, in Joules	~0.13	~0.11	Table 19	~2.5	~2	Table 19	~1	~1	Table 35	~1.1	~1	Table 34
Hysteresis, in Joules	~.02		Table 19	0.7 to 0.1		Table 19	0.04		Table 35	~0.2		Table 34

3.2.4.4 Indicated Modulus of Crosslinked Halar O-rings

The "indicated modulus" was measured using the Instron cyclic load deflection curves of Section 3.2.4.2. As usual, the indicated modulus was measured at a point on each stress-strain cusp corresponding to 50% of the maximum applied load. A cursory examination of the load deflection curves of the crosslinked Halar O-rings of Section 3.2.4.2 shows that the loading portion of each cycle is nearly linear, at least around this 50% point (see Figures 27 to 29). This differs markedly from the Viton, hydraulic seal O-rings discussed in Section 3.1. Consequently, the "indicated modulus" of the loading portion of most cycles was most conveniently measured by simple inspection and a straight edge. The unloading portions of most of the curves, however, were sufficiently curved as to require use of the "Radius Template method" described earlier in Section 3.1.3.4.

The actual numerical results of these indicated modulus measurements are shown in Table 38. The biggest surprise of Table 38 is the relatively small increase in the indicated modulus when the subject crosslinked Halar O-rings were cooled to cryogenic temperatures. In fact, the indicated modulus increased almost as much when the temperature was lowered from 344K to 296K (a decrease of 48K) as when the temperature was lowered from 296K to 83K (a decrease of 213K). Since Halar has a glass transition temperature (T_g) of 413K, at all three test temperatures, the subject Halar O-rings are well within the glassy region, and one would expect the modulus to have a more or less constant temperature coefficient within the glassy region.

Because of the large cyclic hysteresis exhibited by Halar O-rings, the indicated modulus of the "imposed" portion of each cycle is invariably less than that of the recovered portion. It is also apparent that at the two higher temperatures (296K and 344K), the indicated moduli of the "imposed" portion of each load deflection cycle increased steadily with the amount of dynamic cycling, whereas the corresponding indicated modulus of the "recovered" portion remained substantially constant throughout the 100 cycle test. By contrast, at cryogenic temperatures (83K) both the "imposed" and the "recovered" moduli remain unchanged throughout the 100 dynamic cycles.

The reason for this 10% to 30% increase in the indicated moduli on the loading portions of the cycles is unknown. Earlier in this report (Section 3.1.3.4), it was shown that the indicated moduli of the subject Viton O-rings tested in this program remained substantially constant throughout the 100 cycle test regardless of whether the O-rings were in the rubbery or leathery state. In the leathery state [i.e., at 233K (-40F)], the Viton O-rings exhibited indicated moduli during the imposed portions of the cycles ranging from 19 to 23 Kg/cm (106 to

Table 38

Indicated Modulus of Crosslinked Halar O-rings from 344K (160F) to 83K (-310F)

Conditions: 1 cycle/min.
Head speed = (0.02 in./min.)
(0.254 mm/min.)

Temp.	O-ring No.	Applied Force, Max. Kg	(lb)	Cycle No.	Indicated Modulus x 10^3 Imposed Kg/cm	(ppi)	Recovered Kg/cm	(ppi)
344K (160F)	7	635	(1400)	1	13.4	(74.9)	19.6	(109.7)
		631	(1390)	2	14.6	(81.6)	19.6	(109.7)
		608	(1340)	5	15.9	(89.0)	16.3	(91.0)
		581	(1280)	25	16.8	(94.1)	20.1	(112.8)
		576	(1270)	50	17.2	(96.4)	19.3	(108.0)
		590	(1300)	100	18.1	(101.2)	19.6	(109.6)
	8	608	(1340)	1	13.9	(77.7)	17.0	(95.2)
		644	(1420)	2	14.7	(82.5)	19.1	(106.7)
		608	(1340)	5	15.0	(84.2)	19.3	(108.0)
		556	(1225)	25	15.4	(86.4)	18.1	(101.1)
		531	(1170)	50	16.1	(90.0)	17.9	(100.0)
		508	(1120)	100	17.3	(96.8)	18.0	(101.0)
296K (73F)	6	621	(1370)	1	18.9	(106.1)	20.8	(116.3)
		621	(1370)	2	18.9	(106.1)	20.8	(116.3)
		617	(1360)	5	19.1	(107.1)	20.8	(116.3)
		612	(1350)	25	19.7	(110.1)	20.8	(116.3)
		608	(1340)	50	20.2	(113.1)	21.0	(117.7)
		617	(1360)	100	21.0	(117.6)	21.2	(118.8)
	5	1,406	(3100)	1	18.7	(104.8)	27.2	(152.3)
		1,365	(3010)	2	20.6	(115.5)	27.3	(152.7)
		1,338	(2950)	5	22.2	(124.1)	27.3	(152.7)
		1,277	(2850)	25	23.4	(130.8)	26.9	(150.4)
		1,270	(2800)	50	23.4	(130.8)	27.5	(153.9)
		1,270	(2800)	100	24.1	(135.0)	27.0	(151.0)
83K (-310F)	9	2,291	(5050)	1	28.9	(161.9)	32.3	(181.0)
		2,263	(4990)	2	28.8	(161.1)	31.2	(174.9)
		2,268	(5000)	5	29.4	(164.4)	32.1	(179.9)
		2,268	(5000)	25	28.6	(160.1)	30.8	(172.3)
		2,268	(5000)	50	28.8	(161.1)	30.8	(172.3)
	4	2,359	(5200)	1	28.9	(161.9)	30.7	(172.0)
		2,359	(5200)	2	29.5	(165.0)	30.9	(173.0)
		2,395	(5280)	5	29.1	(162.7)	31.2	(174.7)
		2,381	(5250)	25	28.8	(161.2)	30.5	(170.9)
		2,354	(5190)	50	29.6	(166.0)	30.4	(170.1)
		2,313	(5100)	100	28.6	(160.0)	30.8	(172.3)

132 ppi) and a very large cyclic compression set. This is just about the moduli exhibited by the subject crosslinked Halar O-rings at 296K (73F), although accompanied by a much smaller cyclic compression set. It is always dangerous to draw analogies between polymers at different corresponding temperatures,[1] however, it would seem unlikely that the observed increase in indicated modulus displayed by the subject Halar O-rings during the loading cycle was characteristic of all polymeric O-rings in the glassy state.

(1) Corresponding temperatures $\equiv T/Tg$. For the subject Halar at 296K; $\frac{296K}{413K} \simeq 0.7$. For Viton at 233K, $\frac{233K}{243K} \simeq 0.9$.

3. 2. 5 Stress Relaxation Measurements

Stress relaxations of the two surviving Main Propellant System seal candidates (crosslinked Halar and the perfluoroelastomer, AF-E-124D) were measured at two temperatures, 296K (73F), and 344K (160F). In order to obtain the greatest accuracy, all relaxation tests were performed using the procedure and the piezoelectric compression/stress relaxation apparatus previously developed for the 422K (300F) testing of the Viton rubber O-rings (see Section 3. 1. 4. 1).

As might be expected, the stress relaxation behavior of the AF-E-124D O-rings resembled those of the other rubber O-rings of this contract, Viton E-60C and ECD-3234. The initial applied stress required to produce the desired 22% compression was somewhat lower, ~35 Kg (75 lb) at 296K and ~24 Kg (~53 lb) at 344K. The relaxation followed the same relationship:

$$\sigma = \sigma_1 - K \log t$$

where σ_1 = stress at 1 minute

σ = stress at time, t

and the relaxation constant, K, obtained by plotting the stress against log t on semilog paper, averaged 3. 5 Kg at room temperature and ~2 Kg at 344K (160F). Representative stress relaxation plots at 296K and 344K are shown in Figures 27 and 28, respectively. It will be observed that the rate of stress relaxation actually decreased as the temperature increased from 296K to 344K. Part of this decrease is due to the lower initial stress used with the higher temperature specimens. However, even when the data is "normalized" for the imposed stress, i. e., $\frac{\sigma}{\sigma_1} = 1 - \frac{K}{\sigma_1} \log t$, the rate of relaxation is ~30% less at 344K than at 296K (see last column of Table 39). This is exactly the same behavior exhibited by the Viton O-rings (see Section 3. 1. 4).

In contrast to the preceding rubber seal candidates, the rate of stress relaxation of the crosslinked Halar O-rings increased with an increase in temperature. This is shown in Figures 36 and 37 and summarized in Table 39. It is interesting that in spite of the vast difference in material properties between these hard plastic Halar O-rings, and the soft, elastic, low modulus rubbers, the Halar stress relaxation still obeys the same simple relationship, $\sigma = \sigma_1 - K \log t$. This is shown by the very straight lines obtained when the measured stress is plotted against the log of time as in Figures 36 and 37. In spite of the 10-fold greater initial applied stresses[1] (compared with the stresses applied to the rubber O-rings), the normalized relaxation constant $\left(\frac{K}{\sigma_1}\right)$ is almost the same as for the rubber O-rings, except, of course, that the rate of relaxation increased sharply as the temperature increased by 48K.

(1) Because of the hard, non-compliant nature of the Halar O-rings, the usual 22% "sealing squeeze" criteria employed for the rubber O-rings in this program was not applicable. Instead, the load required to achieve sealability as described in Section 3. 2. 6 (Dynamic Sealability, etc.) of this report was used.

Figure 34. Plot of Stress Relaxation of AF-E-124D O-rings at 296K (73F)

$\sigma = \sigma_1 - k \log t$

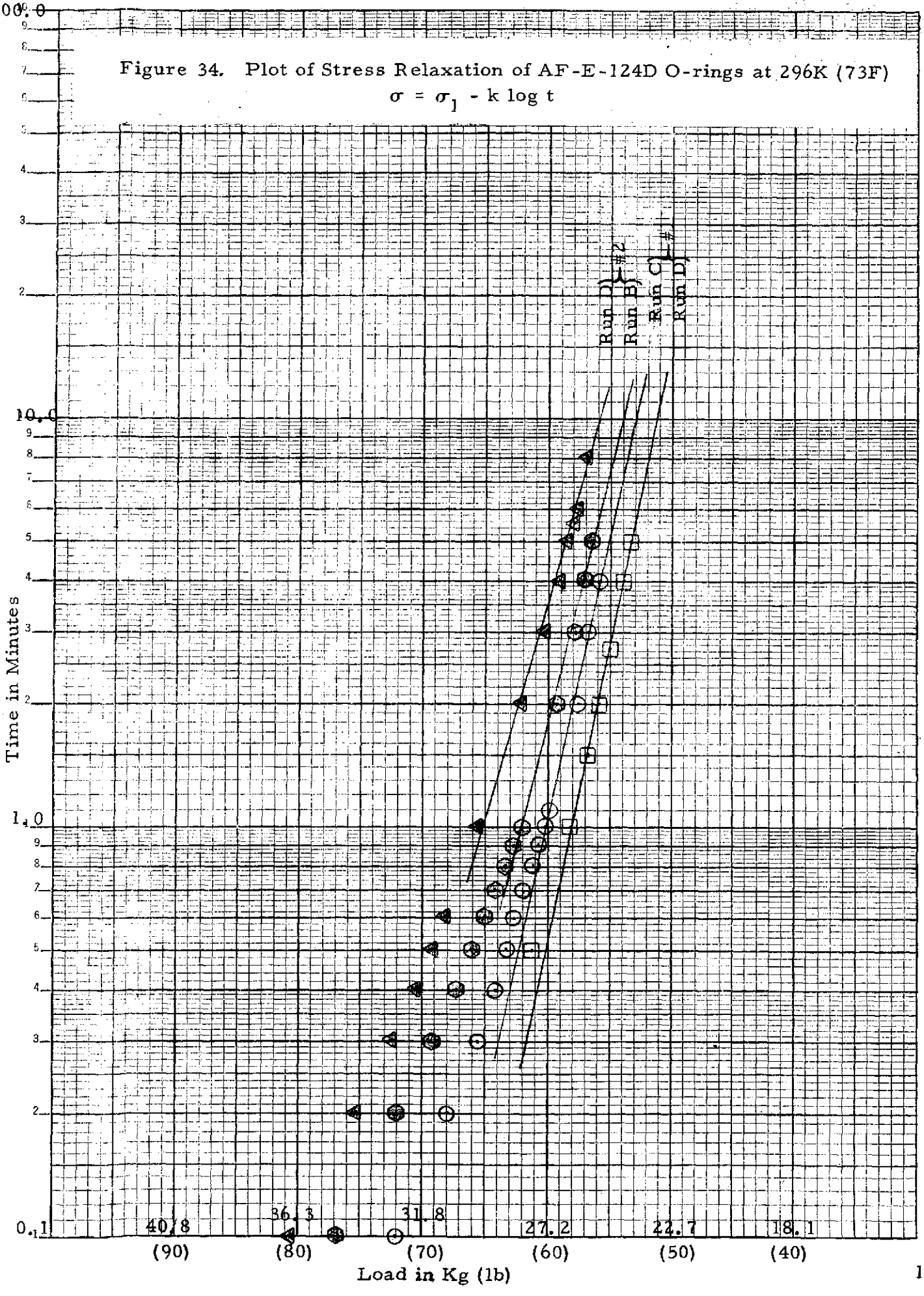

Figure 35. Plot of Stress Relaxation of AF-E-124D O-ring #1 at 344K (160F)

$\sigma = \sigma_1 - k \log t$

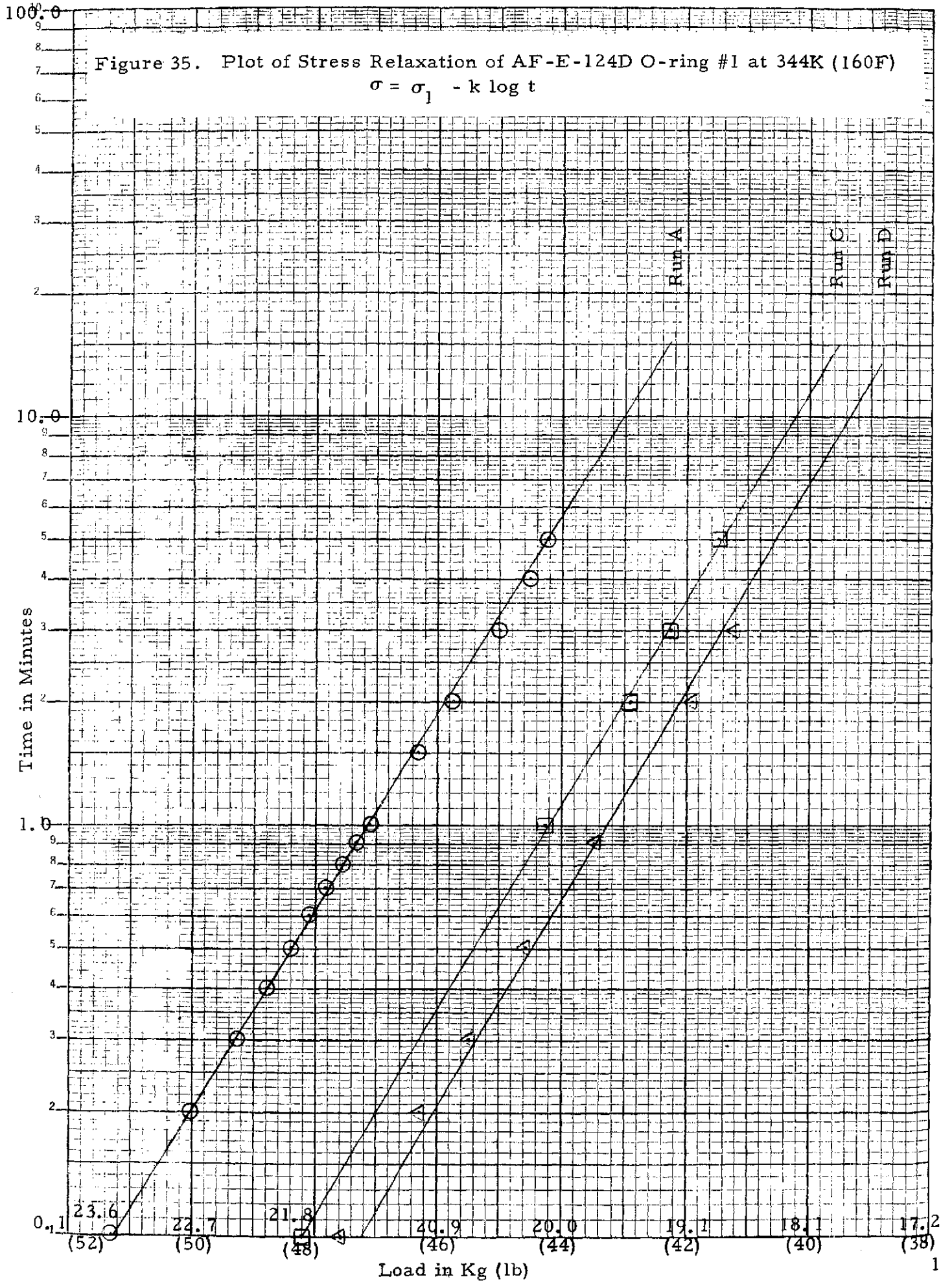

Figure 36. Plots of Stress Relaxation of Crosslinked Halar O-rings at 296K (73F)

$$\sigma = \sigma_1 - k \log t$$

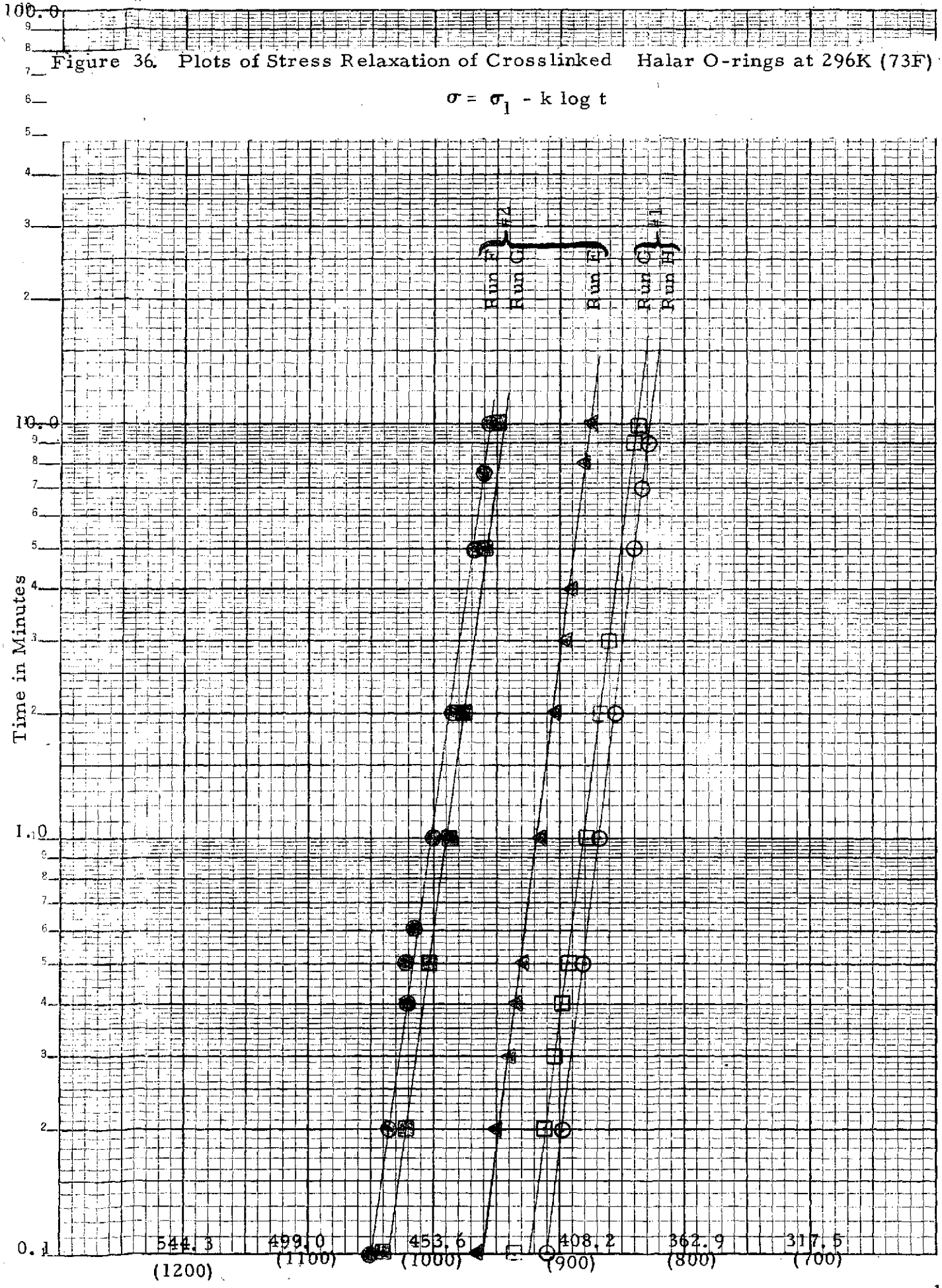

Figure 37. Plots of Stress Relaxation of Crosslinked Halar O-ring #1 at 344K (160F)

$$\sigma = \sigma_1 - k \log t$$

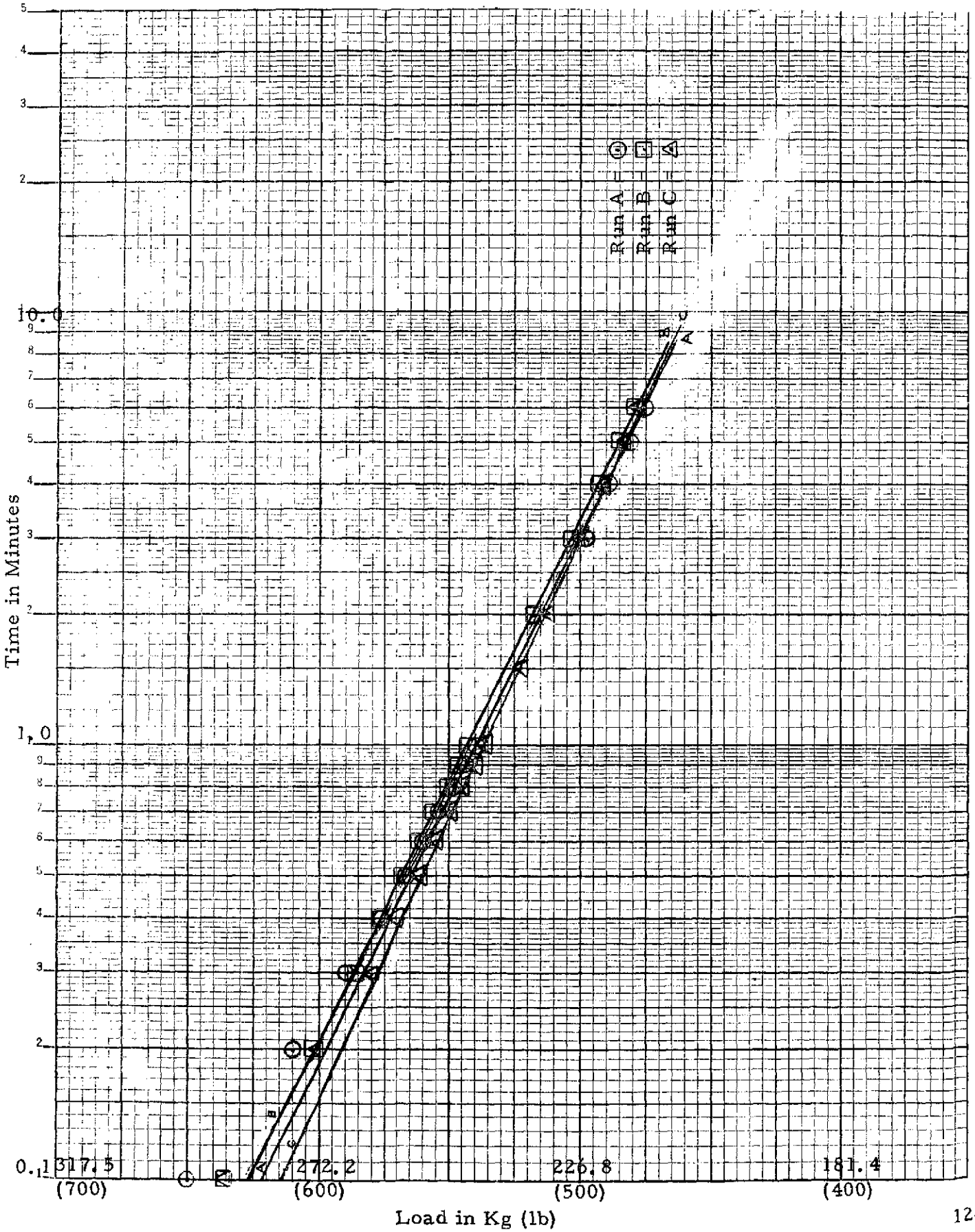

Table 39

Stress Relaxation of Principal Main Propellant System Seal Candidates;
$\sigma = \sigma_1 - K \log t$

Seal Candidate	Run No.	Temperature °K	Temperature (°F)	Stress at 1 min. "σ_1" Kg	Stress at 1 min. "σ_1" (lb)	Relaxation Constant, "K" Kg	Relaxation Constant, "K" (lb)	Normalized Relaxation Const. "K/σ_1"
AF-E-124D								
O-ring #1	C	296	(73)	27.4	(60.5)	3.24	(7.15)	0.118
	D			26.3	(58.0)	3.13	(6.9)	.119
O-ring #2	D'			29.5	(65.0)	4.17	(9.2)	.142
	B			28.1	(62.0)	3.63	(8.0)	.129
Average				27.8	(61.5)	3.53	(7.8)	.127
O-ring #1	A	344	(160)	21	(47)	1.88	(4.15)	0.088
	C'			20	(44)	1.81	(4.0)	.091
	D''			19	(43)	1.77	(3.91)	.091
O-ring #2	A'			22	(49)	2.22	(4.9)	.100
	B'			21	(47.3)	2.04	(4.5)	.095
	D'''			21	(47)	2.04	(4.5)	.096
Average				21	(46.2)	1.96	(4.3)	.094
Crosslinked Halar								
O-ring #1	G	296	(73)	400	(881)	19	(42)	0.048
	H			394	(869)	19	(41)	.047
O-ring #2	F			455	(1002)	21	(47)	.047
	G'			449	(990)	21	(46)	.046
	E			417	(920)	19	(42)	.046
Average				423	(932)	20	(44)	.047
O-ring #1	B	344	(160)	246	(543)	38	(84)	0.155
	A			245	(540)	37	(82)	.152
	C			243	(536)	35	(78)	.146
O-ring #2	C'			275	(607)	37	(81)	.133
	A'			263	(579)	32	(71)	.123
	B'			259	(570)	32	(70)	.123
Average				255	(563)	35	(78)	.139

3.2.6 Cyclic Compression Sealability Tests

Size (-224) O-rings molded from the two surviving seal candidates for the Main Propellant System, crosslinked Halar and the perfluoroelastomer, AF-E-124D, were subjected to the same cyclic sealability test described in Section 3.1.5.

The Instron curves of typical sealability test on crosslinked Halar O-rings at 296K (73F) and 344K (160F) are shown in Figures 38 and 39, and the data is given in Table 40. These Instron sealability curves are similar to those exhibited by the Viton O-rings of Section 3.1.5 at 233K (-40F), i.e., in the leathery region. Like the Viton O-rings at 233K, the crosslinked Halar O-rings start to seal at relatively low loadings (~20 Kg) and compressions (~0.05 mm). At these same temperatures (296K and 344K), loads and compressions required to achieve complete sealing increased to ~500 Kg and ~0.4 mm, respectively, following the first complete compression cycle which, of course, is anomalous (see Section 3.1.5). In spite of the higher loading required, these O-rings exhibited only slight cyclic "compression set" during the 200 test cycles employed.

At cryogenic temperatures, the modulus of the Halar has increased markedly and, as might be expected, the loadings required to obtain complete sealability is significantly higher, i.e., ~1000 Kg. Surprisingly, the compression required to achieve complete sealing did not increase, nor did the loading and compression required to achieve initial sealing (see Table 40). There is, however, one significant difference in the cryogenic use of Halar O-rings. This involves the necessity of compression cycling Halar O-rings under ambient conditions prior to cryogenic use.

Initial attempts to utilize crosslinked Halar O-rings at 86K (-310F) failed due to extensive leakage. Internal pressurization never reached more than 0.90 MN/m^2 to 1.16 MN/m^2 (130 to 168 psi), i.e., 67% to 89% of the applied helium pressure. Only if the O-rings are compression cycled prior to cooling to cryogenic temperatures can good sealability be attained, the efficiency of sealing being proportional to the amount of ambient compression cycling. For example, crosslinked Halar O-ring #4, in Instron test run #2283 (see Table 40), was compression cycled once at 296K (73F) prior to cooling to 86K (-310F). The first and second compression cycles at 86K, required an abnormally high loading force to attain even an imperfect seal holding 1.27 MN/m^2 (185 psi) helium internally. Even this sealing action was not achieved on the loading cycle, but rather on the Instron unloading portion of the cycle. With continued cycling, however, the cryogenic sealing behavior of the Halar O-ring improved dramatically, and by the third cycle the O-ring was sealing completely at a load of 900 Kg (~2,000 lbs) on the loading cycle. It maintained these same sealability characteristics throughout the remainder of the entire 50 cycle test. A composite of the preliminary 296K compression cycle plus the 1st, 2nd, 3rd, and 50th sealability test cycles of this crosslinked Halar O-ring is shown in Figure 40. These 50 cycles at 83K produced only a 0.038 mm (.0015 in.) compression set in the 3.49 mm (.1375 in.) thick O-ring.

Page intentionally left blank

Page intentionally left blank

Table 40

Cyclic Sealability Behavior of Crosslinked Halar O-rings from 86K (-310F) to 344K (160F)

Conditions: Instron Head Speed = .509 mm/min (.02 in./min.)
Internal Pressurization = 1.34 MN/m^2 (190 psi)
He at 500 cc/min.

			Instron Loading Cycle								Instron Unloading Cycle							
			Initial Sealing				Complete Sealing				Initial Leak				Complete Loss of Sealing			
			Load		Compression		Load		Compression		Load		Compression		Load		Compression	
Temp.	O-ring Specimen	Instron Test No.	Kg	(lb)	mm	(inches)	Kg	(lb)	mm	(inches)	Kg	(lb)	mm	(inches)	Kg	(lb)	mm	(inches)
83K (-310F)	O-ring #4*	2283		-			2,200⊛	(4,850)	-	-	522	(1,150)	-	-	<4.5	(<10)	-	
			(incomplete sealing to 1.28 MN/m^2 only)															
	ditto, 1st rerun		~9.1	(~20)	~.07	(~.003)	1,089⊛	(2,400)	.64	(.025)	~590	(~1,300)	.43	(.017)	4.5	(<10)	.03	(.001)
	ditto, 2nd rerun		<4.5	(<10)	~.05	(~.002)	839	(1,850)	.53	(.021)	680	(1,500)	.48	(.019)	4.5	(<10)	.03	(.000)
	ditto, 3rd rerun		4.5	(<10)	~.05	(~.002)	894	(1,970)	.56	(.022)	862	(1,900)	.43	(.017)	4.5	(<10)	.03	(.000)
	ditto, 4th rerun		4.5	(<10)	~.05	(~.002)	972	(2,150)	.61	(.024)	544	(1,200)	.46	(.018)	4.5	(<10)	.03	(.000)
	ditto, 5th rerun ▲		4.5	(<10)	~.05	(~.002)	939	(2,070)	.58	(.023)	771	(1,700)	.56	(.022)	4.5	(<10)	.03	(.001)
	O-ring #5Ⓐ	2284	-	-	-	-	1,043	(2,300)	-	-	454	(1,000)	-	-	9.1	(<20)	-	-
	ditto, 1st rerun		-	-	-	-	1,270	(2,800)	.64	(.025)	465	(1,025)	.46	(.018)	9.1	(~20)	~.05	(.002)
	ditto, 2nd rerun		4.5	(~10)	~.05	(~.002)	998	(2,200)	.58	(.023)	635	(1,400)	.48	(.019)	9.1	(<20)	~.05	(~.002)
	ditto, 3rd rerun		4.5	(<10)	~.05	(.002)	1,043	(2,300)	.61	(.024)	680	(1,500)	.51	(.020)	4.5	(~10)	.03	(~.001)
	ditto, 4th rerun		4.5	(<10)	.05	(.002)	1,043	(2,300)	.58	(.023)	680	(1,500)	.53	(.022)	4.5	(<10)	.03	(.001)
	ditto, 5th rerun †		4.5	(<10)	.03	(.001)	758	(1,670)	.41	(.016)	408	(900)	.25	(.010)		-	-	-
296K (70F)	O-ring #1	2067	36.3	80	<.07	(<.003)	533	(1,175)	.38	(.015)	249	(550)	.46	(.018)	18.1	(40)	.23	(.009)
	ditto, reruns #3 thru #6		45.9	(10-20)	~.07	(~.003)	499	(1,100)	.36	(.014)	290	(640)	.25	(.010)	4.5	(10)	.03	(.001)
	O-ring #2	2068	18.1	(40)	.05	(.002)	1,043	(2,300)	.71	(.028)	340	(750)	.46	(.018)	18.1	(40)	.28	(.011)
	ditto, 1st rerun		36.3	(80)	.05	(.002)	535	(1,180)	.33	(.013)	254	(560)	.46	(.018)	9.1	(20)	.20	(.008)
	ditto, reruns #2 thru #5		27.2	(60)	.05	(.002)	469	(1,035)	.25	(.010)	290	(640)	.18	(.007)	4.5	(10)	.00	(.000)
344K (160F)	O-ring #1	2076	22.7	(50)	.05	(.002)	481	(1,060)	.41	(.016)	272	(600)	.33	(.013)	9.1	(<20)	.25	(.010)
	ditto, reruns #1 thru #5		13.6	(30)	.05	(.002)	435	(960)	.38	(.015)	263	(580)	.18	(.007)	4.5	(10)	.00	(.000)
	O-ring #2	2077	4.5	(~10)	.05	(.002)	499	(1,100)	.46	(.018)	254	(560)	.53	(.022)	4.5	(10)	.25	(.010)
	ditto, 1st rerun		~18.1	(~40)	.07	(.003)	429	(945)	.41	(.016)	254	(560)	.28	(.011)	9.1	(20)	.03	(.001)
	ditto, reruns #2 thru #5		~18.1	(~40)	.07	(.003)	413	(910)	.38	(.015)	254	(560)	.28	(.011)	9.1	(~20)	.03	(.001)

† After 100 compression cycles at 87K.

Ⓐ Compression cycled twice at room temperature to 1,025 Kg (2,260 lb) and pressurized with He prior to cooling to 86K and starting cyclic leak measurements.

* Loaded at room temperature to 1,131 Kg (2,500 lb) and pressurized with 134 MN/m^2 He prior to cooling to 86K and starting load deflection/leak test cycles.

⊛ Maximum sealability not attained until after max. load (~2,270 Kg, i.e. 5,000 lb) had been applied and unloading cycle had started.

▲ After 50 compression cycles at 86K.

Page intentionally left blank

Figure 41 shows a similar composite of Instron run #2284, which is the sealability test for crosslinked Halar O-ring #5. The two preliminary compression cycles at 296K plus the 1st, 2nd and 100th sealability test cycles at 83K (-310F) are shown. Since the 2nd preliminary compression cycle was also helium pressurized, there is a direct comparison of the increase in sealing pressure required upon cooling from 296K to 83K. It will be noted that this crosslinked Halar O-ring sealed at $1,090^{+182}_{-91}$ Kg ($2,499^{+400}_{-200}$ lbs.) on the first three test cycles, and this sealing load (on loading cycle) had reduced to 725 Kg (~1,600 lbs.) after 100 cryogenic cycles. Similarly, the load required to maintain complete sealability on the unloading cycle decreased from 540 Kg (~1,200 lbs.) on the first three cryogenic cycles to ~400 Kg (~900 lbs.) on the 100th cycle. Overall, crosslinked Halar appears sufficiently promising to warrant intensive development as a cryogenic seal material. Since Halar can be radiation crosslinked, whereas the presently accepted cryogenic seal materials (Teflon and Kel-F) cannot, it should prove to be a superior seal material with much wider range of service temperatures.

Instron curves of sealability tests at 296K (73F) and 344K (160F) on O-rings molded from the perfluorocarbon AF-E-124D are shown in Figures 42 and 43. These O-rings failed upon unloading via extrusion between the pressurized gland face and the mating anvil, rather than by simple loss of sealing force. This mode of failure has already been thoroughly discussed in Section 3.1.5, and is typical of the sealing behavior of any highly elastic O-ring mounted in an internally pressurized face seal gland. AF-E-124D O-rings would, therefore, exhibit this behavior throughout their rubbery range, i.e., at any temperature above 233K (-40F). As Figures 42 and 43 indicate, the sealability of AF-E-124D in the rubbery region is excellent. For example, the required sealing force at 296K (73F) is the same as at 344K (160F). This is shown in Table 41 which summarizes the sealability behavior of AF-E-124D. At these higher temperatures, the AF-E-124D O-rings appear to be just as resilient and have just as good sealability as the Vitons discussed under Section 3.1.

At cryogenic temperature, the AF-E-124D O-rings are definitely poorer seals than the crosslinked Halar, when tested under the same conditions of 86K and 0.5 mm/min. Instron head speed. In spite of a four-fold increase in helium flow rate into the pressurized O-ring test gland, the AF-E-124D O-ring sealed assembly never reached the applied 1.34 MN/m^2 (194 psi) internal helium gas pressure. This can be readily seen in Figure 44, which shows the Instron sealability curve of a typical AF-E-124D O-ring at 83K. Attempts to improve the cryogenic sealability by compression cycling the O-rings prior to cooling to 83K or by maintaining the O-ring in a compressed condition during "cool down" did not substantially improve the sealability. In addition, the AF-E-124D exhibited absolutely no improvement in sealability upon continued compression cycling at 83K as witnessed by the continued poor sealability exhibited by the O-ring after 100 cryogenic compression cycles.

Page intentionally left blank

Page intentionally left blank

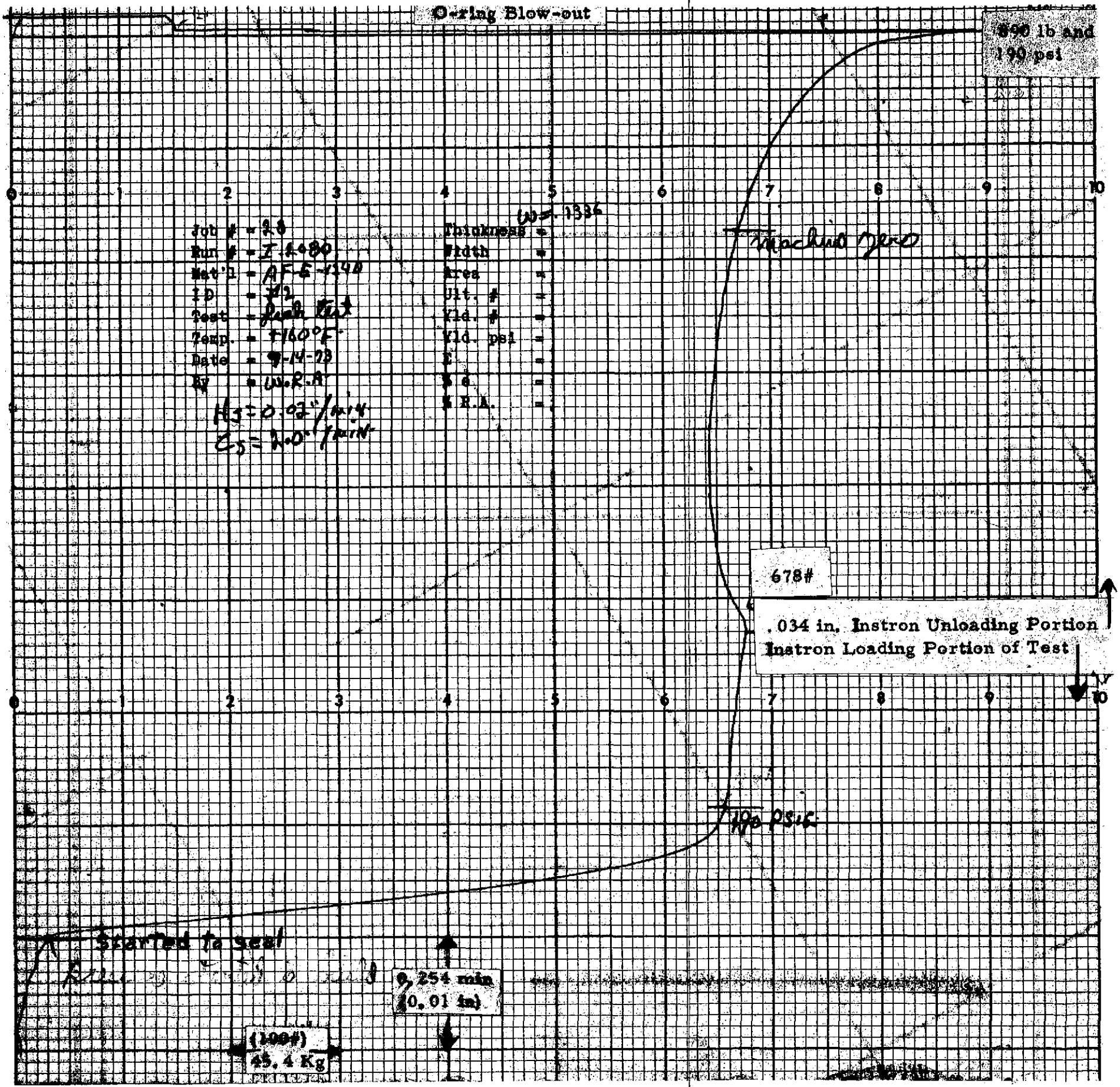

Figure 43. Instron cyclic Sealability Test Curve of AF-E-124D O-ring #2 at 344K (160F).

Table 41

Cyclic Sealability Behavior of Perfluoroelastomer AF-E-124D O-rings from 86K (-310F) to 344K (160F)

Conditions: Instron Head Speed = .509 mm/min. (.02 in/min.)
Internal Pressurization = 1.34 MN/m^2 (195 psi)
He at 500 cc/min.

			Instron Loading Cycle								Instron Unloading Cycle							
			Initial Sealing				Complete Sealing				Initial Leak				Complete Loss of Sealing			
			Load		Compression		Load		Compression		Load		Compression		Load		Compression	
Temp.	O-ring Specimen	Instron Test No.	Kg	(lb)	mm	(inches)	Kg	(lb)	mm	(inches)	Kg	(lb)	mm	(inches)	Kg	(lb)	mm	(inches)
83K	O-ring #1④	2295	4.5	(~10)	.05	(.002)	1,769	*(3,900)	.91	*(.036)	680	(1,500)	.56	(.022)	~4.5	(~10)	.15	(.006)
(-310F)	ditto, 1st rerun		-	-	-	-	1,769	*(3,900)	.99	*(.031)	907	(2,000)	.51	(.020)	4.5	(~10)	.00	(.000)
	ditto, 2nd rerun		~4.5	(~10)	.05	(.002)	2,191	*(4,830)	.94	*(.037)	-	-	-	-	> 4.5	(< 10)	.00	(.000)
	ditto, reruns #3, #4, and #5		4.5	(~10)	.07	(.003)	2,313	*(5,100)	.99	*(.039)	~1,089	(~2,400)	.64	(~.025)	< 4.5	(< 10)	.03	(.001)
	ditto, 6th rerun ▲		4.5	(~10)	.05	(.002)	2,177	*(4,800)	.99	*(.039)	953	(2,100)	.61	(.024)	~4.5	(~10)	.05	(.002)
	O-ring #3④	2305	18.1	(~40)	-	-	2,268	*(~5,000)	.94	*(.037)	590	(1,300)	.30	(.012)	9.1	(20)	.00	(.000)
	ditto, 1st rerun		13.6	(~30)	.05	(.002)	2,393	*(5,275)	.97	*(.038)	680	(1,500)	.43	(.017)	~9.1	(~20)	.00	(.000)
	ditto, reruns #2, #3, and #4		9.1	(~20)	.05	(.002)	2,404	*(5,300)	.91	*(.036)	499	(1,100)	.30	(.012)	9.1	(20)	.03	(.001)
	ditto, 5th rerun ▲		9.1	(~20)		(.002)	2,404	*(5,300)	.94	(.037)	680	(1,500)	.41	(.016)	9.1	(20)	.13	(.005)
296K	O-ring #1	1671	9.1	(20)	.18	(.007)	290	(640)	.36	(.014)	None - Blowout.				375	(826)	-1.19	(-.047)
(73F)	ditto, rerun		9.1	(20)	.20	(.008)	295	(650)	.28	(.011)	None - Blowout.				381	(841)	-1.04	(-.041)
	O-ring #2	1673	13.6	(30)	.20	(.008)	295	(650)	.43	(.017)	None - Blowout.				366	(806)	-1.07	(-.042)
	ditto, rerun		9.1	(20)	.15	(.006)	295	(650)	.41	(.016)	None - Blowout.				376	(828)	-1.04	(-.041)
344K	O-ring #1	2078	13.6	(30)	.23	(.009)	297	(655)	.48	(.019)	None - Blowout.				-			
(160F)	ditto, rerun	2079	13.6	(30)	.23	(.009)	299	(660)	.43	(.017)	None - Blowout, †				402	(887)	-.46	(-.018)
	O-ring #2	2080	13.6	(30)	.25	(.010)	299	(660)	.53	(.021)	None - Blowout, †				404	(890)	-.46	(-.018)
	ditto, rerun	2081	13.6	(30)	.23	(.009)	299	(660)	.51	(.020)	None - Blowout, †				401	(885)	-.46	(-.018)

④ Compression cycled 3 times to 600 lb., once with He pressurization, at room temperature before cooling in LN_2.
* Complete sealing not achieved. Max. pressure = 31% of internal pressurization applied.
▲ After 100 compression cycles at 86K (-310F).
④ Compression cycled 4 times to ~600 lb., once with He pressurization, at room temperature before cooling in LN_2.
† O-rings partially resealed after blowoug out. After Instron load precipitiously dropped to (150-200 lb).
* Complete sealing not achieved although He flow increased to ~2,000 cc/min.

Page intentionally left blank

The leakage rate for the AF-E-124D O-rings was in general more than four times that of the Halar O-rings. In addition, although the AF-E-124D is a soft, compliant, good sealing rubber at ambient temperatures (whereas the Halar is a tough, hard plastic), at cryogenic temperatures the AF-E-124D must be even harder and more intractable than the Halar. This is supported by the much higher Instron loadings (~2,000 Kg) required for the still incomplete sealing of the AF-E-124D O-rings compared with the ~1,000 Kg loading required for the complete sealing of the Halar O-rings (compare Tables 40 and 41). In a practical way, the tremendous change in loading requirements (i.e., required sealing force) of the AF-E-124D O-rings on passing from ambient or elevated temperatures to cryogenic temperatures mitigates against their use as cryogenic seals. For example, while the required sealing force for crosslinked Halar only increased by a factor of two (i.e., from 500 Kg to ~1,000 Kg) on cooling from 296K to 86K, the corresponding sealing force required for AF-E-124D increased almost by a factor of eight (from ~300 Kg to ~2,400 Kg).

3.2.7 Static Thermal Cycling Leak Test

On the basis of the previous liquid oxygen (LO_2) impact tests (Section 3.2.2) and dynamic sealability tests (Section 3.2.6), crosslinked Halar was selected as the outstanding Main Propellant seal candidate. The same static thermal cycling leak test assembly described in Section 3.1.6 and shown in Figure 25 was employed. By inserting 0.508 mm (0.020 in.) shims between the gland shoulders and the anvil, the crosslinked Halar O-ring was subjected to a 15% squeeze. The test fixture containing the crosslinked Halar O-ring was thermocoupled and manually cycled between a 296K (73F) water bath, a 344K (160F) constant temperature oven, and a LN_2 bath. One complete thermal cycle, therefore, consisted of the following successive temperature stages:

296K	→	344K	→	296K	→	83K	→	296K
(73F)		(160F)		(73F)		(-310F)		(73F)
water bath		oven		water bath		LN_2 bath		water bath

The test fixture was maintained at each temperature stage for 30 minutes in order to ensure thermal equilibration. Each of two crosslinked Halar O-rings was subjected to three complete thermal cycles.

Each crosslinked Halar O-ring exhibited the same sealing qualities. Full sealability[1] was maintained through the 296K→344K→296K portion of the test. The O-ring invariably started to leak (very slightly) as the temperature was lowered to 227K (-50F). The leakage rate steadily increased as the temperature decreased, until at 177K (-140F) complete loss of pressure resulted.

(1) Full sealability is defined as no visible loss of pressure over a five minute time period after the gas inlet to the already pressurized O-ring test gland is shut off.

When these failed O-rings were warmed, i.e., as the thermal cycling was continued, the rings started to reseal. By the time ~239K (~-30F) had been reached, full sealability had been achieved. The process thus appeared to be essentially reversible, at least over the three complete cycles to which each of the subject Halar O-rings were subjected.

It is tempting to think that the low temperature leakage was simply due to the normal thermal contraction of the hard crosslinked Halar O-ring. Unfortunately, after three thermal cycles, these crosslinked Halar O-rings exhibited a 50% compression set as a percentage of the original (15%) deflection. One Halar O-ring which after the usual thermal cycling was held under compression for 19 days at ambient temperatures suffered 74% compression set, based on percent of original deflection. These observations support the previous evidence that the subject Halar O-rings were probably not as heavily crosslinked as had been hoped. Even more important,in the absence of comparable data on the presently accepted cryogenic seal materials (such as Kel-F and Teflon), it is difficult to judge the validity of this static thermal cycling leak test. It may be that this test is unduly severe.

3.3 Orbital Maneuvering Seals

3.3.1 Long Term Compatibility Tests of Seal Candidates with Monomethyl Hydrazine

Three tensile specimens each of linear Halar, linear Tefzel, and phosphazine fluoroelastomer #1884-34 were 80% immersed in monomethyl hydrazine (MMH) and sealed in pyrex pressure tubes, 16 mm O.D. by 13.2 mm I.D. by 155 mm long. The Halar and Tefzel specimens had dimensions 9.53 by 63.5 mm, per ASTM D638-71, Type V. The individual tensile specimens were separated by bent glass rod spacers, 2 mm O.D. The general arrangement is shown in Figure 45. The subject capsules were run outdoors, under ambient conditions from 16 October 1972 to 24 July 1973, a period of 281 days (~9 months). The ambient temperature ranged from 275K (36F) to 314K (105F). The capsules were visually examined every month and the appearance of the supernatant MMH as well as the test specimens was noted. The results are summarized in Table 42. It is apparent that only the phosphazine fluoroelastomer suffered any visible degradation.

Upon opening the MMH-filled sealed tubes, the degradation of the phosphazine fluoroelastomer No. 1884-34, which had been visually detected as early as December of 1972, was fully confirmed. The three phosphazine fluoroelastomer tensile dumbbells had completely degraded to a solid mass of soft putty. It will be recalled that during the hydraulic system-compatibility work (Section 3.1.1 and Appendix C) it was discovered that the No. 1884-34 stock used in this contract was an old type vulcanizate which does not adequately reflect the present state-of-the-art for phosphazine fluoroelastomers. However, in view of the observed catastrophic degradation, it is doubtful if even the new, improved phosphazine vulcanizates would survive 9 months' immersion in MMH. Degradation to the observed extent probably indicates an inherent phosphazine fluoroelastomer/MMH incompatibility.

Unlike the phosphazine fluoroelastomer, the fluoroplastics (linear Halar and Tefzel) showed only minor losses of tensile strength and even smaller changes in ultimate elongation and hardness. The effect of this 9 to 10 month immersion in both N_2O_4 and MMH on linear Halar and Tefzel are summarized in Tables 43 and 44, respectively. Based on this data, linear Halar and linear Tefzel are equally suitable for prolonged use with MMH.

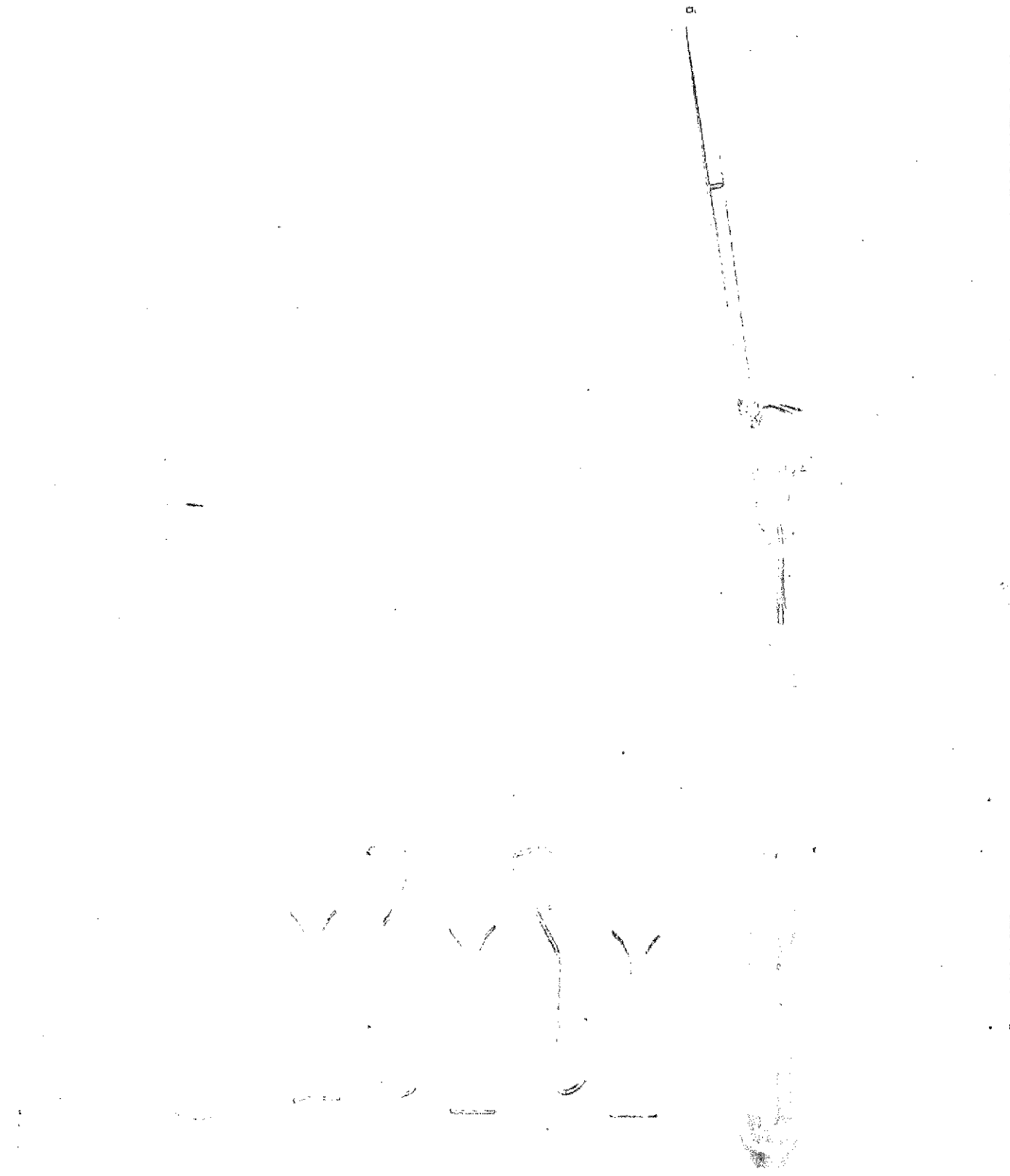

Figure 45. Pyrex Glass Sealed Capsules for Long Term Compatibility Tests With MMH/N_2O_4.

Table 42

Long Term Compatibility Test of Orbital Maneuvering System Seal Candidates with Monomethyl Hydrazine
(Visual Examination)

Time	Phase Propellent vs Seal Material	Linear Halar	Linear Tefzel	Phosphazine Fluoroelastomer #1884-34
14 days	MMH; Tensile spec.	Water white No visible change	Very slightly yellow No visible change	Light brown color No visible change
44 days	MMH; Tensile spec.	Water white No visible change	Very slight yellow No visible change	Clear light gold color No visible change
77 days	MMH; Tensile spec.	Water white No visible change	Very slightly yellow No visible change	Clear gold color 1 spec. slightly swollen
104 days	MMH; Tensile spec.	Water white No visible change	Very slightly yellow No visible change	Clear gold color 1 spec. definitely swollen
134 days	MMH; Tensile spec.	Water white No visible change	Very slightly yellow No visible change	Clear gold color 1 spec. definitely swollen
170 days	MMH; Tensile spec.	Water white No visible change	Very slightly yellow No visible change	Clear gold color All specimens swollen
224 days	MMH; Tensile spec.	Water white No visible change	Very slightly yellow No visible change	All MMH imbibed by specimens Swollen specimens occupy 3/4 of the volume of the capsule
248 days	MMH; Tensile spec.	Water white No visible change	Very slightly yellow No visible change	Specimens are now so swollen as to completely fill the capsule
279 days	MMH; Tensile spec.	Water white No visible change	Very slightly yellow No visible change	Specimens are now so swollen as to completely fill the capsule

Table 43

Effect of Orbital Maneuvering Propellants on Linear Halar

Conditions: Sealed tubes; ambient temperature
San Diego, October to July
Tested: RT, 5.08 mm/min
(0.2 in/min head speed)

Fluoroplastic	Instron Run No.	Tensile Strength at Yield Newtons/m^2 in millions	(PSI)	Tensile Strength at Break Newtons/m^2 in millions	(PSI)	% Elongation at Yield	% Elongation at Break	Shore-D Hardness
Linear Halar-Grade #302								
As Is	4464	33.6	(4,878)	72.1	(10,476)	3.0	122	76
As Is	4465	32.6	(4,740)	74.9	(10,881)	2.8	126	76
As Is	4466	33.0	(4,788)	76.5	(11,105)	2.8	128	76
Average		33.1	(4,802)	74.6	(10,821)	2.9	125	76
After 291 days' immersion in N_2O_4	1623	19.2	(2,790)	63.0	(9,150)	1.8	128	64-5
↓	1624	19.1	(2,780)	64.2	(9,318)	2.1	138	64-6
	1625	18.3	(2,665)	62.1	(9,014)	2.0	146	65-7
Average		18.8	(2,745)	63.1	(9,161)	2.0	137	65
Average Change		-14.3	(-2,057)	-11.5	(-1,660)	-0.99	+12	-10
Average % Change		-43	-43%	-15%	-15%	-31	+96	-13%
After 281 days' immersion in MMH	1626	29.3	(4,255)	66.0	(9,573)	2.5	124	72
↓	1627	28.9	(4,205)	74.2	(10,771)	2.3	128	72
	1628	28.2	(4,100)	73.5	(10,672)	1.9	144	73
Average		28.8	(4,187)	71.2	10,339	2.3	132	72
Average Change		-4.3	(-615)	-3.4	(-482)	-0.6	+7%	-4
Average % Change		-13%	-13%	-4.6%	-4.6%	-21%	+5.6%	-5.3%

Table 44

Effect of Orbital Maneuvering Propellants on Linear Tefzel

Conditions: Sealed tubes - ambient temperature, San Diego, October to July
Tested: RT, 5.08 mm/min (0.2in/min) head speed

Fluoroplastic	Instron Run No.	Tensile Strength at yield Newtons/m^2 in millions	(PSI)	Tensile Strength at break Newtons/m^2 in millions	(PSI)	% Elongation at Yield		% Elongation at Break	Shore-D Hardness
Linear Tefzel									
As Is	4461	27.8	(4,045)	44.4	(6,448)	3.4*	(11.5)	338	75
	4462	27.8	(4,039)	32.6	(4,721)	3.5	(15.3)	196	75
	4463	27.6	(4,009)	39.5	(5,743)	3.3	(13.7)	314	75
Average		27.7	(4,031)	38.8	(5,637)	3.4	(13.5)	283	75
After 291 days' immersion in N_2O_4	1629	25.2	(3,660)	40.0	(5,806)		3.0	324	64
	1630	24.8	(3,600)	38.3	(5,558)		3.3	326	65-6
	1631	24.4	(3,540)	37.9	(5,505)		3.3	308	64-7
Average		24.8	(3,600)	38.7	(5,623)		3.2	319	65
Average Change		-2.9	(-431)	-0.1	(-14)		-0.2	+36	-10
Average % Change		-10%	-11%	0%	0%		-6%	+13%	-13%
After 281 days' immersion in MMH	1632	25.0	(3,640)	38.8	(5,632)		3.0	322	75
	1633	24.8	(3,610)	41.9	(6,077)		3.9	328	75
	1634	25.2	(3,660)	33.1	(4,815)		3.4	248	73
Average		25.0	(3,637)	37.9	(5,508)		3.4	333	74
Average Change		-2.7	(-394)	-0.9	(-129)		0	+50	-1
Average % Change		-9%	-97%	-23%	-22%		-0%	+18%	0%

* Newly calculated values compared with originally calculated value, "( )". See text for explanation.

3.3.1.2 Long Term Compatibility Tests of Seal Candidates with Nitrogen Tetroxide

Three tensile specimens each of linear Halar, linear Tefzel, and the perfluoroelastomer AF-E-124D were 80% immersed in nitrogen tetroxide (N_2O_4) and sealed in the same type of pyrex pressure tubes described in Section 3.3.1.1 and shown in Figure 45. Like the MMH immersion specimens, the N_2O_4 immersion capsules were run outdoors in San Diego from 6 October 1972 to 24 July 1973, a period of 291 days (almost 10 months). These N_2O_4-charged capsules were visually inspected once a month. The appearance of both the supernatant N_2O_4 and the seal specimens are summarized in Table 45.

It can be seen that, except for a slight warping of the linear Halar specimens, there was no visually detectable changes in the subject seal specimens. Color changes of the supernatant liquid N_2O_4, however, indicated that some type of chemical reaction or extraction from the specimens was occurring.

When the N_2O_4-filled sealed tube capsules were opened, the earlier continuing visual observations concerning the condition of the exposed seal specimens were confirmed. All three seal specimens (linear Halar, linear Tefzel, and perfluoroelastomer AF-E-124D) appeared to be in good condition. After rinsing and soaking in water for 48 hours, the specimens were allowed to air dry for 72 hours. The specimens were then tensile tested; the Halar and Tefzel at 5.08 mm/min. (0.20 in/min.) head speed, and the AF-E-124D at 50.8 cm/min (20 in/min.). This Instron test data is summarized in Table 43 for the linear Halar, in Table 44 for the linear Tefzel, and in Table 46 for the perfluoroelastomer, AF-E-124D. The linear Halar suffered the greatest loss (43%) of tensile strength, followed by the AF-E-124D with 25 percent loss, and linear Tefzel with the least ($\sim$10%) loss. The AF-E-124D obviously suffered a typical polymeric degradation related to scission of either the main polymer chains or (less likely) the crosslinks. Modulus decreases of 20 percent to 30 percent accompanied the above-mentioned decrease in strength. The AF-E-124D softened by 6 points, and the elongation increased by 20 percent.

Table 45

Long Term Compatibility Test of Orbital Maneuvering System Seal Candidates with Nitrogen Tetroxide

(Visual Examination Only)

	Time	Phase Propellent vs Seal Material	Linear Halar	Linear Tefzel	Fluoroelastomer AF-E-124D
N_2O_4	24 days	N_2O_4; Tensile spec.	Clear brown color Slightly warped	Cloudy brown color No visible change	Dark brown color No visible change
	55 days	N_2O_4; Tensile spec.	Clear brown color Slightly warped	Brown color No visible change	Darker brown color No visible change
	87 days	N_2O_4; Tensile spec.	Clear brown color Slightly warped	Cloudy brown color No visible change	Greenish brown color No visible change
	114 days	N_2O_4; Tensile spec.	Clear brown color Slightly warped	Cloudy brown color No visible change	Greenish brown color No visible change
	144 days	N_2O_4; Tensile spec.	Clear brown color Slightly warped	Cloudy brown color No visible change	Greenish brown color No visible change
	180 days	N_2O_4; Tensile spec.	Clear brown color Slightly warped	Cloudy brown color No visible change	Greenish brown color No visible change
	234 days	N_2O_4; Tensile spec.	Clear brown color Slightly warped	Cloudy brown color No visible change	Dark brown color No visible change
	258 days	N_2O_4; Tensile spec.	Clear brown color Slightly warped	Cloudy brown color No visible change	Dark brown color No visible change
	289 days	N_2O_4; Tensile spec.	Clear brown color Slightly warped	Cloudy brown color No visible change	Dark brown color No visible change

Table 46

Effect of N_2O_4 Exposure on Perfluoroelastomer, AF-E-124D

Conditions: 292 days, Sealed Tubes - Temperature:ambient San Diego, October to July, Instron Tested at RT, head speed 50.8 mm/min (20 in/min)

Rubber Compound	Instron Run No.	Tensile Strength Newtons/m^2 in millions	Tensile Strength (PSI)	% Elongation at Break	Rubber Modulus (*) at 20% Newtons/m^2 in millions	Rubber Modulus (*) at 20% (PSI)	Rubber Modulus (*) at 100% Newtons/m^2 in millions	Rubber Modulus (*) at 100% (PSI)	Shore A Hardness
Perfluoroelastomer AF-E-124D									
GDC slab "as is"	4758	13.2	(1,920)	180	.83	(120)	3.79	(550)	75
GDC slab "as is"	4447	19.9	(2,886)	190	.77	(112)	3.70	(538)	75
	4760	15.2	(2,210)	160	.89	(130)	3.76	(545)	75
Average		16.1	(2,339)	177	.83	(121)	3.75	(544)	75
After 292 days' immersion in N_2O_4	1620	13.1	(1,907)	225	.64	(93)	2.5	(361)	67
	1621	12.1	(1,749)	210	.65	(95)	3.0	(430)	71
	1622	11.0	(1,601)	204	.67	(98)	2.4	(352)	69
Average		12.1	(1,752)	213	.65	(95)	2.6	(381)	69
Average Change (-less) (+gain)		-4.0	(-587)	+36	-.18	(-26)	-1.15	(-163)	-6
Average % Change		-25%	-25%	+20%	-21%	-21%	-31%	-30%	-8%

3.3.2 Thermal Cycling of Orbital Maneuvering Seal Candidates in Monomethyl Hydrazine

Three tensile specimens of each of the two surviving seal candidates of Section 3.3.1.1, linear Halar and linear Tefzel, were sealed in thermocoupled pyrex glass capsules containing MMH. The capsules are similar to those shown in Figure 4 except that the thermocouple was sealed into the capsule via a graded glass seal. The capsules are hermetically sealed. The same mechanical "dipping" machine successfully employed in thermal cycling both the hydraulic and the main propellant seal specimens was used. The principal modification was the replacement of the refrigeration chest employed as the cold sink in Section 3.1.2.1 by a 18.9 liter (5 gal) dewar flask charged with dry ice and Freon MF. Use of this cold bath plus the constant temperature, Marshall tube furnace permitted a 222K/377K (-60F/220F) cycle to be completed in ~100 minutes. Upon completion of the 200 cycles, the specimens were removed, rinsed, and air dried 2 to 3 days before tensile testing.

The results are summarized in Table 47. It is apparent, except for changes in elongation, that the linear Tefzel underwent only negligible changes in properties during the 200 cycles between 222 and 377K. The linear Halar proved to be even more resistant to MMH under these conditions. All changes exhibited by the linear Halar were well within experimental error.

3.3.3 Stress Relaxation Measurements of the Orbital Maneuvering Seal Candidates

The three surviving Orbital Maneuvering seal candidates were the perfluoroelastomer AF-E-124D, linear Tefzel, and linear Halar. Stress relaxation measurements of the AF-E-124D had already been performed under the Main Propellant seal work of Section 3.2.5. Typical semilog plots of the stress relaxation of AF-E-124D O-rings at 296K (73F) and 344K (220F) are shown in Figures 27 and 28, while the values of the relaxation constant "K" at 296 and 344K are summarized in Table 33. Similar stress relaxation measurements were performed at 296K and 377K on linear Tefzel and Halar O-rings using the same piezoelectric compression/stress relaxation apparatus described in Section 3.1.4.1. The stress relaxation measurements followed the same relationship:

$$\sigma = \sigma_1 - K \log t$$

where: σ_1 = stress at 1 min.

σ = stress at time, t

K = relaxation constant

and plots of load (stress) against the log of time gave the straight lines shown in Figures 46 and 47 for linear Tefzel O-rings at 296K and 377K. Figures 48 and 49

Table 47

Effect of Temperature Cycling in MMH on Linear Tefzel and Halar

Conditions: Two Hundred 100 min. cycles
222K (-60F) to 377K (220F)
Tested - RT, 0.2 in/min. head speed

Fluoroplastic	Instron Run No.	Tensile Strength at Yield Newtons/m^2 in millions	(PSI)	Tensile Strength at Break Newtons/m^2 in millions	(PSI)	Elongation Yield	Elongation Break	Shore D Hardness
Linear Tefzel "As Is"	4461	27.8	(4,045)	44.4	(6,448)	11.5%	338%	75
	4462	27.8	(4,039)	32.6	(4,721)	15.3%	196%	75
	4463	27.6	(4,009)	39.5	(5,743)	13.7%	314%	75
Average		27.7	(4,031)	38.8	(5,637)	13.5%	283%	75
After 200 Cycles -60F to +220F	1635	26.9	(3,910)	43.8	(6,358)	2.9%	362%	74
	1636	26.9	(3,910)	44.1	(6,397)	2.6%	366%	74
	1637	26.7	(3,880)	35.5	(5,155)	3.8%	282%	72
Average		26.8	(3,900)	41.1	(5,970)	3.1%	336%	73
Average change		(-0.9)	(-131)	(+2.3)	(+333)	(-10.4%)	+53.0%	-2
Average % change		-.3%	-.3%	+6%	+6%	-7.7%	+1.8%	-2.6%
Linear Halar-Grade #302 "As Is"	4464	33.6	(4,878)	72.1	(10,476)	3.0%	122%	76
	4465	32.6	(4,740)	74.9	(10,881)	2.8%	126%	76
	4466	33.0	(4 788)	76.5	(11,105)	2.8%	128%	76
Average		33.1	(4,802)	74.6	(10,821)	2.9%	125%	76
After 200 Cycles -60F to +220F	1638	31.9	(4,637)	74.9	(10,876)	2.7%	132%	75
	1639	32.5	(4,721)	74.7	(10,841)	2.5%	120%	76
	1640	30.2	(4,380)	73.0	(10,590)	2.8%	139%	74
Average		31.5	(4,579)	74.2	(10,769)	2.6%	130%	75
Average change		(-1.6)	(-223)	(-.4)	(-52)	(-0.3%)	(+5%)	(-1)
Average % change		-.5%	-.5%	-.5%	-.5%	-1%	+4%	-.1%

Figure 46

Stress Relaxation of Linear Tefzel O-ring at 296K (73°F)(Specimen No. 2)

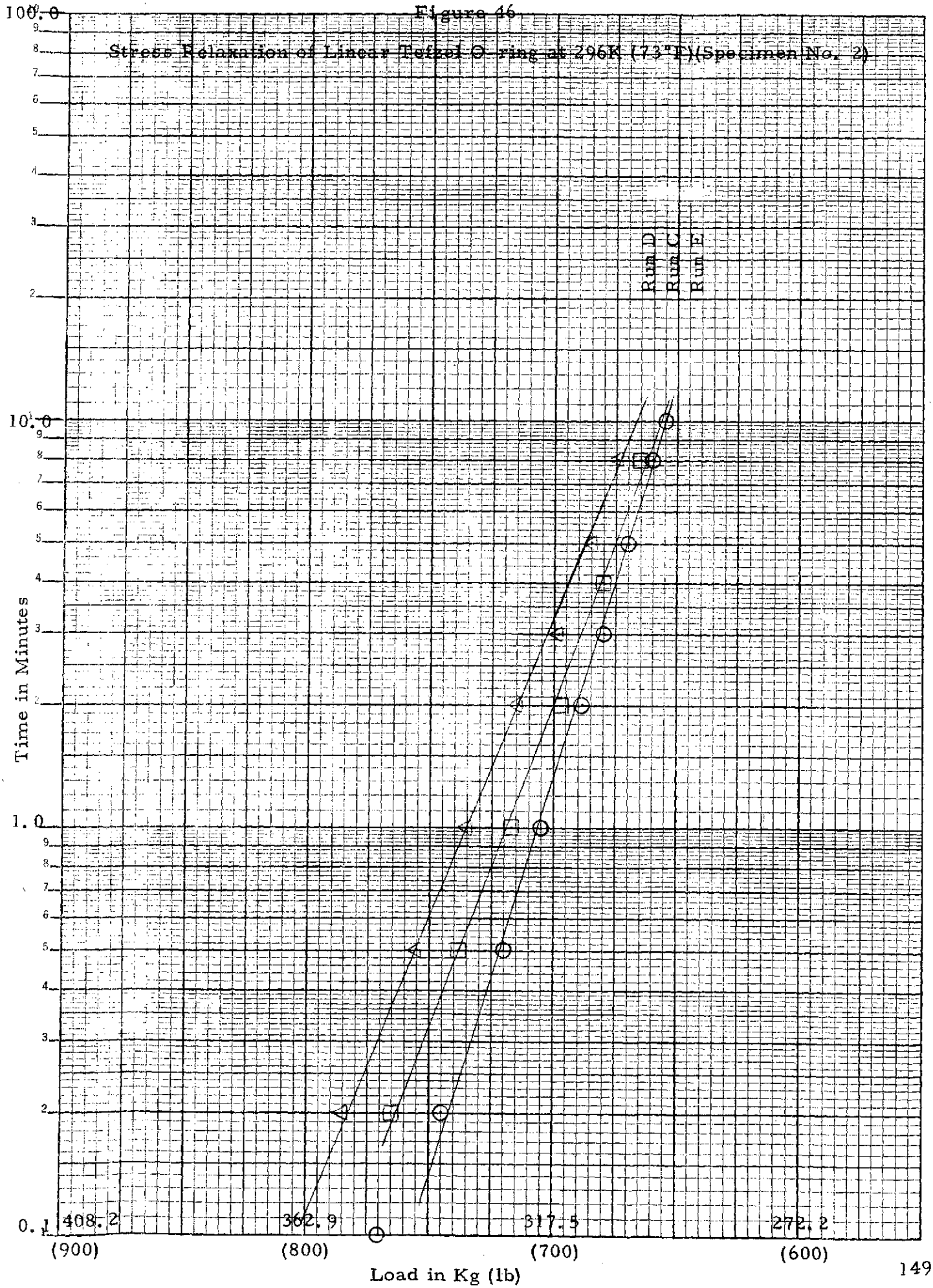

Figure 47

Stress Relaxation of Linear Tefzel O-ring at 177K (220°F) (Specimen No. 2)

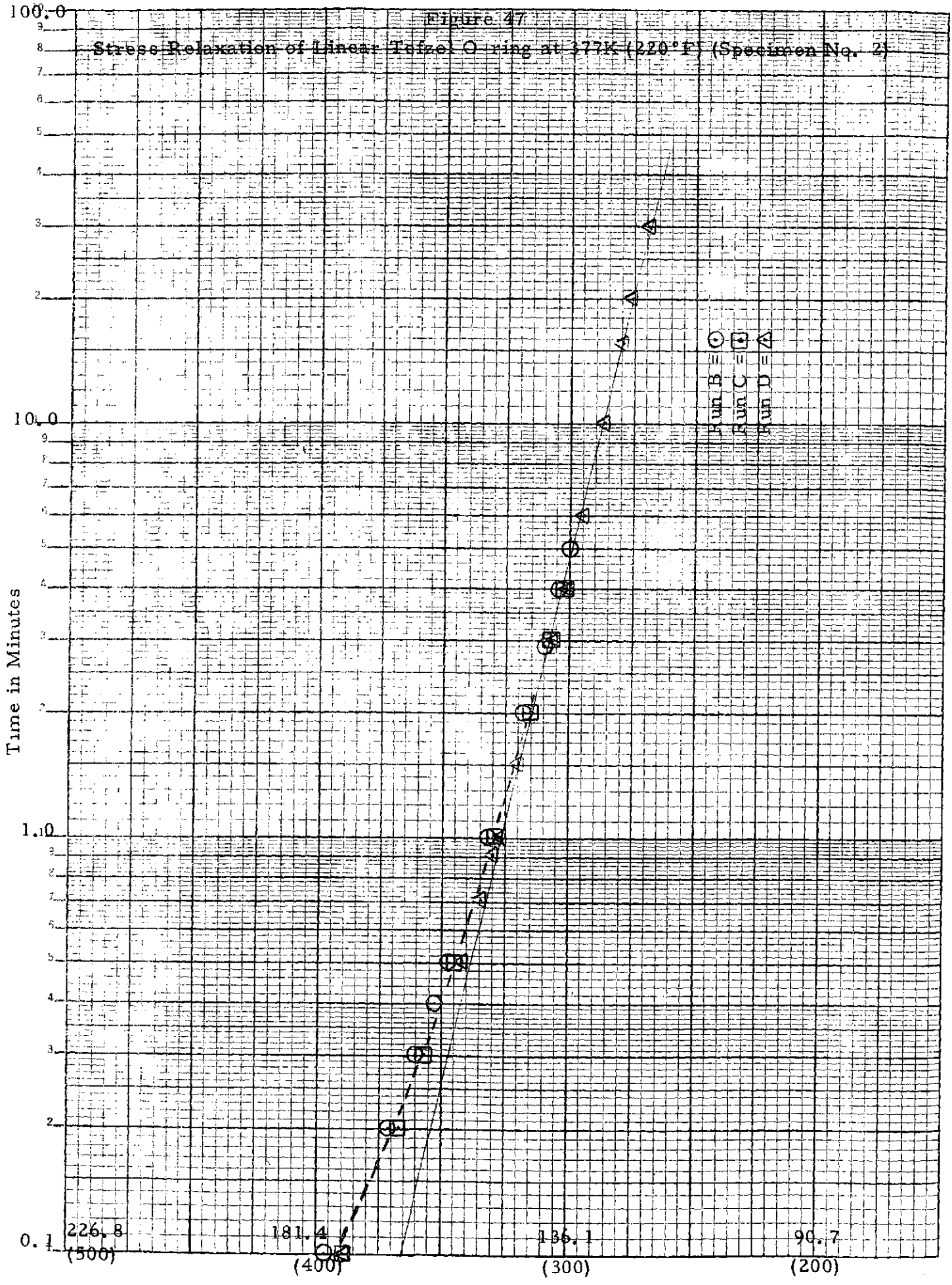

Figure 48

Stress Relaxation of Linear Halar O-rings at 296K (73°F)
(Specimen No. 1 and 2)

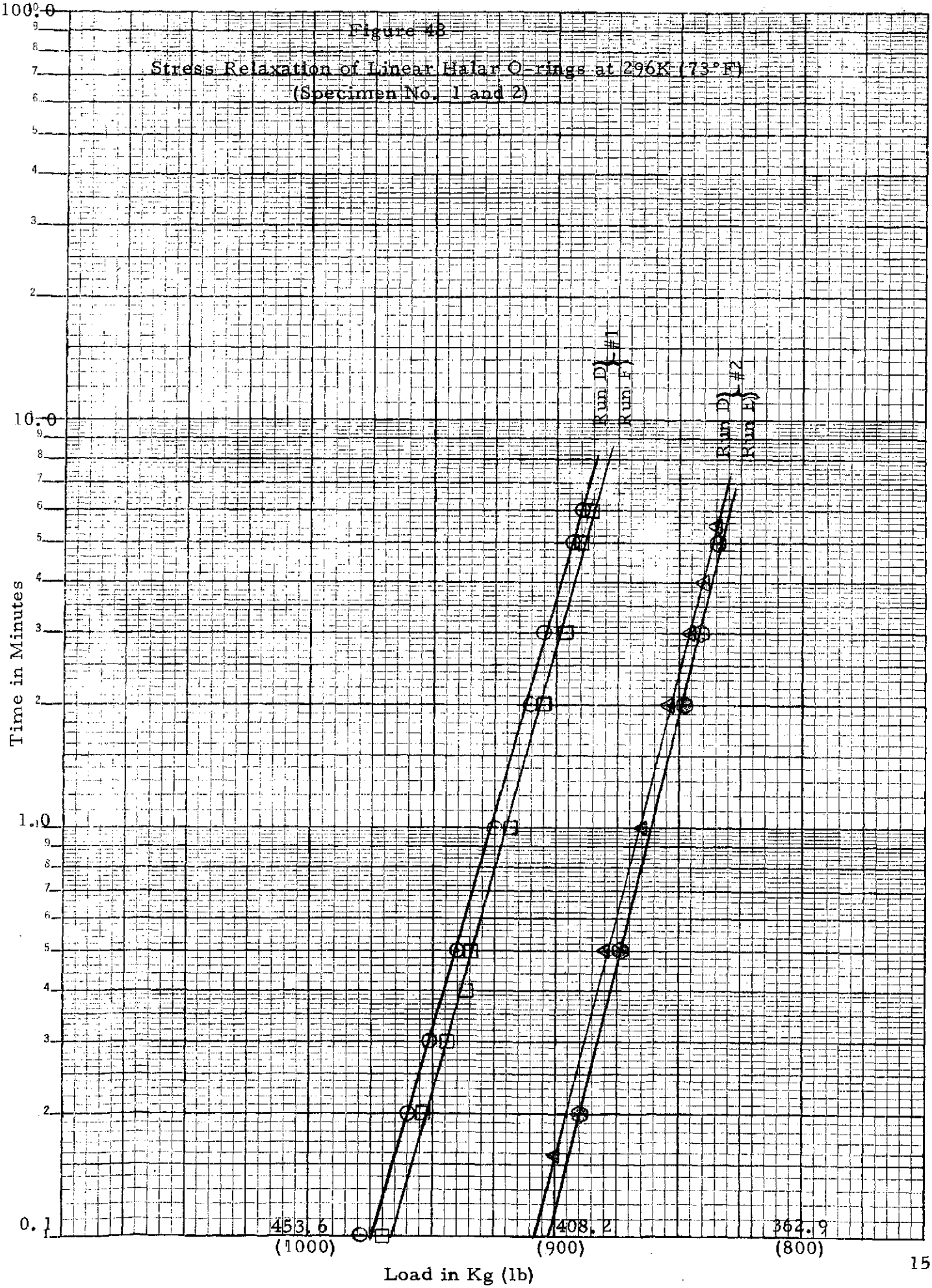

Figure 49

Stress Relaxation of Linear Halar O-rings at 377K (220°F)

(Specimens No. 1 and 2)

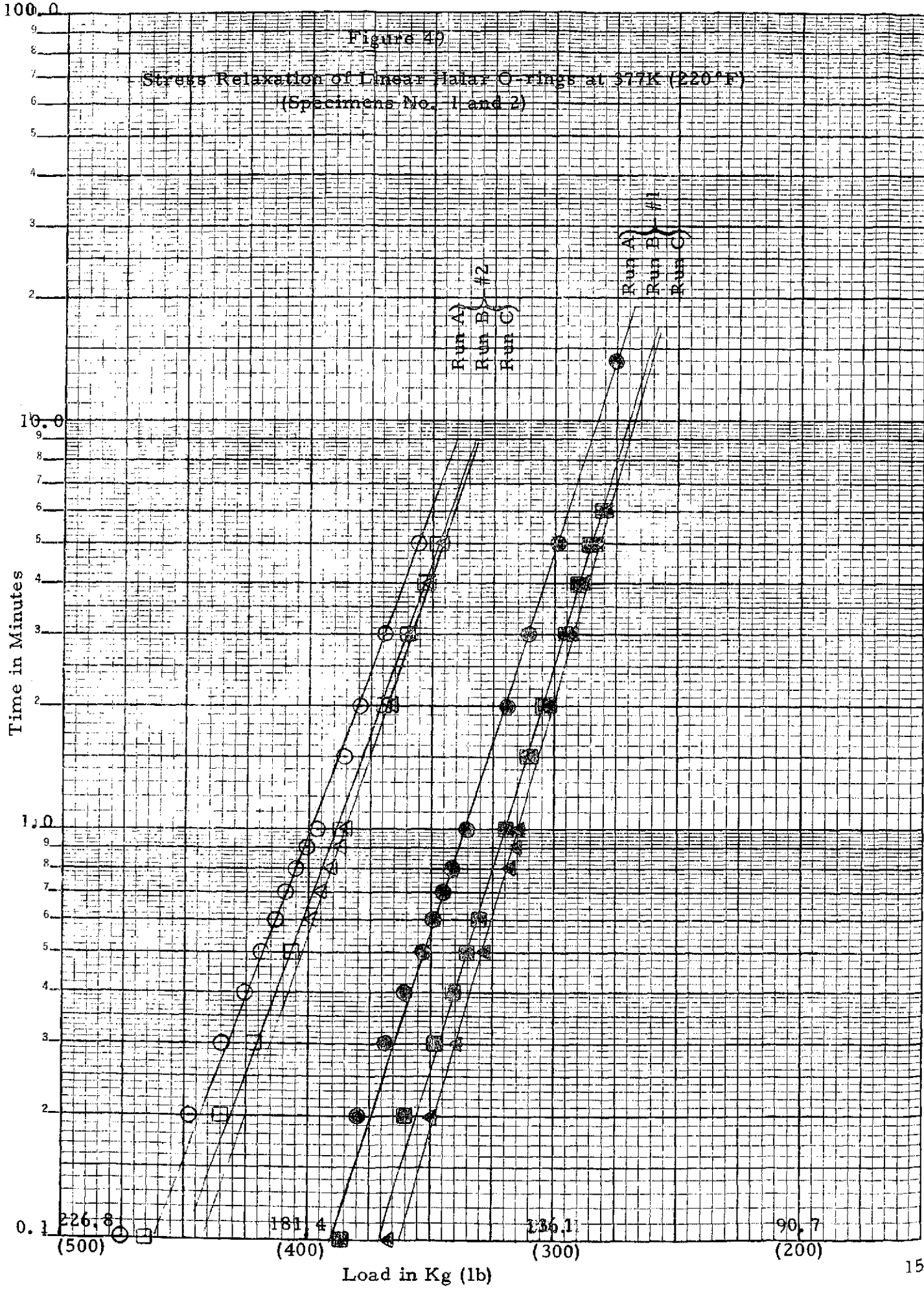

are the same types of plots for linear Halar O-rings at 296K and 377K, respectively. The stress relaxation results for these two fluoroplastics at the two subject temperatures is summarized in Table 48. As expected, stress relaxation behavior resembled that of the previously measured crosslinked Halar O-rings (see Section 3.2.5) in that the rate of stress relaxation increased sharply as the temperature was raised. In fact, the relaxation constant, K, of these linear Halar O-rings is almost exactly equal to that of the crosslinked Halar O-rings (compare Tables 33 and 48). At 296K, Tefzel O-rings had a significantly higher rate of stress relaxation than the Halar O-rings (i.e., $\frac{K}{\sigma_1}$ = .088 vs. 050). However, when the temperature was raised to 377K (220F), the Tefzel O-rings displayed a lower rate of stress relaxation than the Halar O-rings (i.e., $\frac{K}{\sigma_1}$ = .121 vs. .155).

3.3.4 Cyclic Compression Sealability of the Orbital Maneuvering Seal Candidates

O-rings molded from linear Tefzel and linear Halar were subjected to the same cyclic sealability leak tests previously described in Section 3.1.5. As might be expected, the sealing characteristics are similar to those of the crosslinked Halar O-rings described in Section 3.2.6.

Because of its outstanding N_2O_4 resistance discussed previously (Section 3.3.1.2), the sealability of the linear Tefzel O-rings was tested at four (4) temperatures: 222K (-60F), 233K (-40F), 296K (73F), and 377K (220F). Results of these tests are summarized in Table 49. Typical Instron sealability curves are shown in Figures 50, 51, and 52 for the 296K (73F), 222K (-60F), and 378K (220F) temperature tests, respectively. It can be readily seen that linear Tefzel displays fair to good sealability at ambient and low temperatures. Once the first compression sealing cycle (which is always typically high, see Table 40 for similar effects) was completed, the linear Tefzel sealed at quite low pressures. In fact, at 296K the Tefzel O-rings sealed at lower pressures than the previously measured crosslinked Halar O-rings (compare Table 49 with Table 40). Measurements of the cross section of these Tefzel O-rings before and after these dynamic leak tests also disclosed no compression set. At 222K (-60F), the Tefzel O-rings failed to achieve complete internal pressurization until after the unloading portion of the cycle had started (see Figure 51), although this was not considered important. At 377K (220F), however, these linear Tefzel O-rings failed to seal. This poor sealability of the linear Tefzel O-rings is evident in Figure 52. In spite of the two preliminary "non-pressurized" compression cycles, the Tefzel O-ring retained less than 70% (i.e., 0.93 MN/m^2) of the maximum possible internal pressure of 1.34 MN/m^2 (195 psi) He, with a flow rate (~1500 cc/min.) three times the 500 cc/min. flow rate customarily employed during these sealability tests. This poor sealability of the Tefzel at 377K (220F) is particularly surprising in view of the excellent resistance of Tefzel O-rings to stress relaxation at 377K. In fact, at 377K linear Tefzel has a lower average normalized relaxation constant, $\frac{K}{\sigma_1}$ = 0.121 (Table 48), than crosslinked Halar has at 344K, $\frac{K}{\sigma_1}$ = 0.139 (Table 33).

Table 48

Stress Relaxation of Principal Orbital Maneuvering Seal Candidates,
$\sigma = \sigma_1 - K \log t$

Seal Candidate	Run No.	Temperature °K	Temperature (°F)	Stress At 1 min., " " Kg	Stress At 1 min., " " (lb)	Relaxation Constant, "K" Kg	Relaxation Constant, "K" (lb)	Normalized Relaxation Const., "K/σ_1
Linear Tefzel								
O-ring #1	B	296	(73)	331	(730)	32	(71)	0.097
	C			319	(703)	28	(61)	.087
	A			263	(580)	24	(52)	.090
O-ring #2	D			333	(735)	31	(68)	.093
	C			327	(720)	29	(63)	.088
	E			321	(707)	24	(52)	.074
Average				316	(696)	28	(61)	0.088
O-ring #1	A	377	(220)	228	(502)	26	(57)	0.114
	B			226	(498)	26.5	(58)	.116
	C			224	(494)	24.5	(54)	.109
O-ring #2	B'			151	(332)	21	(46)	.138
	C'			150	(330)	20	(44)	.133
	D			145	(320)	17	(37)	.116
	E			148	(327)	18	(39)	.119
Average				182	(431)	22	(48)	0.121
Linear Halar								
O-ring #1	D	296	(73)	420	(927)	22	(48)	0.052
	F			417	(920)	21	(46)	.050
O-ring #2	D'			393	(867)	20	(44)	.051
	E			391	(861)	19	(41)	.048
Average				405	(894)	20.5	(45)	0.050
O-ring #1	A	377	(220)	152	(336)	24	(53)	0.158
	B			145	(320)	23	(50)	.156
	C			143	(315)	22	(48)	.152
O-ring #2	A			181	(399)	29	(63)	.158
	B			176	(389)	28	(61)	.157
	C			175	(385)	26	(57)	.148
Average				162	(357)	25	(55)	0.155

Table 49

Cyclic Sealability Behavior of Linear Tefzel O-rings from 222K (-60F) to 378K (220F)

Conditions: Instron Head Speed = 0.509 mm/min. (0.02 in/min.)
Internal Pressurization = 1.34 MN/m^2 (195 psi)
GN_2 at 500 cc/min.

			Instron Loading Cycle								Instron Unloading Cycle							
			Initial Sealing				Complete Sealing				Initial Leak				Complete Loss of Sealing			
			Load		Compression		Load		Compression		Load		Compression		Load		Compression	
Temp.	O-ring Specimen	Instron Test No.	Kg	(lb)	mm	(inches)	Kg	(lb)	mm	(inches)	Kg	(lb)	mm	(lb)	Kg	(lb)	mm	(inches)
222K (-60F)	O-ring #2	1686	<4.5	(<10)	0.051	(.002)	726	(1600)	0.457	(.018)	318	(700)	0.406	(.016)	<4.5	(<10)	0.178	(.007)
	ditto, 1st rerun		4.5	(10)	0.051	(.002)	435	(960)	0.305	(.012)	322	(710)	0.229	(.009)	~0.9	(~ 2)	0.025	(.001)
	ditto, 2nd & 3rd reruns		9.1	(20)	0.051	(.002)	431	(950)	0.279	(.011)	277	(610)	0.203	(.008)	~0.9	(~ 2)	0.025	(.001)
	ditto, 5th rerun		4.5	(10)	0.051	(.002)	431	(950)	0.279	(.011)	340	(750)	0.229	(.009)	~0.9	(~ 2)	0.025	(.001)
	O-ring #3	1689	~13.6	(~30)	0.051	(.002)	508	(1120)	0.330	(.013)	304	(670)	0.381	(.015)	~4.5	(~10)	0.152	(.006)
	ditto, reruns #1 thru #3		4.5	(10)	0.051	(.002)	435	(960)	0.279	(.011)	277	(610)	0.203	(.008)	3.2	(~ 7)	0.051	(.002)
	ditto, reruns #4 & #5		9.1	(20)	0.051	(.002)	449	(990)	0.279	(.011)	286	(630)	0.203	(.008)	2.3	(5)	0.051	(.002)
233K (-40F)	O-ring #4	1685	~4.5	(~10)	0.076	(.003)	635	(1400)	0.406	(.016)	281	(620)	0.330	(.013)	~4.5	(~10)	0.152	(.006)
	ditto, reruns #1 & #2		4.5	(10)	0.051	(.002)	440	(970)	0.279	(.011)	259	(570)	0.203	(.008)	~2.3	(~ 5)	0.076	(.003)
	ditto, reruns #3 thru #5		4.5	(10)	0.051	(.002)	440	(970)	0.305	(.012)	268	(590)	0.178	(.007)	~4.5	(~10)	0.051	(.002)
296K (73F)	O-ring #1	1677	~9.1	(~20)	0.076	(.003)	431	(950)	0.330	(.013)	249	(550)	0.533	(.021)	18.1	(40)	0.356	(.014)
	ditto, 1st rerun		~13.6	(~30)	0.025	(.001)	431	(950)	0.229	(.009)	249	(550)	0.305	(.012)	11.3	(25)	0.127	(.005)
	O-ring #7	1678	22.7	(50)	0.076	(.003)	372	(820)	0.279	(.011)	277	(610)	0.178	(.007)	6.8	(15)	0.051	(.002)
	ditto, 1st rerun		13.6	(30)	0.025	(.001)	386	(850)	0.229	(.009)	268	(590)	0.127	(.005)	4.5	(10)	0.025	(.001)
	ditto, reruns #2 thru #4		6.8	(15)	0.025	(.001)	367	(810)	0.203	(.008)	277	(610)	0.152	(.006)	4.5	(10)	0.025	(.001)
377K (220F)	O-ring #10	2795	9.1	(20)	0.051	(.002)	494	(1090)*	0.660	(.026)*	254	(560)	0.432	(.017)	<4.5	(<10)	0.127	(.005)
	ditto, rerun		4.5	(10)	0.051	(.002)	508	(1120)*	0.711	(.028)*	231	(510)	0.406	(.016)	<2.3	(< 5)	0.025	(.001)
	O-ring #11	2796	<2.3	(< 5)	0.076	(.003)	408	(900)*	0.559	(.022)*	245	(540)*	0.432	(.017)	<2.3	(< 5)	0.025	(.001)

* Complete sealing was never achieved. Measured pressurization = 1.0 MN/m^2 compared with applied pressure of 1.34 MN/m^2

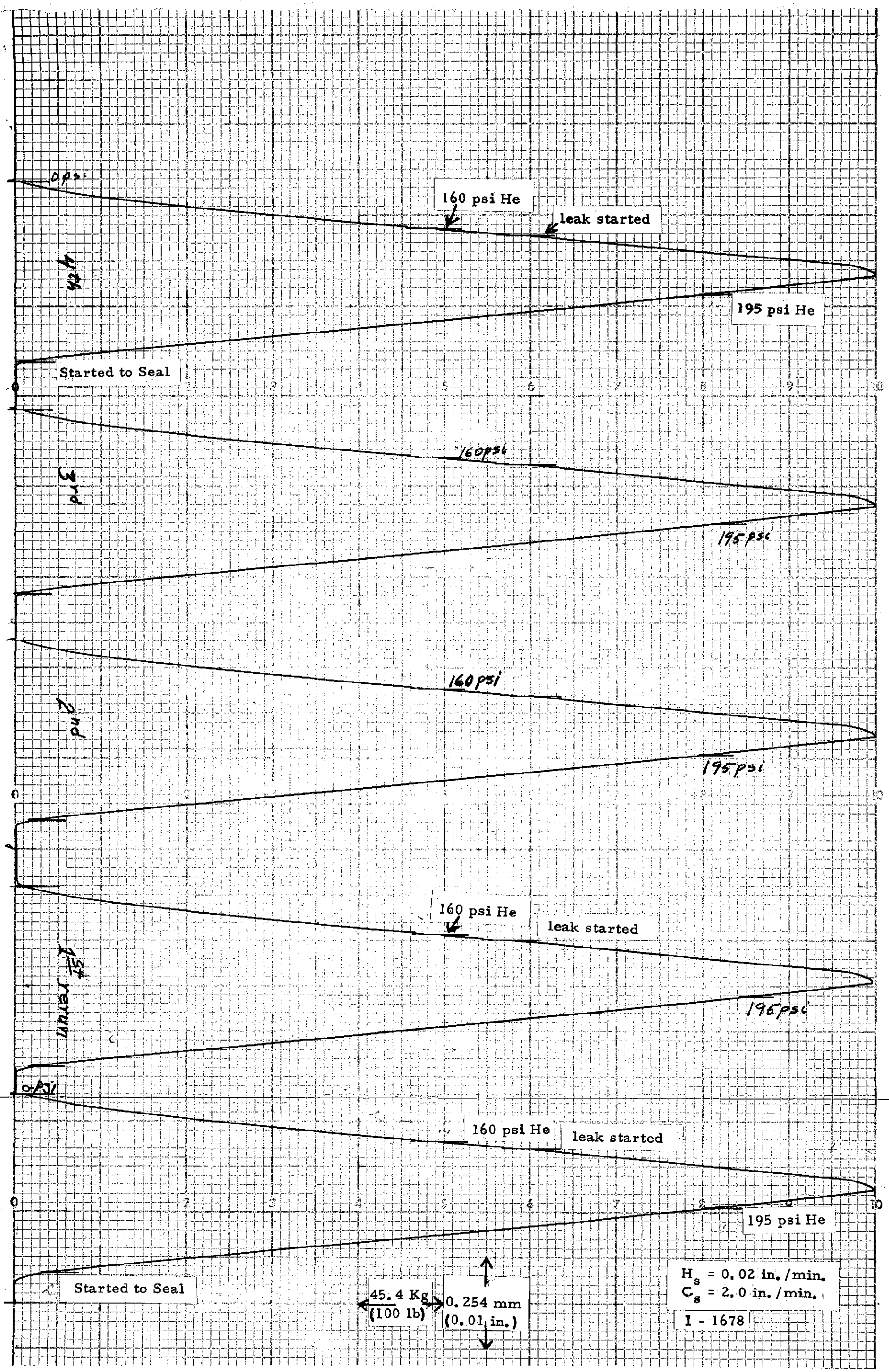

Figure 50. Instron cyclic Sealability Test Curves of Linear Tefzel O-ring #7 at 296K (73F)

Page intentionally left blank

Page intentionally left blank

The dynamic sealing performance of the linear Halar O-rings resembled those of the linear Tefzel O-rings except at high temperatures the performance of the linear Halar was significantly better. Typical Instron dynamic sealability curves at 222K (-60F) and 296K (73F) are shown in Figures 53 and 54. The results are summarized in Table 50. It will be noted that the initial sealing action of these linear Halar O-rings required about the same 5 to 20 kg load as the linear Halar O-rings. In order to get complete sealing, however, significantly higher loading forces were required. At low temperatures (222K), these Halar O-rings exhibit the same peculiar delay as the Tefzel O-rings in that complete sealing was not achieved until after the maximum pressure had been applied and the unloading portion of the cycle had started (compare Figure 54 with Figure 51).

Like the linear Tefzel O-rings, the linear Halar O-rings failed to achieve complete sealing at 377K (220F). However, as shown in Figure 55, a significantly greater degree of sealing action was obtained with the linear Halar O-rings. About 82% of the applied internal pressurization, i.e., 1.1 MN/m^2 (160 psi), was achieved on the first three sealing cycles. This increased to >86% [1.17 MN/m^2 (169 psi)] after the O-ring had been compression cycled 100 times. Although compression set was not apparent during the first four compression cycles (i.e., through the third "rerun"), there was a large compression set by the end of 100 cycles. Based upon maximum load values, the compression set amounted to ~17%. This is somewhat more than the 8-10% compression set calculated from actual measurements of the O-ring thicknesses before and after the 100 compression cycles of this sealability test (see Appendix E).

Regardless of the exact figures employed, these data indicate that 377K (220F) is above the service capabilities of both linear Tefzel and linear Halar. Although linear Halar has a somewhat higher service temperature, the linear Tefzel has much better N_2O_4 resistance and requires lower sealing forces. It should be possible to raise the Tefzel service temperature without compromising the latter two favorable characteristics by crosslinking the Tefzel with radiation. This, unfortunately, is beyond the scope of this present program, and as the best viable alternature, it was decided to attempt to utilize the crosslinked Halar O-rings produced as seals for the Main Propellant System (see Section 3.2) in the last remaining test of this program; namely, the thermal cycling static seal test.

3.3.5 Static Thermal Cycling Leak Test

In view of the failure of the preferred linear Tefzel to satisfy the high temperature dynamic sealability requirement of the Orbital Maneuvering System, it was decided (see Section 3.3.4) to attempt to use crosslinked Halar. It will be remembered that crosslinked Halar had demonstrated satisfactory dynamic sealing properties from 344K (160F) to 83K (-310F), with, in fact, outstanding performance at the

Page intentionally left blank

Page intentionally left blank

Page intentionally left blank

latter cryogenic temperature. There was, however, some question concerning the completeness or extent of radiation crosslinking of the subject crosslinked O-rings.

The same static thermal cycling leak test assembly described in Section 3.1.6 and illustrated in Figure 25 was employed. The same 0.508m (0.020 in.) shims, decribed in Section 3.2.7, were employed to obtain a 15% squeeze on the O-ring specimen. One complete thermal cycle consisted of the following successive temperature stages:

296K	→	222K	→	296K	→	377K	→	296K
(73F)		(-60F)		(73F)		(220F)		(73F)
water bath		cold bath		water bath		oven		water bath

A Freon MF (trichlorofluoromethane)/dry ice bath served as the 222K cold bath. In order to protect the O-ring specimen from the solvating effect of the Freon, the entire test fixture was encased in a polyethylene bag during this stage. The thermocoupled test fixture was stabilized at each test temperature for 30 minutes before passing on to the next thermal stage.

In contrast to the results of the Main Propellant Static Thermal Cycling Leak Tests of Section 3.2.7 (where the O-ring specimen had been carried through the temperature sequence: 296K → 344K → 296K → 83K → 296K) the crosslinked Halar O-ring specimens of this present test passed the first four stages with flying colors but failed on the 5th stage, i.e., on cooling from the 377K (220F) test temperature to room temperature (296K). Thus, crosslinked Halar showed full sealability from 296K (73F) down to 222K (-60F) and back through 296K (73F) up to 377K (220F). Full sealability is defined as no detectable drop in pressure for five minutes after the gas inlet tube is closed off from the pressurized O-ring gland. During the 5th stage, i.e., upon cooling from 377K (220F) to 296K (73F), the crosslinked Halar O-ring invariably started to leak at ~ 336K (145F) and was leaking badly by the time the temperature had dropped to 313K (100F). Results of the critical 4th and 5th stages of a typical test cycle are shown below.

Time:	12:45 p.m.	1:20 p.m.	1:45 p.m.	2:05 p.m.
Test Temperature:	296K (73F) →	322K (120F) →	352K (175F) →	366K (200F)
Sealability:	F.S.(1)	F.S.	F.S.	F.S.

2:12 to 2:42 p.m. →	3:00 p.m. →	3:30 p.m.
377K (220F)	335K (144F)	315K (108F)
F.S.	very slight leak	internal pressure dropped to 60 psi with a gas flow of 500 cc/min. Helium gas

→ 4:30 p.m.
296K (73F)
internal pressure = 0 psi
i.e., very heavy leak

(1) F.S. = full sealability

When the cross section of this subject O-ring was measured at the conclusion of this static leak cycle, the average W dimension = 2.95 mm (0.1261 in.) compared with an original W dimension of 3.56 mm (0.1400 in.) corresponded to 0.353 mm (0.0139 in.) compression set, or 66% compression set based on the initial 15% squeeze.

Although these crosslinked Halar O-rings do seal completely at 377K (220F), sufficient plastic flow (i.e., compression set) has occurred over 30 minutes' time so that the O-rings leak when the temperature is reduced by as little as 45K (≈80F). Crosslinking does increase the upper service temperature of these fluorocarbon plastics. However, the subject Halar O-rings, crosslinked with 5M rads of radiation, still exhibited an unacceptable amount of compression set at 377K (220F).

SECTION 4

ANALYTICAL STUDIES

The primary object of this program was to select and develop seal materials capable of satisfying the high reliability, multiple reuse requirements of the Space Shuttle. The performance of selected promising seal candidates was therefore studied under conditions simulating those encountered in the three primary space shuttle systems, i.e., the Hydraulic System, the Main Propellant System, and the Orbital Maneuvering System. Considerable progress was made in pursuit of this primary objective.

A secondary and probably the ultimate, long range objective of this program was to develop methods for calculating the effective lifetime of a given type of seal via short term measurements of specific, critical (but still unknown) parameters. In an attempt to accomplish this secondary objective, the performance tests utilized in this program were carefully designed, and the results analyzed to yield the maximum amount of basic rheological data concerning the subject seal candidates.

Rheological properties measured include stress relaxation, cyclic compression set, cyclic work, and hysteresis. Unlike the primary objective, only the surface of this secondary objective was "scratched." There are several reasons for this. First, although many of the critical material parameters which govern seal life are recognized, this knowledge is largely qualitative rather than quantitative. Secondly, although the essential criteria for effective sealing action such as a smooth compliance surface and retention of sealing pressure are obvious, and their direct relationship to material properties (such as retention of load bearing ability and stress relaxation) apparent, the precise mode of failure is often not only unknown, but undoubtedly changes with the operating conditions and service requirements. Thus, the primary failure modes encountered in sealing a high energy propellent such as N_2O_4 is far different from the failure modes encountered by a seal operating against a cryogenic fuel such as LH_2.

Similarly, the failure modes dominating static O-ring applications are far different from those dominating dynamic O-ring applications. In the first (static) case, the sole critical criterion is retention of sufficient sealing force to maintain a zero clearance against the gland walls, and this is easily and precisely determined via stress relaxation measurements. The stress relaxation data generated in this contract, over the time period measured, reasonably followed the simple log t plot:

$$\sigma = \sigma_1 - K \log t$$

where: σ_1 = stress at unit time

σ = stress at time t

K = relaxation constant

regardless of whether the O-ring was fabricated from a soft elastomer, such as Viton E-60C, or from a hard tough plastic, such as crosslinked Halar. It is entirely possible that the form of this stress relaxation curve is determined by the O-ring shape factor rather than the viscoelasticity of the O-ring material itself (Note 1). It will be noted that,when the "K's" of the various seal materials (from Viton to Tefzel) are normalized for the initial stress (i.e., K/σ_1), the normalized 296K (73F) values all fall between 0.035 (for Viton) and 0.140 (for AF-E-124D). Even at elevated temperatures, the normalized relaxation constant (K/σ_1) never exceeded 0.158 (for linear Halar O-rings at 378K (220F). These small relaxation constants virtually assure that the O-rings of this program would not fail by stress relaxation at ambient temperatures.

For example, taking the value of K = 4.2 lb/min. for ECD-3234 (black) O-rings, and assuming the empirical relationship $\sigma = \sigma_1 - K \log t$ is valid for large values of time, then the time, t, required for complete stress relaxation can be calculated

$$\sigma = \sigma_1 - K \log t = 0$$

$$\sigma_1 = K \log_{10} t, \quad t = 10^{\left(\frac{\sigma_1}{K}\right)}$$

$$t = 10^{\frac{\sim 125 \text{ lb}}{4.2 \text{ lb/min.}}} = 10^{\sim 30 \text{ min}} \quad \text{or}$$

$$2 \times 10^{24} \text{ years}$$

Obviously, this 10^{24} years is an artificial figure. However, the absence of significant stress relaxation is supported by work performed at Convair Aerospace several years ago on NBR (i.e., Buna N) O-rings (Reference 11). This work disclosed that O-rings from used aircraft components exhibit virtually no compression set. O-rings tested were as old as fifteen years.

Unfortunately, under even the simple cyclic conditions of this program, failure modes other than simple stress relaxation must predominate. Otherwise,the linear Tefzel O-rings would have sealed satisfactorily at 377K (220F).

If the failure controlling mode can be related to a given rheological factor, then it is possible to predict long range behavior at one temperature from a series of short range behaviorsat a higher temperature by the time-temperature superposition principle. Time-temperature superposition is a useful relationship in that stress or modulus time functions, when plotted on a log time graph, have identical shaped curves for different temperatures. The sketch below shows the log

Note 1. It must be emphasized that all the basic rheological data of this program relates to O-rings fabricated from the various seal candidates, rather than to the seal candidates themselves.

of the tensile modulus (M) plotted against the log of the time, at three different temperatures (T_1, T_2 and T_3) for a typical rubber.

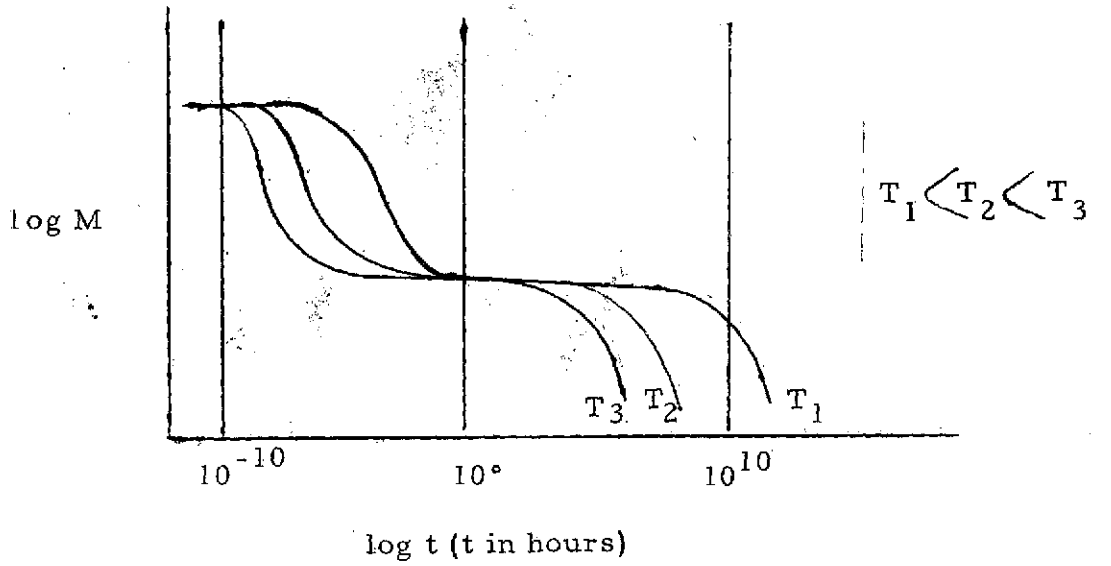

The fact that the stress or modulus magnitude (vertical scale) may also be plotted as a log function is unimportant as far as time-temperature superposition principle is concerned. The stress or modulus of the material is a function of the temperature and, as pictured above, a different curve is shown for three different temperatures. However, the shape of each curve is the same, there being only a horizontal time shift between each curve. The horizontal log time shift is a constant between common stress values for any one set of curves.

To make maximum use of the time-temperature superposition, one needs to be able to establish one curve throughout its entire range. Then by knowing any one point (not on a horizontal portion of the curve) for any other temperature, one can construct the entire curve for this other temperature.

Conversely, if portions of all the ranges were covered by several different but overlapping curves (overlapping at other than horizontal portions of the curves), they could be composed into one complete curve. The ability to directly establish any one curve throughout its entire range is severely limited by the extremes in times required at each end of the curve. If one goes to a high temperature so that the test does not extend into hundreds of years, then the start of the curve requires measurement times less than nanoseconds (which is difficult or impossible in most seal situations). If one goes to a cold temperature so that the initial time measurements become physically possible, the other end of the curve will never be seen in normal lifetimes. Of course, the exact times depend on the material and environment, but in general, this is the basic problem associated with these relationships.

When one tries to compose one curve out of many separate curves, one is then faced with making the proper matches between the curves. The proper matches must be done on non-horizontal lines, and the accuracy of these matches are dependent upon the comparative or absolute accuracy of the data. The smaller the slope, the greater the accuracy has to be for reasonable time correlations.

The data which was obtained in this program, by its very purpose and nature, was confined to materials which were expected to be very stable over the environments to be imposed. Any seal candidate found to be unstable was eliminated from the program. Therefore, most of the data obtained was in regions where the log plots were relatively linear and horizontal. Moreover, because of the very nature and intent of the basic work, the extremes which are desirable to accomplish a time-temperature superposition relationship was automatically excluded.

To obtain a time-temperature superposition relationship by matching a series of curves requires a relatively good fitting or matching of absolute values. In other words, if a high temperature run is really going to be compared to a lower temperature run, there would have to be a match between their absolute stress or modulus. In this program, testing consisted only of measuring total forces, and the comparison of these forces as a stress or modulus relationship is valid only to the extent that each O-ring at every temperature and force being related maintains identical geometry. This, of course, is not a reasonable assumption for the complicated geometry of O-ring contacts where the area of contact varies with force and modulus.

SECTION 5

DISCUSSION AND CONCLUSIONS

5.1 Hydraulic Seals

The Viton rubber compounds E-60C, ECD-3234 (black), and ECD-3234 (white) displayed good to fair high temperature resistance against the three different variants of the new MIL-H-83282 hydraulic fluid under both isothermal and thermal cycling conditions. There was some indication that this resistance was a function of the oxygen concentration. At both ambient and elevated temperatures these Vitons displayed excellent rheological, load bearing, and cyclic deflection properties. Cyclic work (determined by measuring the area under the stress-strain cusp via a compensating polar planimeter) remained constant throughout the 200 cycle test, and the cyclic hysteresis remained low and constant from 296K (73F) to 422K (300F). Stress relaxation measurements confirmed outstanding thermal stability of these Viton rubbers. Relaxation occurs by a log t type equation:

$$\sigma_t = \sigma_1 \quad - K \log t$$

which is in accord with physical relaxation rather than a chemical degradative process. Within the above temperature range, these Vitons are highly elastic and the dynamic sealability tests disclosed that an internally pressurized elastic O-ring mounted in a face seal gland will continue to seal long past the zero load point due to extrusion of the O-ring into the clearance between the gland face and the sealing anvil. Leaking occurred only after the clearance had become so large that the O-rings could blow completely out from between the gland and the anvil.

At 233K (-40F), the Vitons lose all their elasticity and are tough, leathery plastics. The load bearing and cyclic load deflection measurements are from 10 to 20 times greater in this leathery range than in the elastic range. In addition, under the 22% compression employed, all measurements (such as load bearing force, cyclic work, hysteresis, etc.) decreased steadily during the cycling so that after 200 cycles the measurements had decreased to between one-half and one-tenth of their value displayed on the first cycle. The indicated modulus is the sole rheological parameter which did not exhibit this decay. A new, accurate method of measuring this indicated modulus confirmed the complete absence of modulus decay at 233K (-40F). Higher anvil loading is required to achieve complete sealing, and the modulus in this leathery region is much too high to permit the Viton O-rings to extrude into the clearance between the gland shoulder and the sealing surface. As a result, at 233K (-40F) these Vitons exhibited a more normal type of sealing and leaking versus anvil loading action.

To recapitulate, the subject Vitons are excellent sealing rubbers at ambient or elevated temperatures, but they exhibit a drastic change in sealing characteristics at ~240K (-22F); sealing failures occur at 236K (-35F) and lower. The data of this program gave little evidence that the subject Vitons could perform satisfactorily as conventional O-ring seals below 240K (-22F). It must, however, be remembered that all the subject sealability data was derived from virgin Viton O-rings. Saturating the Viton O-rings with MIL-H-83282 hydraulic fluid could conceivably extend the Viton elastic range as far as 236K (-35F), or even 233K (-40F). It is highly unlikely, that the Vitons would become sufficiently plasticized by the hydraulic fluid to be useful for service at 219K (-65F).

In order to meet the standard 219K (-65F) military requirements, it is imperative that other oil resistant rubbers be considered. Of the two oil resistant rubbers evaluated in this program (the perfluoro Viton elastomer AF-E-124D and the phosphazine fluoroelastomer), only the latter appears promising since AF-E-124D has even poorer low temperature properties than the subject Vitons (Reference 9).

By contrast, phosphazine fluoroelastomers are still highly elastic at 219K (-65F) (Reference 10). As was mentioned in Section 3.1.1.3, the #1884-34 phosphazine specimen available to this program is not representative of the current generation of phosphazine fluoroelastomers which have excellent high temperature resistance to MIL-H-83282 fluid.

5.2 Main Propellent Seals

Of the six seal candidates considered for use on the Space Shuttle main propellent system only two, the perfluoroelastomer AF-E-124D and the fluoroplastic Halar, passed the critical LO_2-impact test. In addition, both of these candidates passed both the 20K (-424F) cryogenic soak and the 76K (-320F) to 344K (160F) thermal cycling tests without difficulty. Cyclic load deflection tests, however, disclosed that at 344K (160F) the crosslinked Halar O-rings exhibited significant compression set, while the AF-E-124D O-rings exhibited a smaller but still appreciable compression set at both the 344K (160F) and the 296K (73F) temperatures.

This susceptibility to physical relaxation is confirmed by the stress relaxation measurements of Section 3.2.5. For example, the normalized relaxation constants (K/σ_1) at 344K (160F) of both the crosslinked Halar and the AF-E-124D O-rings are 0.139 and 0.094, respectively. This is considerably higher than the normalized relaxation constants of the subject Viton O-rings at the much higer temperature of 422K (300F).

In view of the strong thermally stable nature of fluorocarbon polymer molecules, it would appear that these high compression set/stress relaxation phenomena are due to weak crosslinks or incomplete cures. In the case of the AF-E-124D O-rings,

a poor or non-stable crosslinked system is also suggested by the 50% decrease in load bearing properties when the temperature is raised from 296K to 344K (160F).

When the test temperature is lowered to 83K (-310F), neither seal candidate exhibited any compression set, however, neither did the AF-E-124D satisfactorily seal even though loadings as high as ⩾2,000 Kg (4,400 lb) were applied. By comparison, the crosslinked Halar O-rings sealed very well under ~1,000 Kg load, providing the Halar O-rings are "seated" (by compression cycling) at room temperature prior to cooling to cryogenic temperatures. In addition, although the crosslinked Halar O-rings require higher sealing loadings (~600 Kg) at room temperature than do the soft, elastic O-rings (such as the Vitons or AF-E-124D), on cooling from ambient to cryogenic temperatures the required sealing force only doubles, whereas the required sealing force for the elastic AF-E-124D increases more than 8-fold. The hysteresis of these crosslinked Halar O-rings is also of the same order as the measured cyclic hysteresis of the elastic Viton O-rings even though the low temperature test range of the Halar O-rings was 150K (270F) below that of the Vitons.

To summarize, although the crosslinked Halar O-rings of this contract were inadequately crosslinked, they still exhibited outstanding properties as cryogenic seals. There is every reason to suppose that their high temperature properties can be considerably improved by higher degrees of crosslinking without compromising their already excellent low temperature properties.

5.3 Orbital Maneuvering Seals

Ten-month immersion tests indicated that linear Tefzel has outstanding resistance to monomethyl hydrazine (MMH), as well as to the much more destructive nitrogen tetroxide (N_2O_4). Under the test conditions employed, linear Tefzel suffered only a 10% loss in tensile strength after the long N_2O_4 immersion. Judging from the stress relaxation measurements, linear Tefzel has surprisingly good resistance to stress relaxation at 377K (220F). However, when compression cycled in the internally pressurized O-ring leak test assembly, the linear Tefzel O-ring failed to seal adequately at this same temperature. This poor sealing performance of the linear Tefzel O-rings is particularly disappointing, since linear Halar O-rings which exhibited a larger compression set at 277K (220F) (K/σ_1 equaled 0.15 for Halar versus 0.12 for Tefzel) also displayed significantly better sealability. Radiation crosslinking should increase the service temperature of the Tefzel just as it did for Halar. As a partial confirmation of this assumption, some crosslinked Halar O-rings (prepared for application in the main propellent system) were evaluated in the static thermal cycling leak test of Section 3.3.5. As anticipated, the crosslinked Halar O-rings did seal perfectly at 377K (220F). However, under the loading forces employed, they also exhibited excessive compression set at this temperature. Tefzel O-rings, radiation crosslinked to various degrees,

therefore appears to be the most promising seal candidate for the orbital maneuvering system. As an alternative orbital maneuvering seal candidate, the perfluoroelastomer AF-E-124D is worth further consideration in spite of its high cost. The AF-E-124D suffered only a 25% loss in tensile strength after 10 months' immersion in N_2O_4. This perfluoroelastomer, however, does display considerable evidence of an incomplete or inadequate cure as witnessed by significant cyclic compression set and the large temperature dependence of load bearing properties. It is probable that the present cure system does not do justice to the inherently tough, stable polymeric backbone of the AF-E-124D rubber.

SECTION 6

RECOMMENDATIONS

It is recommended that the current employment of tensile coupons for the compatibility tests and O-rings for the cyclic load deflection, stress relaxation and sealability tests be continued, Some improvement in instrumentation is warranted. It is further recommended that the policy of evaluating seal candidates at three temperatures (encompassing the projected service range) be retained, but that in the case of the hydraulic and orbital maneuvering seal candidates the emphasis be shifted from virgin specimens to specimens which have undergone long term compatibility test exposure. As far as practical, specimens should be tested while still saturated with the test fluid. In this way the relationship of service conditions and time (static and cyclic) to O-ring sealing capabilities could be acertained; i. e., Sealing Capability = f (t/T°/test fluid/air). Hopefully, this data would lead to a determination of the critical parameters which control seal life. Once the critical parameter or parameters have been determined, it should be possible to measure the rate of change of this parameter. This, in turn, should permit predicting seal life from short time high temperature measurements via the time-temperature superposition principle.

6.1 Hydraulic Seals

In view of the poor low temperature properties of the various fluorocarbon rubbers (Viton, AF-E-124D, etc), it is recommended that the newer types of the phosphazine fluoroelastomers be evaluated for compatibility against MIL-H-83282 hydraulic fluid. A 234g. sample of one of these new phosphazine fluoroelastomer compounds is now available for fabricating the necessary O-rings and tensile specimens. As already indicated, compatibility should include both high temperature static and thermal cycling tests in presence and absence of oxygen. Physical, load bearing, and cyclic load deflection properties should be determined on both virgin and exposed specimens from the highest to the lowest service temperatures. If the subject phosphazine fluoroelastomer O-rings are sufficiently promising, and if time and money permit, functional tests should be performed on the subject O-rings in standard high pressure, dynamic, hydraulic systems containing MIL-H-83282 fluid.

6.2 Main Propellant Seals

Crosslinked Halar offers every indication of developing into an outstanding LO_2-compatible cryogenic seal material. The present program, however, strongly suggested that the 5 Megarads of radiation employed to cure the Halar moldings was insufficient to prevent an unacceptable amount of viscous flow,

particularly at high loadings and/or elevated temperatures. It is believed that these deficiencies can be corrected by increasing the amount of crosslinking. In order to develop a more nearly optimum cure, it is recommended that the effect of increased radiation doses on the physical, cyclic load deflection, and sealability properties of crosslinked Halar O-rings be determined. Crosslink-density measurements on selected members of this series of crosslinked Halars would also be helpful. An alternate method of inhibiting viscous flow involves fibrous reinforcement. If the fibrous filler is inorganic and incorporated in appreciable amounts, the coefficient of thermal expansion can also be substantially reduced, although at the expense of decreased elongation and ductility. At least some exploratory work with filled Halar should be considered.

Since most of the tests developed during this program are nonstandard, it is essential to obtain a direct comparison between the best of the crosslinked or filled Halar compounds developed above, and the current commercial cryogenic seal materials, filled Teflon, and Kel-F. Tests should include static and dynamic sealability, load deflection measurements, etc., from elevated to cryogenic temperatures. In addition, the impact resistance of all of the main propellent seal candidates should be determined at cryogenic temperatures.

6.3 Orbital Maneuvering Seals

It is recommended that a parallel development of radiation crosslinking and fibrous filling be performed also on the linear Tefzel in order to correct its poor sealability at 377K (220F). Testing should employ Tefzel specimens which have been both continuously and intermittently exposed to the test fluid (N_2O_4 or MMH) for varying lengths of time. In addition, these exposed specimens should be tested, as far as practical, while still immersed in, or at least saturated with, the test fluid.

In view of the powerful nitrating ability of N_2O_4 and its proven ability to form explosive mixtures with organic substrates, it is further recommended that the test program include an ASTMD-2512 type impact test, modified to use N_2O_4 rather than LO_2. In this connection, the broken tensile specimens (Tefzel, Halar, and AF-E-124D) used in the 10 month-long N_2O_4-compatibility test have been saved. After a two-month interval of atmospheric exposure, the specimens were again resealed in a N_2O_4 filled capsule. These specimens have, therefore, undergone a series of prolonged N_2O_4-atmosphere-N_2O_4 exposures, and are ideal vehicles for determining whether the subject fluorocarbon plastics or rubbers are capable of forming dangerous reaction products with N_2O_4.

As in the case of the preceding section, a direct testing comparison should be obtained between the best of the crosslinked or filled Tefzel specimens developed by work outlined in the foregoing paragraph and the currently acceptable N_2O_4-service seal material.

Although Tefzel possesses the very best N_2O_4/MMH resistance of any material tested to date, it is still a hard, high modulus material. For applications requiring a soft, compliant elastomeric seal, the AF-E-124D perfluoroelastomer should be considered. The principal defects of AF-E-124D (high compression set, sharp reduction in load bearing properties with temperature, etc.) appear related to an undercured condition. This present AF-E-124D situation is reminiscent of the situation which existed for the commercial fluorocarbon rubbers (Viton-A and Fluorel) eight years ago. The excessive compression set exhibited by parts molded from Viton-A or Fluorel severely limited their use. These difficulties were solved by the development of vastly superior curing systems typified by Viton-80 and Fluorel LCS. The AF-E-124D perfluoroelastomer requires a similar improvement in cure efficiency. TRW and AFML, Wright-Patterson AFB are working along these lines and their achievements should be followed closely.

REFERENCES

1. "Fluid Resistance of Silastic," p 7, Dow Corning Corp., Bulletin 09-013.

2. Table entitled "Fluid Immersion of Poly (fluoroalkoxy-phosphazine) Vulcanizate included with letter from Dr. K. A. Reynard, Horizons, Inc. to Dr. P. L. Merz, Convair Aerospace, April 5, 1973.

3. Casgarea, et al, "Aging of Cure Dated Items and Various Elastomeric Compounds," AD432369, 9/30/63

4. Bellanca and Harris, "Literature Survey on the Effects of Long Term Shelf Aging on Elastomeric Materials," Tech. Rpt. AFML-TR-67-235, AD831119 (March 1968).

5. Parker Seal Co. engineering report No. 03-176, "O-ring Compressive Force," 8 July 1969.

6. "Seal Material Development Program, Phase I," N71-165-77, TRW Report No. 14771-6001-RO-00 (31 December 1970).

7. Allied Chemical Corp. data sheet, "Halar Fluorocarbon Resin Chemical Resistance," C-8.

   Letter from E. F. C. Cain, North American Rockwell, to M. J. Fernandi, Allied Chemical Corporation, 14 September 1971.

8. "Properties and Structure of Polymers," p 78-83, Tabolsky, A. V. (John Wiley & Sons, New York, N. Y.) 1960.

9. "Vulcanizate Properties from a New Perfluoroelastomer," Barney, Kalb and Khan, Contribution No. 237, Research Laboratory, Elastomer Chemicals Dept., E. I. duPont de Nemours & Co., Wilmington, Del.

10. "Synthesis of New Low Temperature Petroleum Resistant Elastomers," S. L. Rose and J. Cable, AMMRC CR69-07(F), March 1969.

11. "Extend Elastomeric Seal Life," Value Engineering Proposal, #2283,GD/C 9 May 1968, Contract F04701-68-C-0023.

APPENDIX A

Rubber Formulations and Cure Schedules

Viton ECD-3234 (Black)

100 parts Viton ECD-3234
3 parts Maglite D
30 parts MT Carbon Black
6 parts Calcium Hydroxide

Bend on cool, tight mill

Premix in clean polyethylene container; add to rolling bank over 2-3 minute time

Mill mix 6 to 7 minutes, cutting and blending approximately four times from each side of the mill. Shut off and air cool 10 minutes. Cure in a preheated press for 20 minutes at 450K (350F) and 2500 psi with delayed bumping of press. Cool under pressure in mold. Postcure as follows:

4 hours from room temperature to 422K (300F)
4 hours from 422K to 450K (350F)
4 hours from 450K to 480K (400F)
4 hours from 480K to 504K (450F)
24 hours at 504K (450F)

Viton ECD-3234 (White)

Exactly the same formulation as shown above for the ECD-3234 (black) except that the 30 parts of carbon black are replaced by 30 parts of Wollostanite P-4 (or Cab-O-Lite).

Mill mixing, curing, and postcuring schedules are the same as those described above.

Viton E-60C (Black)

Formulation identical with that for ECD-3234 (black) except, of course, that the E-60C base replaces the ECD-3234 base.

Mill mixing, curing, and postcuring schedules are the same as those described above.

Viton ECD-3233 (Black)

Formulation identical with that for ECD-3234 (black) except, of course, that the -3233 base replaced the ECD-3234 base.

Mill mixing, curing, and postcuring schedules are the same as those described above.

Fluorosilicone LS-2380

100 parts Silastic LS-2380
0.5 parts Vorax [i.e. 2,5 bis (tert-bulyl peroxy)-2,5 -dimethyl hexane]

Mill mix on cold mill. No breakdown required.
Cure for 10 minutes at 444K (340F).
Postcure for 8 hours at 473K (392F) in a circulating air oven.

Fluorosilicone LS-2249

Formulation, compounding, curing, and postcuring similar to that of LS-2380 above.

Phosphazine Fluoroelastomer

100 parts of poly (fluoroalkoxyphosphazine) base
100 parts Burgess KE
6 parts Elastomag 170
1.5 parts Chemlink 30
6 parts DiCup 40 KE

Compound on cold mill, incorporating the peroxide catalyst (Di Cup 40KE) last. Allow to bin age for three days.

Cure in a preheated press for 15 minutes at 434K (320F).
Postcure for 24 hours at 373K (212F).

AF-E-124D (Viton ECD-006)

Formulation is proprietary (duPont and AFML-WPAFB).
Masticate on a hot, 340K (160F) mill until the crumbly raw gum stock coalesces. Masticate for an additional three minutes. Slab out hot masticated stock, and cut preforms. Place in a hot (340K) mold. Cure in a preheated press at 408K (275F) for 45 minutes at >7 MN/m^2 (>1,000 psi). Bump twice. Postcure as follows:

24 hours at 423K (302F)
24 hours at 450K (351F)
24 hours at 477K (399F)
6 hours from 477K (399F) to 558K (545F)
24 hours at 558K (545F)

APPENDIX B

Fluoroplastic O-ring Molding Procedures

Tefzel

a) Rings $2.01 \pm .005$ inches O.D. and $1.72^{+.02}_{-.00}$ inches I.D. having a cross section shown at the right, were machined from Tefzel rod.

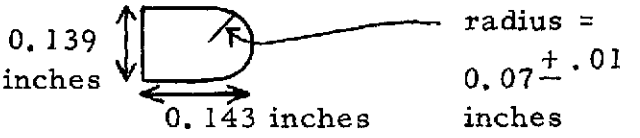

b) The Tefzel preforms were then placed, round side down, in a nickel plated, rubber type, 4-cavity O-ring mold equipped with a thermocouple.

c) The large 2-platen press is preheated to 533K (500F). Only light contact pressure is applied until the mold temperature reaches 504K (450F).

d) 20,000 lb. ram pressure is applied for three minutes with the temperature maintained at 504K (450F).

e) The mold is slowly cooled while maintaining ram pressure. The rate of cooling should not exceed 2K/minute for the first ten minutes.

Halar #302

a) Rings $2.00 \pm .005$ inches O.D. and $1.72^{+.02}_{-.00}$ inches I.D. having a cross section shown at the right, were machined from Halar rod.

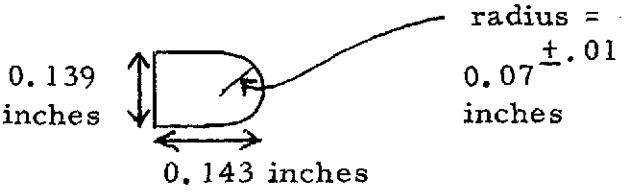

b) The Halar preforms were then placed, round side down, in a nickel plated, rubber type, 4-cavity O-ring mold equipped with a thermocouple.

c) The mold is closed and placed in a large 2-platen press preheated to 477K (400F). Only light contact pressure is applied until the mold temperature reaches 450K (350F).

d) 20,000 lb. ram pressure is then applied for three minutes while maintaining the temperature at 450K (350F).

e) The mold is slowly cooled while maintaining ram pressure. The rate of cooling should not exceed 2K/minute for the first ten minutes.

APPENDIX C

Poly [fluoroalkaxyphosphazine]
A New Generation Phosphazine Fluoroelastomer

The base polymer is essentially a copolymer of di(trifluoroethyloxy) phosphazine and di(heptafluorobutoxy) phosphazine:

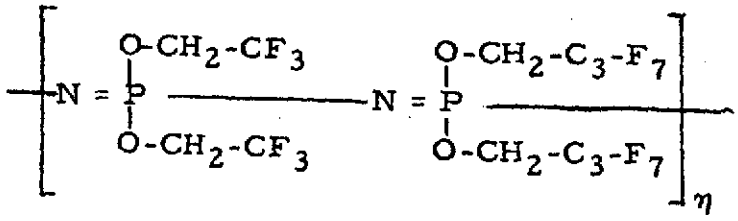

modified with small amounts of butane-1, 3 diol or N-ethyl-ethanolamine to give functionally reactive terpolymers which can be crosslinked with polyisocyanates.

This new improved elastomer is the result of improvements in the vulcanizing/compounding of the phosphazine fluoelastomer rather than any change in the chemical structure or molecular weight distribution of the base polymer. The pertinent data from Horizons, Inc. (Reference 2) is summarized below. For purposes of comparison, comparable results obtained on the older #1884-34 vulcanizate in NAS8-29060 are also included.

It is apparent that these new phosphazine fluoroelastomer vulcanizates exhibit not only improved physical properties, but vastly improved resistance to reversion. For example, after 144 hours of 423K in MIL-H-83282 hydraulic fluid, these new vulcanizates still retained 77 percent of their original tensile strength, and all (100%) of their ultimate elongation. Even when the shorter exposure time (144 hours of the Horizons work versus 200 hours in the Convair tests) is taken into account, the retention of physical properties by these new phosphazine fluoroelastomer vulcanizates is impressively better than the retention of properties exhibited by any of the seal candidates (white or black) tested in this program. In fact, the physical property values, reported by Horizons for these new phosphazine fluoroelastomer vulcanizates after 144 hours' immersion in the hot hydraulic oil was superior to the properties exhibited by the virgin specimens of the #1884-34 vulcanizates tested in this program.

Table 51

Effect of High Temperature MIL-H-83282 Hydraulic Fluid on Various Phosphazine Fluoroelastomers

Vulcanizate	Test Conditions	Ultimate Tensile Newton's/$m^2 \times 10^6$	Ultimate Tensile (Psi)	Ultimate Elongation	Hardness Hardness
"Old" 1884-34	0 hr. (virgin)	8.90	(1,291)	140%	68*
"Old" 1884-34	200 hr. /422K/ MIL-H-83282 Fluid (1)	1.54	(224)	243%	34-46*
% Retention of Physical Properties		17.4%		--	59%
"New"Horizons data	0 hr. (virgin)	11.45	(1,660)	80%	70%
"New"Horizons data	24 hr. /423K/ MIL-H-83282 Fluid (1)	9.72	(1,410)	60%	60 (*)
"New"Horizons data	72 hr. /423K/ MIL-H-83282 Fluid (1)	8.96	(1,300)	60%	60 (*)
"New"Horizons data	144 hr. /423K/ MIL-H-83282 Fluid (1)	8.83	(1,280)	80%	65 (*)
% Retention of Final Physical Properties		77%		100%	93%

(1) Royal Lubricants, Inc.
* = Shore A
(*) = microhardness

APPENDIX D

Pertinent Stress Relaxation Considerations

When the strain in a rubber material is quickly changed from one fixed value to another, the stress likewise quickly changes. However, even when the strain is held constant following a change, the change in the stress initially developed by this change in strain is often found to decrease with time. This change in stress with time under the condition of fixed strain is called stress relaxation.

Stress relaxation can actually be caused by several factors: 1) a non-conservative irrecoverable viscous flow effect, 2) heat distribution or thermal equilibrium effect, 3) chemical reactions (such as oxidation, cission, crosslinking changes to the number and/or type of crosslink bonds, etc.). All of these effects are to some extent present in most stress relaxation measurements, and under many conditions, are the particular parameters that are being controlled or investigated.

There is another factor associated with stress relaxation which is not directly related to these first factors. The term used to describe it is often given as physical stress relaxation, and is represented as a combination of elastic and viscoelastic components. All materials undergo physical stress relaxation. For most materials, neither the times nor magnitude of the physical stress relaxations are sufficient to be noticed. In rubber, however, the times and magnitudes are both sufficient to be readily observed.

Sketch #1 indicates the action associated with physical stress relaxation. At points A to B, a positive increase in imposed strain occurred, and at points C to D, a decrease in strain occurred. Following the positive increase in strain, the stress is shown to decrease with time, "B-C" (i.e. stress relaxation). Now following instantaneous partial removal of the imposed stress to point "D," the stress is shown to actually increase with time to "E." This is compatible with the initial description of stress relaxation in that it is the change in stress which decreases with time.

If the change in strain is such as to make the initial change in stress negative, the stress will then algebraically increase with time. If the strain in a specimen were instantly changed, the stress will also instantly change, but the stress developed by this change in strain will decrease with time even if the strain were held at a constant, fixed value. This decrease in stress which occurs when the strain is held constant is called stress relaxation.

SKETCH NO. 1

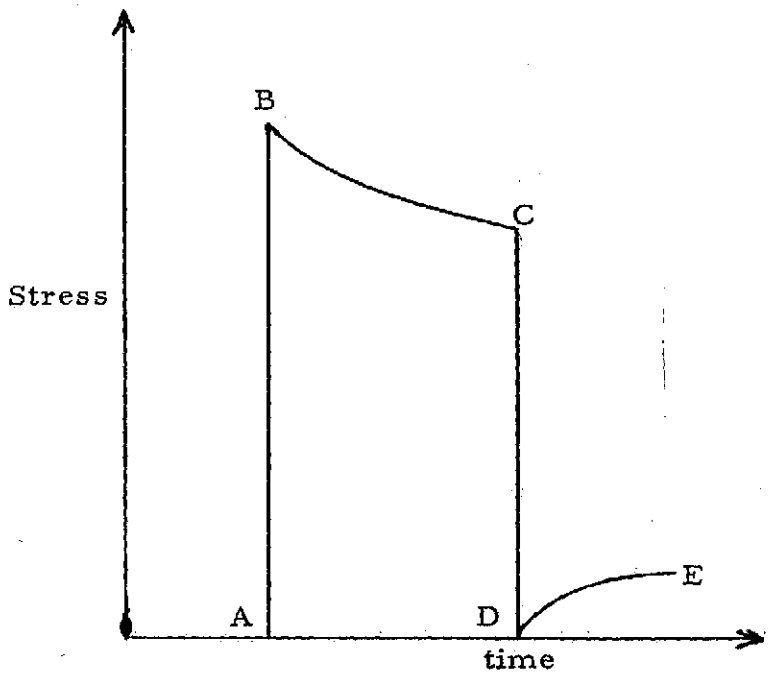

The various points in this stress/time curve are often approximated by a generalized Voigt-Kelvin model as shown.

A	B	C	D	E
Unloaded State	Instantaneous Stress	Relaxing State	Unloaded State	Retraction

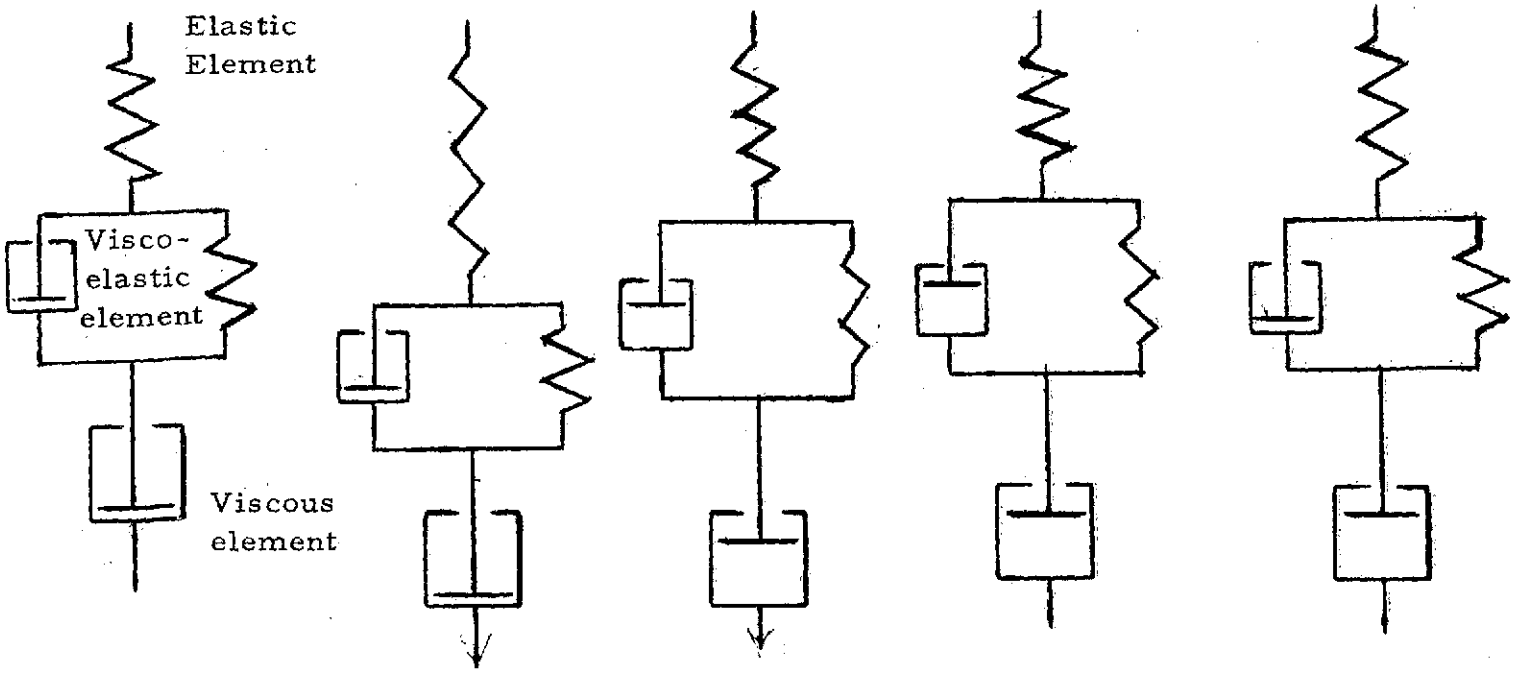

This decrease of stress with time can result from several factors: chemical changes in the material, thermal equilibrium changes, cold flow or yielding functions, and what could be called physical stress relaxations. Each of these factors have various time constants, are affected in different ways by the external environment, and include mathematical relationships of a variety of forms and/or functions. Some of these factors are permanent, non-conservative type reactions; others are conservative. In a stress relaxation measurement, the effects from each of these factors which may be present are superimposed upon each other, and one cannot always distinguish their effects individually. In general, however, it has been found that many chemical reactions follow a power law, and by following a stress relaxation over a long time period, the different time constants can sometimes be separated and different mathematical relationships can be seen to predominate during these different times.

For the materials tested in this program, there did not appear to be any strong chemical reactions occurring, either in terms of that seen in the stress relaxation measurements, or in other supporting tests. Also, very little cold flow, yielding or permanent set seemed associated with these tests. Therefore, the stress relaxations which were measured (after a short time required for thermal equilibrium to occur) must be assumed to be almost entirely associated with physical stress relaxation.

All materials undergo physical stress relaxations. For most materials, neither the time nor magnitude of this stress relaxation are sufficient to be noticed. In rubber, the time and magnitude are both sufficient to be readily observed.

To understand physical stress relaxations requires a knowledge of the molecular actions of a material, and certain relationships between stress and strain. Under long term equilibrium conditions, the molecules of a material, which are constantly moving, reach a state of balance in which motions or displacements in one direction are balanced by the motions or displacements in another direction, and all statistical norms remain constant over finite time periods. When a material which has reached this statistical balance is suddenly forced to change its shape (e. g. a strain is placed upon it), there must be a change in relative positions between the molecules. This change in relative positions of the molecules occurs almost immediately in the direction of the strain, being a forced motion, but the motion in the other dimensions occur somewhat randomly and with a speed limited by molecular motion itself. It takes a finite time for the molecules to rearrange themselves into a new statistical balance. For most materials, the location for the new statistical balance points are only fractions of an atom away from the original balance points (in any and all directions), and the time to establish this new balance is usually less than the time it takes to apply the original strain. Therefore, no stress relaxation is seen on the practical level. For other materials, such as rubbers, the mechanical complications that are present are such that new statistical balances are not quickly

achieved. Sketch #2 shows the complications of molecular chains which are associated with rubber-like materials.

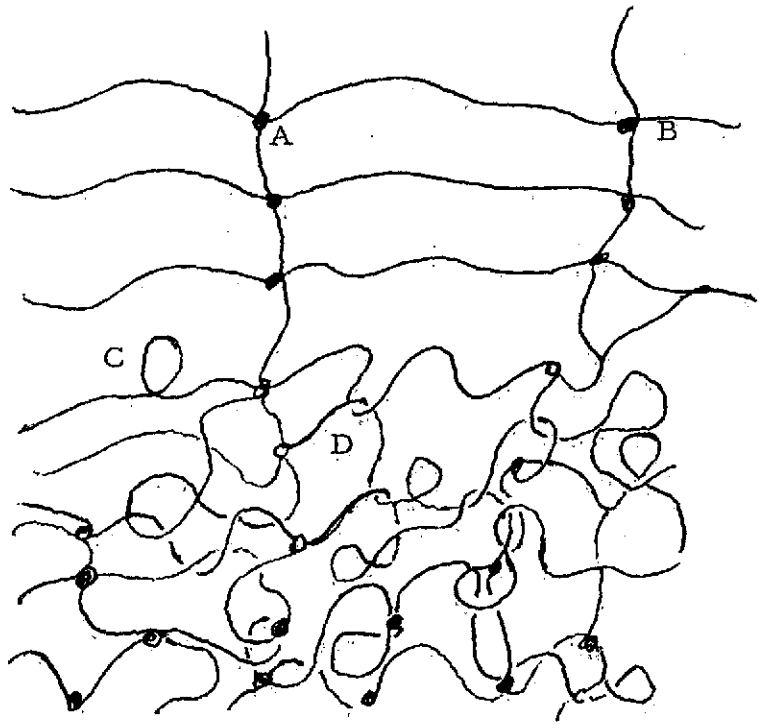

Sketch #2. Links in Molecular Chains: Points A and B – Standard (normal) Crosslinks. Point C – Internal Knot or Loop. Point D – Cross-cross entanglement.

In the upper portion of Sketch #2, the chain linkages are shown in a very simple, uniform arrangement. Because the molecules represented here are long chains of a very large number of atoms, their molecular motions, due to their large total mass and other factors, are much reduced, and stress relaxation times would be larger than single atomic molecular materials. However, for small strains, there are no changes in the simple, uniform, geometry or general relationship shown in this part of the sketch. In the lower part of the sketch, various entanglements are indicated. Because the chains are much longer than the distances between their crosslinking, these chains are constantly inter-wrapping themselves around each other and even upon themselves in loops and

"knots." The degree to which these inter-wrappings occur is highly dependent upon the differences in their total lengths and the distances between their formal crosslinking. Thus, each particular position of strain would have its own degree of entanglement associated with that position.

Under equilibrium conditions, the number of entanglements which are constantly developing are balanced by the disintanglements which are also constantly occurring. These events are statistical in nature. Depending on each individual entanglement, whether it is a cross-cross, or a loop, or a cross-cross with two or more other links, and the total lengths and forces involved, each has its own apparent time constant for disengagement. Sometimes, a particular chain is trapped into a position where two or more random events must occur simultaneously in order for it to be released. The time constant for this type of relationship can be very long.

When a material such as that shown in the lower part of the sketch is suddenly stretched or placed under strain, many of the original entanglements are temporarily trapped and even other entanglements or additional point contacts are created by this act of change. One can easily look at the sketch and can see how additional points of contacts can be created if a large strain occurred in any one direction. The time it takes for the original and the new entanglements to reach an equilibirum with the natural entanglements expected or associated with that particular new point of strain is the time associated with stress relaxation.

The following points are easily seen. The larger the strain (positive strain or stretching or pulling), the less entanglements expected or capable of occurring. To maximize stress relaxation, one would like to allow the material to remain in a minimum volume until maximum entanglements occur, then quickly move to a maximum strain point. The effects of temperature is not directly apparent. An increase in temperature results in faster molecular motions which would appear to result in shorter time constants, but the degree of entanglement is also increased so much more that this could offset this reduction. The total amount and number of entanglements which exist at any one time therefore increased with temperature. Whether this causes a decrease or an increase in relaxation times depends on the differences between the two strain positions, differences in terms of total number of entanglements, and their average release in stress forces when these entanglements disengage, as well as in the average rate of these disengagements.

APPENDIX E

Compression set calculations of linear Halar O-rings after 100 compression cycles during dynamic sealability testing at 377K (220F). O-ring thickness measured a 4 equidistances around the O-ring periphery.

O-ring #8 - Instron Run #2787 -				
before cycling	0.1400"	0.1394"	0.1398"	0.1401"
after 100 cycles	0.1256"	0.1306"	0.1300"	0.1290"
decrease in thickness	0.0144"	0.0088"	0.0098"	0.0111"
compression set as % of total thickness	10.3%	6.3%	7.0%	7.9%
compression set as % of est. 15% deflection	68%	42%	47%	53%
O-ring #9 - Instron Run #2788 -				
before cycling	0.1387"	0.1393"	0.1397"	0.1387"
after 100 cycles	0.1250"	0.1250"	0.1240"	0.1237"
decrease in thickness	0.0127"	0.0143"	0.0157"	0.0150"
compression set as % of total thickness	9.7%	10.3%	11.2%	10.8%
compression set as % of est. 15% deflection	65%	69%	75%	73%